A STUDY OF THE WAKE REGION OF THE FLOW OF DILUTE POLYMER SOLUTION ABOUT CIRCULAR CYLINDERS

John Norman Schimmels

NAVAL POSTGRADUATE SCHOOL
Monterey, California

THESIS

A STUDY OF THE WAKE REGION
OF THE FLOW OF DILUTE POLYMER SOLUTION
ABOUT CIRCULAR CYLINDERS

by

John Norman Schimmels

Thesis Advisor: T. M. Houlihan

December 1971

A Study of the Wake Region of the Flow of Dilute Polymer Solution about Circular Cylinders

by

John Norman Schimmels
Ensign, United States Navy
B.S., Marquette University, 1970

Submitted in partial fulfillment of the
requirements for the degree of

MASTER OF SCIENCE IN MECHANICAL ENGINEERING

from the

NAVAL POSTGRADUATE SCHOOL
December 1971

ABSTRACT

The wake region of the flow of dilute polymer solution about a circular cylinder was studied. Polyox WSR-301 at a concentration of 25 WPPM was dissolved in tap water. The investigation was performed in the drag transition flow regime. Turbulence intensity, wake width, microscale of turbulence and frequency spectra were measured at various points in the wake region of water flow and polymer solution flow.

The polymer additive suppressed turbulence intensity outside the wake and caused a corresponding increase in the wake core. The effect was dependent upon degradation, and Reynolds Number. Frequency spectra were also suppressed. The amount of suppression was dependent upon degradation, Reynolds Number and distance from the wake center. Microscale was reduced outside the wake, as a function of degradation only. Wake width was reduced, dependent upon degradation and Reynolds Number. Results indicated a premature transition which was dependent upon the above factors.

TABLE OF CONTENTS

LIST OF FIGURES

Figure Page

ACKNOWLEDGEMENT

The author is indebted to Professor Thomas Houlihan for his invaluable insight into the theoretical aspects of this experiment, and for his continual guidance with the measurement techniques involved. The assistance of Messrs. K. Mothersell, T. Christian, G. Baxter, G. Bixler, J. McKay, and J. Beck in the construction and maintenance of test equipment was also greatly appreciated. Thanks are also extended to my wonderful wife, Sue Ann, for her understanding and patience.

I. INTRODUCTION

A. ORIENTATION

The engineer is constantly "searching for a bargain" at nature's bartering table. Invariably, he comes away with less than he went in with, for nature is a ruthless bargainer. However, through innovative thinking, the engineer has often been able to reduce his losses to nature. The so-called "Toms' Effect" has proved to be an example. In 1948, Toms [Ref. 1] discovered that a dilute solution of polymer in a Newtonian solvent greatly reduced frictional drag in internal turbulent flow. Since that time, a considerable amount of research has been undertaken in the field of fluid dynamics, for the purpose of optimizing the efficiency of submersible propulsion systems through drag reduction.

Great strides have been made in the study of internal flow drag reduction. However, a relatively sparse amount of information is presently available concerning external flow behavior of such solutions.

The rheological effects of polymer additives have been studied extensively. It has been found that polymer additives impart a degree of viscoelasticity to a Newtonian solvent, which is dependent upon concentration. This effect is due to the high degree of flexibility of the polymer molecule. The solutions have also been found to be time-dependent. Under any imposed shearing action, the high molecular weight,

long-chain polymer molecules are torn apart, and eventually lose their drag-reducing capabilities. This phenomenon is referred to as solution degradation. These additional solution parameters, concentration and degradation, add to the already complex nature of the study of external flow.

B. SYNOPSIS OF PREVIOUS WORKS IN EXTERNAL POLYMER SOLUTION FLOWS

It has long been known that the low pressure region behind bluff bodies is reduced as the boundary layer flow changes from laminar to turbulent, at well-defined Reynolds Numbers. This reduction of the low pressure region is accomplished by a momentum transfer to the fluid in the boundary layer. This enables the flow to advance farther against the adverse pressure gradient before separation. Transition is accompanied by a reduction of drag, due to the increased pressure recovery.

A number of researchers have reported drag reductions to varying extents, for various ranges of Reynolds Numbers, and for several basic geometries, with polymer solution flow. An exhaustive survey of this early work has been presented by Sarpkaya and Rainey [Ref. 2].

Studies of the flow of polymer solution about circular cylinders have been performed by Sarpkaya and Rainey [Ref. 2] and Kell [Ref. 3]. Sarpkaya and Rainey reported a premature transition from laminar to turbulent boundary layer characteristics with polymer solution flow. Drag was measured directly

and was found to decrease in this flow region. The change in transition was attributed to two effects. The first was a roughening effect by which a continuous transition was observed, similar to the effect observed with roughened cylinders. The second was a drag crisis or tripping wire effect, which was observed at a certain flow condition and degradation state of the solution.

Kell reported the same reduction of drag in the transition Reynolds Number region, and further studied the effect of polymer solution on the Strouhal frequency. No change was observed in the characteristic Strouhal frequency, but a general suppression of the frequency spectrum obtained at 120° from the forward stagnation point on the cylinder surface was noted.

Kowalski [Ref. 4] studied the effect of dilute polymer solution injection into the boundary layer in open channel flow. He noted energy spectrum changes and a large reduction of viscous dissipation due to the additive. He also noted that the additive was most effective near the position of maximum turbulence production in the boundary layer, that is, the separation point. His studies were performed with fresh solutions only.

Several theories have been offered to explain the effects of polymer additives. Patterson [Ref. 5] summarized them as follows:

1. Aggregation Theory

Clusters of polymer molecules in a flow have a retarding effect upon the intensity of shear layers. This retarding effect is accomplished by an exchange of momentum normal to the shear layers.

2. Anisotropic Viscosity Theory

This theory suggests that the long, chain-like molecules align themselves with the direction of shear, and reduce the momentum transfer normal to the direction of shear. Due to this preferred alignment, the viscosity is found to be anisotropic.

3. Viscoelastic Theories

a. The polymer molecule coil has associated with it a characteristic relaxation time. For processes with a shorter time scale, the molecule has solid-like behavior.

b. The flexibility of the polymer molecule provides the polymer coil with an elastic capability. This results in the absorption, storage, and release of energy, depending upon influences of the surrounding fluid.

4. High Effective (Tensile) Viscosity Theory

Due to large polymer molecule deformations, a high effective viscosity is observed in an irrotational strain field. It is surmised that drag reduction is directly related to this effect.

Since these theories were classified by Patterson, several more recent works have provided the basis for the following theories.

5. The Entanglement Hypothesis

This theory was proposed by Kowalski [Ref. 4] in conjunction with his studies. He suggested that drag reduction is accomplished via the interaction of networks of polymer molecules. These networks are of the same order as the dissipative eddies of the flow field.

6. Shear Wave Theories

a. Sarpkaya and Rainey [Ref. 2] suggested that a finite critical shear wave speed was the fundamental property which changes the characteristics of the flow. It is through this parameter that a hydro-polymeric boundary layer results, which controls the transition characteristics of the flow.

b. Tulin [Ref. 6] suggested that dilute polymer solutions exhibited a frequency-dependent shear stiffness. Shear waves due to this shear rigidity are produced by turbulence in shear flow. There is a direct conversion of turbulence energy into shear wave energy. This effectively "short-circuits" the usual process of scale reduction through inertial interactions.

Because of the diversity of the studies from which these theories were deduced, and the complex nature of the problem, a satisfactory theory has not yet been presented to explain all of the apparent anomalies.

C. SYNOPSIS OF PREVIOUS WORK: WAKE OF FLOW ABOUT CIRCULAR CYLINDERS

Very little quantitative work has been reported in the wake region of the flow about circular cylinders. The

complex nature of the wake flow has thus far defied any sort of analytical approach. The subtle effects of the end conditions, test section geometries, test specimen surface conditions and a host of other elusive parameters render test conditions which are uncontrollable to some extent. However, a great deal of knowledge of the wake region has been obtained, qualitatively speaking. An excellent survey of early work was presented by Goldstein [Ref. 7].

In 1953, Rosenhead [Ref. 8], realizing that the brilliant contributions of von Kármán and Föppl were by no means a complete explanation of vortex shedding phenomena, suggested an investigation of vortex systems in terms of rates of generation and dissipation of vorticity.

Humphreys [Ref. 9] studied the flow about a circular cylinder at transition Reynolds numbers. He stressed the importance of end conditions in the assumption of two-dimensionality. In this flow regime, he observed a spanwise cellular structure on the cylinder surface. This structure was periodic in nature and swept across the cylinder in the spanwise direction. He further noted that the structure became increasingly noticeable as the transition was approached. He reported a spanwise cell length of 1.4 to 1.7 diameters.

The three-dimensionality of bluff body flow has been noted by several other experimenters. Schmidt [Ref. 10] found spanwise correlations for the flow about a circular cylinder. Keefe [Ref. 11] found that end conditions strongly influenced

the magnitude of fluctuating lift and drag forces acting upon a circular cylinder.

Prendergast [Ref. 12] made surface pressure and velocity correlation measurements on the surface of a circular cylinder, between Reynolds Numbers of 20,000 and 100,000. Measurements were made at the side and rear of the cylinder. The correlation length, defined as the area under the correlation coefficient curve versus probe spacing, was found to be 3.5 diameters at the side, but only 1.0 diameter at the rear. El Baroudi [Ref. 13] also studied two-point correlations at the side of the cylinder with hot-wire techniques. He found correlation lengths which were 30% to 80% higher than Prendergast's. Differences were attributed to end effects.

The actual wake region away from the cylinder surface has been studied by several researchers. In 1948, Kovasznay [Ref. 14] used hot-wire anemometry techniques to study the vortex shedding phenomenon at low Reynolds Numbers. In the Reynolds Number range 40 to 160, he noted that vortices were not shed directly from the cylinder, but formed some distance downstream in the wake.

Bloor [Ref. 15] also used hot-wire anemometry to study the positions of the onset of turbulence in the wake, and the mode of the transition. Studies were made in the Reynolds Number range 1,300 to 45,000. She found that in the lower range, the region of turbulence moved closer to the cylinder with increasing Reynolds Number. She also noted that the manner of transition underwent a basic change as the region

of transition moved from the periodic wake into the region immediately behind the cylinder, where the separated layers had not yet rolled into vortices. She suggested that transition to turbulence in the periodic wake was a result of the distortion due to three-dimensional effects. At the higher Reynolds Numbers, however, transition to turbulence occurred immediately behind the cylinder via two-dimensional Tollmien-Schlichting waves, which she called transition waves. She also studied the length of the formation region, which was defined as the downstream length at which low frequency irregularities in the wake were suddenly reduced. This signified the initiation of periodicity, as the shear layers rolled up into vortices. She observed that the formation region rapidly approached the separation point on the cylinder surface as the Reynolds Number increased to the pre-transition range. It was also observed that as the hot-wire was moved closer to the wake center, shedding frequency amplitude gradually increased. The edge of the wake was defined as that point at which there was a jump in signal amplitude. For higher Reynolds Numbers, the wake width was determined from the point at which high frequency spikes were first observed in the free shear layer, as the hot-wire was moved toward the center of the wake.

Gerrard [Ref. 16] studied the flow past the circular cylinder in the Reynolds Number range 2,000 to 50,000. Hot-wire measurements were made near the shoulder of the cylinder. He noted the same transition waves as those observed by Bloor.

He further found that if the flow contained disturbances of the same frequency as the transition waves, a large increase in the fluctuating velocity and the pressure coefficient was observed at the shoulder.

In a later work, Gerrard [Ref. 17] further studied the wake flow behind circular cylinders in the Reynolds Number range 1,000 to 50,000. He proposed two characteristic lengths in the wake flow. The first was the formation region, l_f, which was similar to that defined by Bloor. The second was the diffusion length, L, which was a measure of the width to which the free shear layer diffused.

He proposed that a certain amount of fluid was entrained by the rolling shear layer at the end of the formation region, and a certain amount was drawn into the formation region itself, every half cycle of the vortex shedding. He observed that as the Reynolds Number increased, the formation region decreased, and the rate of entrainment of fluid by the rolling shear layer increased. From the corresponding decrease of entrainment into the formation region, he reasoned that the frequency of vortex shedding would be reduced as Reynolds Number increased. He further found that the diffusion length, L, had the opposite effect on the Strouhal frequency. Thus, the frequency of vortex shedding was influenced by these two opposing effects. He offered this explanation for the constancy of the Strouhal number in this flow regime.

Roshko [Ref. 18] measured the drag coefficient in the supercritical Reynolds Number range one million to ten million,

and found an increase from the lower supercritical value, at a Reynolds Number of 3.5 million. He also observed a return of periodic vortex shedding in the wake above this Reynolds Number.

From this discussion, it is apparent that a thorough understanding of the wake region of the flow about circular cylinders is yet to be uncovered.

D. OBJECTIVES OF THE EXPERIMENT

This experiment was performed to obtain the wake characteristics of the flow of dilute polymer solutions about a circular cylinder, at the Reynolds Numbers limited to the range before, during and after the drag crisis region observed by Sarpkaya and Rainey [Ref. 2] and Kell [Ref. 3]. Measurements of turbulence intensity, wake width, microscale of turbulence and frequency spectra were to be compared between the wake flow of water and the wake flow of polymer solution.

E. DEFINITION OF MEASURED QUANTITIES

1. Turbulence Intensity

Turbulence intensity, as defined by Dryden and Kuethe [Ref. 19], is a measure of the violence or intensity of turbulent fluctuations. The velocity in a given direction of a flow can be characterized by two components, the mean velocity and the fluctuating velocity. This is represented by the following relation:

$$U = \bar{U} + u$$

where $\bar{U}$ is the mean velocity component and u is the fluctuating velocity component. Turbulence intensity is defined by the following ratio:

$$I = \frac{u'}{\bar{U}}$$

where u' is the root-mean-square of u.

The measurement of these quantities through the use of hot-film anemometry is based upon the measurement of the heat transfer rate from the hot sensor. The relation used for the calibration of the sensor, as developed by Hinze [Ref. 19], is stated as follows:

$$V^2 = V_o^2 + B\sqrt{U}$$

where V is the voltage across the sensor, corresponding to a flow velocity U. V_o is the voltage across the sensor at zero flow velocity. B is a constant which is dependent upon the sensitivity of the sensor.

The turbulence intensity as a function of voltage signals can be derived from these relations, the end result being the following:

$$I = \frac{u'}{\bar{U}} = \frac{4xV_m xe'}{(V_m^2 - V_o^2)}$$

where V_m is the D. C. level of the sensor signal in volts and e' is the root-mean-square of the fluctuating component of the sensor signal in volts.

The turbulence intensity in the longitudinal direction of the flow field, that is, parallel to the free stream flow direction, was measured in all phases of the investigation.

2. Microscale of Turbulence

The microscale of turbulence, as defined by Hinze [Ref. 19], is a measure of the average dimension of the smallest eddies in a flow field. This quantity is also called the "dissipation scale," since it represents a measure of the eddies which are primarily responsible for the dissipation of kinetic energy into heat. The relationship defining the longitudinal microscale of turbulence is derived from the longitudinal correlation coefficient and is developed fully by Hinze. With the assumption that Taylor's hypothesis is valid at points of interest, the definition reduces to the following:

$$\frac{2}{\lambda_f^2} = \frac{1}{\bar{U}^2 u'^2} \left(\overline{\frac{\partial u}{\partial t}}\right)^2$$

where λ_f is the longitudinal microscale of turbulence. The above relation is valid only if the flow field is homogeneous with a constant mean velocity. These restraints limit the applicability of the relation to the discrete points outside the periodic wake, where a long-time average of the mean velocity is not necessary.

The microscale as a function of sensor voltage signals can be derived from the above relations to the following:

$$\lambda_f = \sqrt{2} \times e' \times (V_m^2 - \bar{V}_o^2)^2 / B^2 \left(\frac{dV}{dt}\right)'$$

where $(dV/dt)'$ is the root-mean-square of the differentiated sensor signal. The longitudinal microscale of turbulence was measured in this investigation.

II. EQUIPMENT AND PROCEDURE

A. EQUIPMENT

1. NPS Water Tunnel

The experiments were performed in a recirculating water tunnel (Fig. 1) which had a capacity of approximately 500 gallons. The galvanized test section was four inches wide, eight inches high, and sixteen inches long. A low-rpm, high-capacity, fourteen-inch-diameter-discharge centrifugal pump was used to circulate the fluid through the test section at velocities ranging from five to twenty-five fps. The upstream section of the tunnel, having been previously modified with the addition of three flow straighteners, provided a test section velocity profile which was uniform in both mean velocity and turbulence intensity.

Associated with the tunnel are a 150-gallon stainless steel storage tank, a small recirculating pump filter system, and a 15-gallon head tank.

2. Test Specimens

Circular cylinders (Fig. 2) of 3/4 inch, one inch, and 1-1/2 inch diameter were used as the test specimens. The cylinders were made of plexiglass and were located in the center of the test section, perpendicular to the flow field. The cylinders were mounted in place through the plexiglass side walls of the test section, with O-ring type seals at each end. The cylinder could then be rotated through 360° if necessary. The cylinder was held rigidly

in the desired position with a bolt which was fastened to the outside of the test section wall.

Forward stagnation pressure measurements on the surface of the cylinders were taken at midspan. A small 1/32 inch diameter hole was drilled radially into the cylinder, to a larger 1/8 inch diameter hole, which was drilled axially into the cylinder. The larger hole extended to the end of the cylinder, making the pressure signal easily accessible. Static pressure was measured with a pressure tap on the test section wall, near the entrance to the test section.

The one-inch diameter plexiglass cylinder was used for the bulk of the experimentation, since it provided an excellent Reynolds Number range, which was limited by the range of test section velocities attainable. The 3/4 inch cylinder was used only to measure forward stagnation pressure in experiments to determine the turbulence intensity of the flow field at the entrance of the test section. The 1-1/2 inch diameter cylinder was found to be too large to accommodate the relatively small test section. Measurements in the wake of the 1-1/2 inch diameter cylinder showed a substantial amount of wall interference at relatively small downstream location from the cylinder axis. The one-inch diameter cylinder proved to be the optimum size, for it provided the proper Reynolds Number range and did not enhance wall interference with the wake at moderate downstream locations. Thus, the one-inch diameter cylinder was used as the primary test specimen throughout the experiment.

3. Sensor and Sensor Support

TSI conical hot-film sensors with a right angle bend (Model 1231) were used throughout the experiment to measure fluctuating and mean components of velocity in the longitudinal direction. The eight-inch long cylindrical sensor support was strengthened with a concentric 1/4 inch diameter stainless steel tube which provided the sensor with stability at all transverse positions in the wake flow. A small plexiglass splitter plate was also mounted on the rear of the sensor itself. The splitter plate effectively broke the vortices shedding off the rear of the sensor. This gave the sensor further stability and strength (Fig. 3).

Through the course of the experimentation it was necessary to use a number of sensors, due to the relatively short life expectancy of each sensor, and the lengthy test procedure.

The sensor and sensor support unit extended through the top or bottom of the test section via several plexiglass plugs, which were fitted to mount flush on the interior wall of the test section (Fig. 4). Three plugs were made for the top of the test section and were placed at distances of two inches, 3-1/2 inches, and five inches downstream of the longitudinal axis of the cylinder. One plug was made for the bottom of the test section and was placed at a distance of 1-1/2 inches from the longitudinal axis of the cylinder. A small-clearance hole was drilled in each plug through which the sensor support was extended. The plugs were sealed with

O-ring type seals. The sensor support was then fastened to an aluminum traversing mechanism which was bolted to the top or bottom of the test section. The sensor was moved transversely across the flow field by this means.

This set-up provided the sensor with a range of position extending from +2.5 inches from the center of the test section at minimum extension to -1.25 inches from the center of the test section at maximum extension.

Several experimenters in the past have reported anomalous hot-film measurements in dilute polymer solution. Metzner and Astarita [Ref. 20] found the convection coefficient of the sensor, h, to be independent of free stream flow velocity above a critical velocity. The effect was attributed to a layer of stagnant fluid on the tip of the probe. Their data were obtained using cylindrical sensors. Smith, Merrill, Mickley and Virk [Ref. 21] also reported a change in the heat transfer characteristics of a hot-film cylinder in dilute polymer solution. The heat transfer was found to be a function of mean velocity, the molecular weight of the polymer and the polymer concentration.

Preliminary investigations concerning the feasibility of the use of conical hot-film sensors were performed. All calibrations of the conical hot-film sensors showed excellent response in both water and dilute polymer solution for the full range of test section velocities. No change of the heat transfer characteristics of the sensor was found.

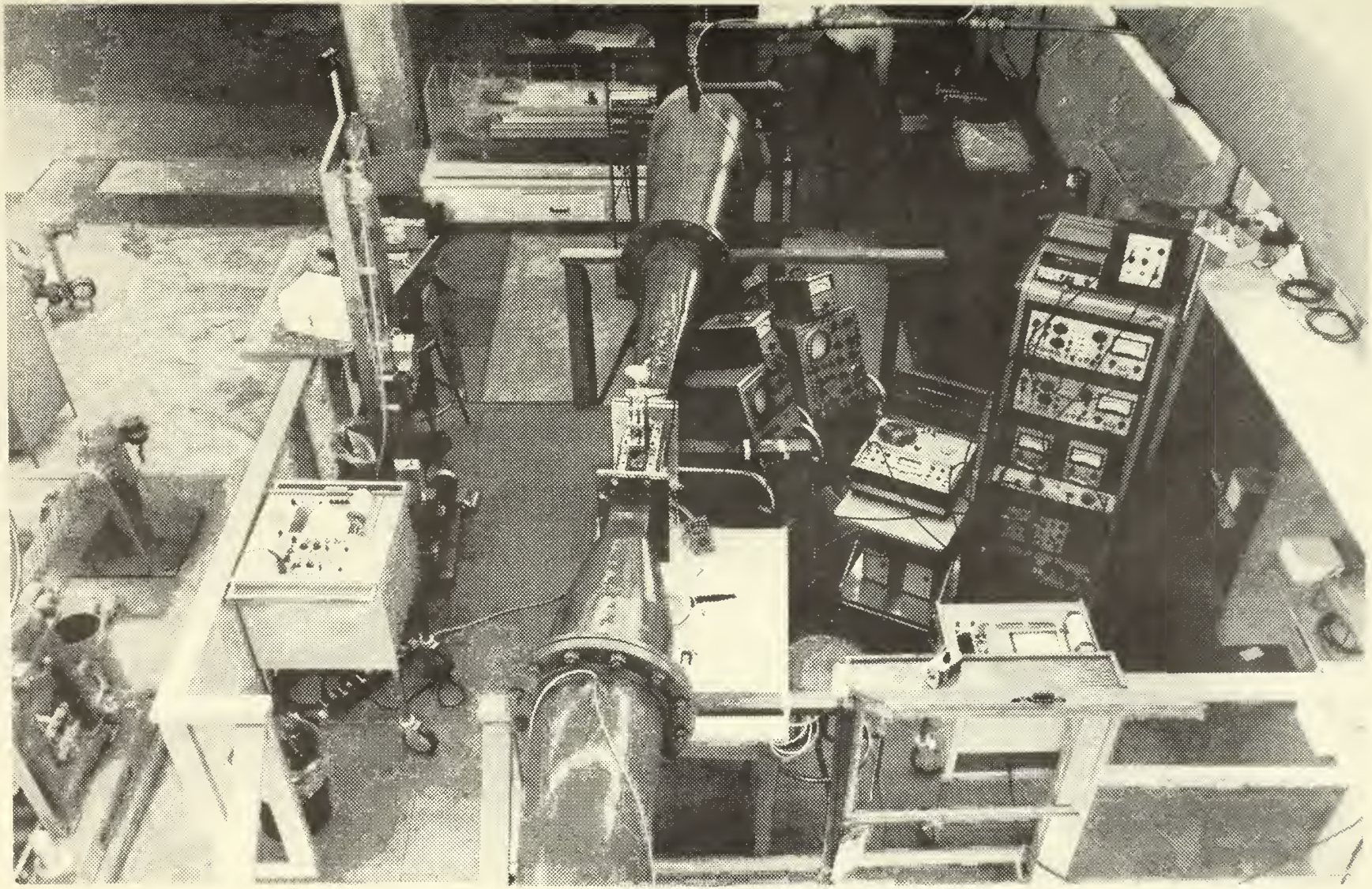

Figure 1: NPS WATER TUNNEL AND INSTRUMENTATION

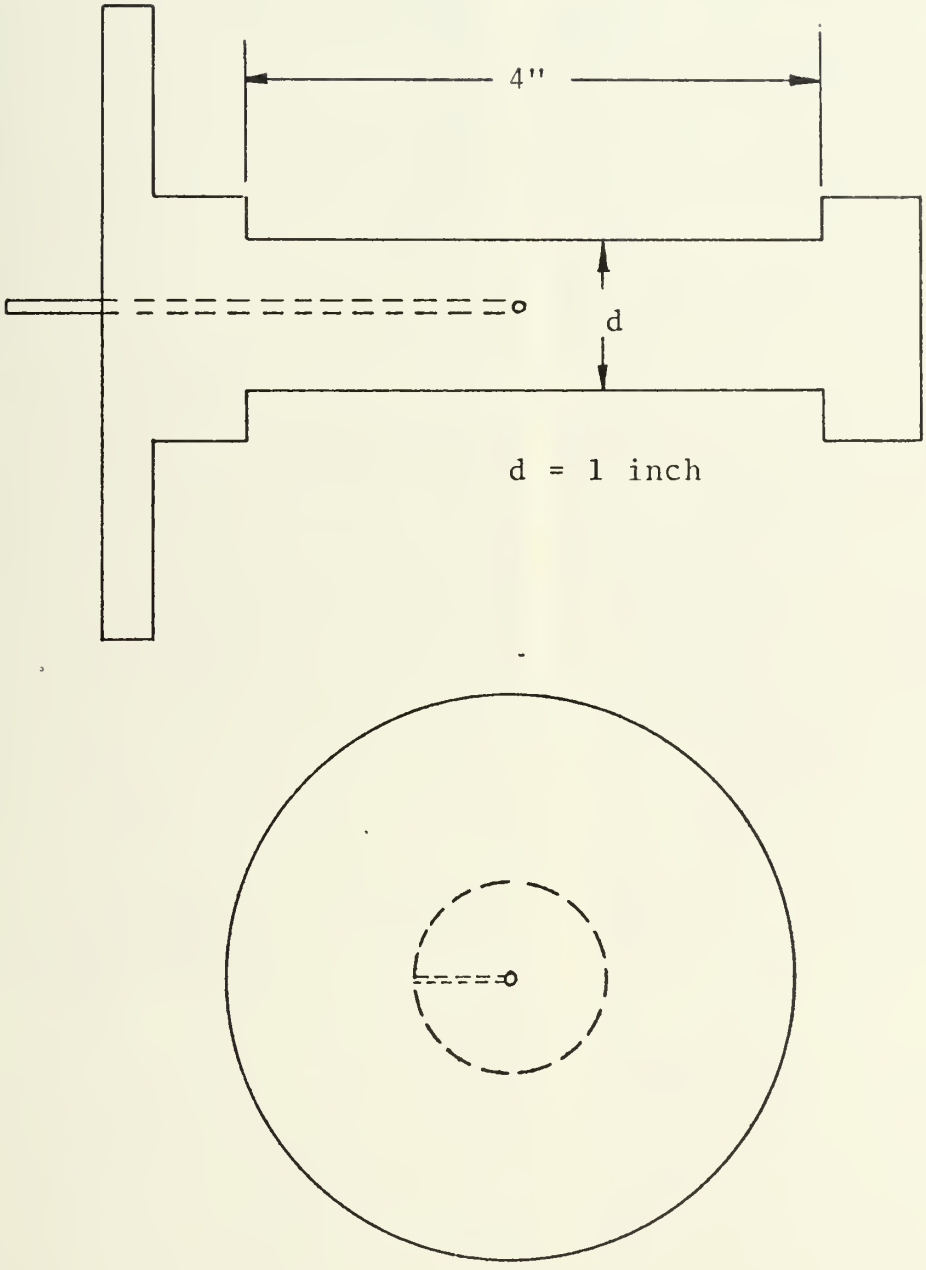

Figure 2: PLEXIGLASS CYLINDER

Figure 3: CONICAL HOT-FILM SENSOR UNIT

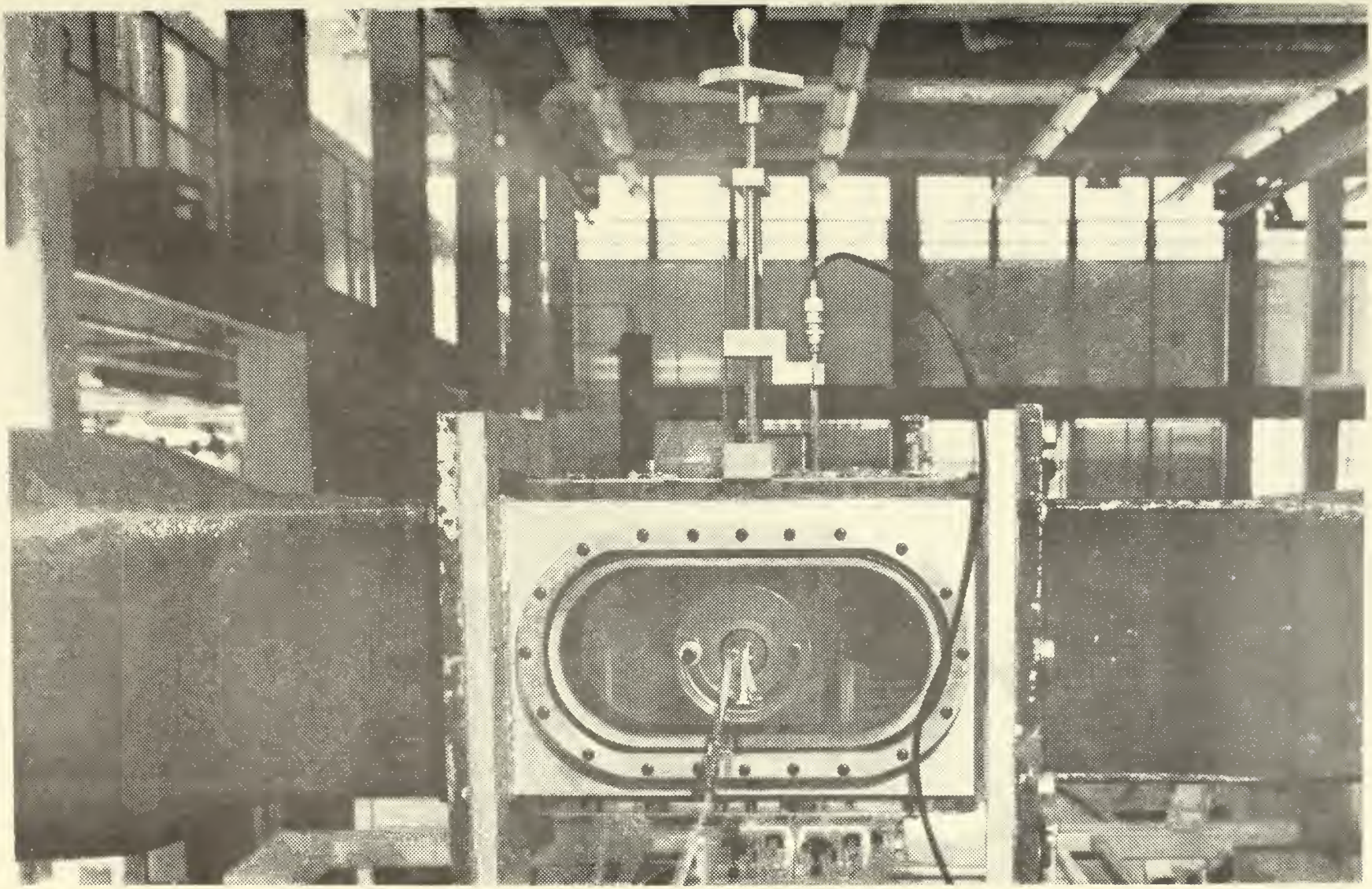

Figure 4: TEST SECTION

4. Instrumentation

Differential pressure measurements were effected with a Pace pressure transducer (Model P70) having a range of zero to six psig. The signal was amplified and recorded on a Hewlett-Packard strip chart recorder (Model 7702B).

A TSI Constant Temperature-Type Anemometer Unit (Model 1050) was used in conjunction with the hot-film probes. The anemometer unit was set to provide a high frequency cut-off at 2,000 cps. The bridge output of the unit was fed to a Simpson digital voltmeter (Model 2700), from which the mean velocity component of the signal was extracted. The output was also paralleled to a TSI RMS Voltmeter (Model 1060) with a three-second time constant from which the RMS of the fluctuating component of velocity was extracted. Upon calibration of the probe, these signals were used to calculate the turbulence intensity of the flow. The sensor signal was constantly monitored on a Textronix Oscilloscope (Model 531). The sensor signal was also amplified by a Keithley Amplifier (Model 103) to either 100X or 1,000X, with a low and high frequency cut-off of .1 and 1,000 cps, respectively. The amplified signal was the input to one channel of a Hewlett-Packard Instrumentation Tape Recorder (Model 3960). The output of the recorder was constantly monitored on the second channel of the oscilloscope, and further checked for the proper amplification with a Hewlett-Packard RMS Voltmeter (Model 3400A).

Microscale measurements were obtained by feeding the bridge output signal of the anemometer unit to a Flow Corporation Sum-Difference Differentiator Unit (Model 900-6), from which the derivative (with respect to time) of the sensor signal was obtained. This signal was fed to a TSI RMS Voltmeter (Model 1060), and to another Keithley Amplifier with a low and high cut-off of .1 and 1,000 cps, respectively. This signal was constantly monitored on another Textronix oscilloscope and provided the input to a second channel of the tape recorder. Again, the output of the tape was monitored on the second channel of the oscilloscope, and also checked for proper amplification with another Hewlett-Packard RMS Voltmeter (Model 3400A). A schematic of this system is presented in Fig. 5.

Frequency spectrum measurements were made by band passing the taped hot-film sensor signal through a Krohn-Hite Band Pass Filter (Model 3750). The filtered signal was fed to a TSI RMS Voltmeter (Model 1060) with a time constant of three seconds.

5. Turbulent Pipe Rheometer

As has been done by previous experimenters, the disposition of the polymer solution being tested was characterized by its ability to reduce pressure loss in turbulent pipe flow. The turbulent pipe flow rheometer unit consisted of a .073-inch inside diameter stainless steel pipe, which was mounted vertically. A 100 cc graduated syringe was connected to the lower end of the pipe. A glass

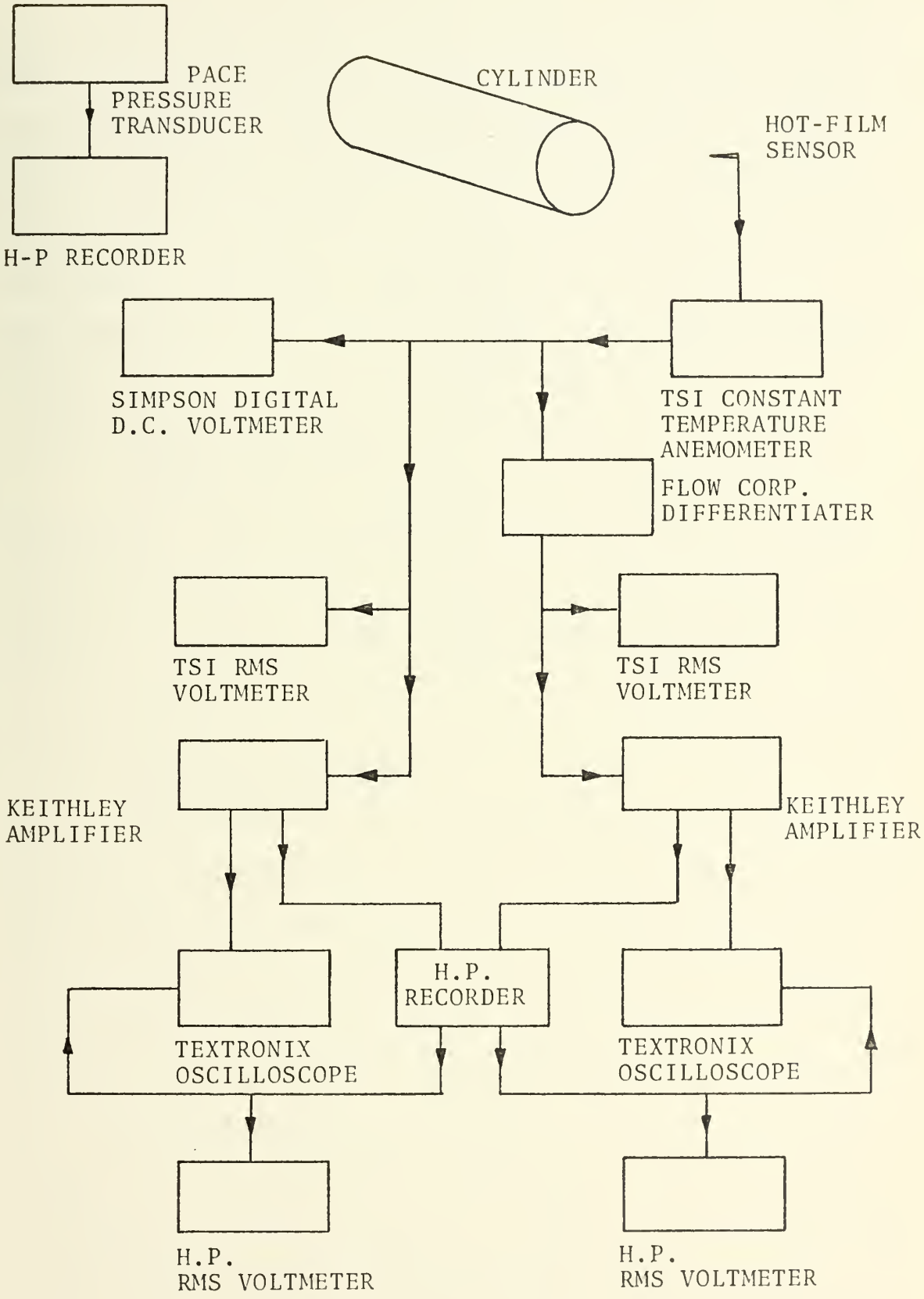

Figure 5: SCHEMATIC OF INSTRUMENTATION

reservoir was connected to the top end. A variable speed motor produced the input torque to a worm-gear box which forced the fluid in the syringe through the pipe. Two pressure taps were placed six inches apart on the length of the pipe, and the pressure loss was measured with a Pace transducer. The signal was amplified and recorded on a Hewlett-Packard strip chart recorder. The Reynolds Number of the pipe flow was in the range 5000-5500.

6. Polymer Additive

Polyox WSR-301, Blend 1267A was used in all of the experiments. This polyethylene-oxide additive is produced by Union-Carbide. Polyox is a water soluble resin with a molecular weight of approximately five million [Ref. 22].

B. PROCEDURE

1. Rheometer Operation

The fluid to be tested was poured into the top reservoir and allowed to fill the whole system. The syringe plunger was then slowly lowered to slightly below the 100 cc level, drawing in fluid as it was lowered. The variable speed motor was then started at a pre-selected speed by closing a relay. When the syringe plunger had reached the 100 cc level, an electric timer was activated. The time elapsed for the flow of 80 cc of fluid through the pipe was measured by instantaneously stopping the timer and the motor when the plunger had reached the 20 cc level.

The pressure drop and elapsed time were recorded and used to calculate the pipe friction factor. Values of

the Fanning friction factor for water flow were used as a basis for comparison with polymer solution flow at the same Reynolds Number. Thus, the Fanning friction factor for water, f_t, was first obtained as a function of Reynolds Number. Subsequent tests of the polymer solution were run and consequent pressure drops were obtained. From this data, the friction factor for polymer solution was obtained. The Per cent Pipe Drag Reduction (P.D.R.) of the polymer solution relative to laminar flow was then calculated.

$$P.D.R. = 100X\ (f_t - f)/(f_t - 64/Re)$$

The polymer solutions were tested at a Reynolds Number of approximately 5,000. The Reynolds Number was always based on the viscosity of water at ambient temperature.

Samples of the test fluid were drawn from the tunnel before every traverse of the flow field at a given Reynolds Number, corresponding to an elapsed running time of 10-15 minutes. Ample quantity was withdrawn to allow one flush through the rheometer and three test runs. A sample was run only once, then discarded. The PDR was then calculated for each test run, and the average of the three runs was used as the PDR for the given traverse.

2. Preparation of Test Fluid

Before any data could be taken at all, it was necessary to filter fresh tap water for at least eight hours. The water seemed to contain an incredibly large amount of foreign material, the source of which remains unknown. It

was necessary to change filters in the filtering system after each fresh input. More significant, however, is the fact that the addition of polymer to fresh, unfiltered water provided negligible pipe drag reduction. The initial pipe drag reduction capabilities of a solution increased proportionally to the time fresh water was filtered prior to the addition of polymer. More than eight hours of prior filtering caused no change in the initial PDR of the solution, and the fresh solution reached an expected value of 80% PDR.

The polymer solution was prepared by the same procedure as in previous investigations [Ref. 2]. The desired amount of polymer was weighed out on a laboratory scale, $\pm$.05 gm. In all tests, a 25 weight-part-per-million (WPPM) solution was used. The level in the tunnel was then dropped to below the center of the test section. The water was displaced to the storage tank. The pump was then turned on to its lowest speed, and the polymer was slowly sprinkled into the water. Upon completion, the water in the storage tank was pumped back into the tunnel. The pump was then turned on, and allowed to mix the solution for five minutes. The pump was then shut down, and the solution was aged for approximately 24 hours before any tests were run.

After the solution had degraded to zero PDR, the tunnel was emptied and flushed twice before refilling. Prior to taking water data, the tunnel was chemically treated with potassium bicarbonate and allowed to sit for 72 hours.

3. Tunnel Correction Factors

Tunnel correction factors for solid blockage and wake effects were applied to all stagnation pressure measurements to obtain the actual free stream velocity in the test section. The total correction factor (e_t) was calculated from

$$e_t = \frac{\pi^2}{12} \left(\frac{d}{h}\right)^2 + \frac{1}{2} \left(\frac{d}{h}\right) C_d$$

where $\frac{d}{h}$ is the ratio of cylinder diameter to test section height, and C_d is the drag coefficient of the cylinder. The drag coefficient of the cylinder was obtained from the data of Sarpkaya and Rainey [Ref. 2], since no direct drag measurements were made in this experiment.

The actual free stream velocity in the test section was then obtained from

$$U = V(1 + e_t)$$

where V is the free stream velocity calculated from the measurements of forward stagnation pressure on the cylinder surface.

4. Definition of Coordinate Axes

Throughout the experiment, all positions of the sensor were referenced to the coordinate system shown in Fig. 6. All X-coordinates and Y-coordinates presented here refer to this system.

5. Measurement of Tunnel Turbulence Intensity

The turbulence intensity of the tunnel flow field with water was measured at the location -3.5 X/DIAM, in front

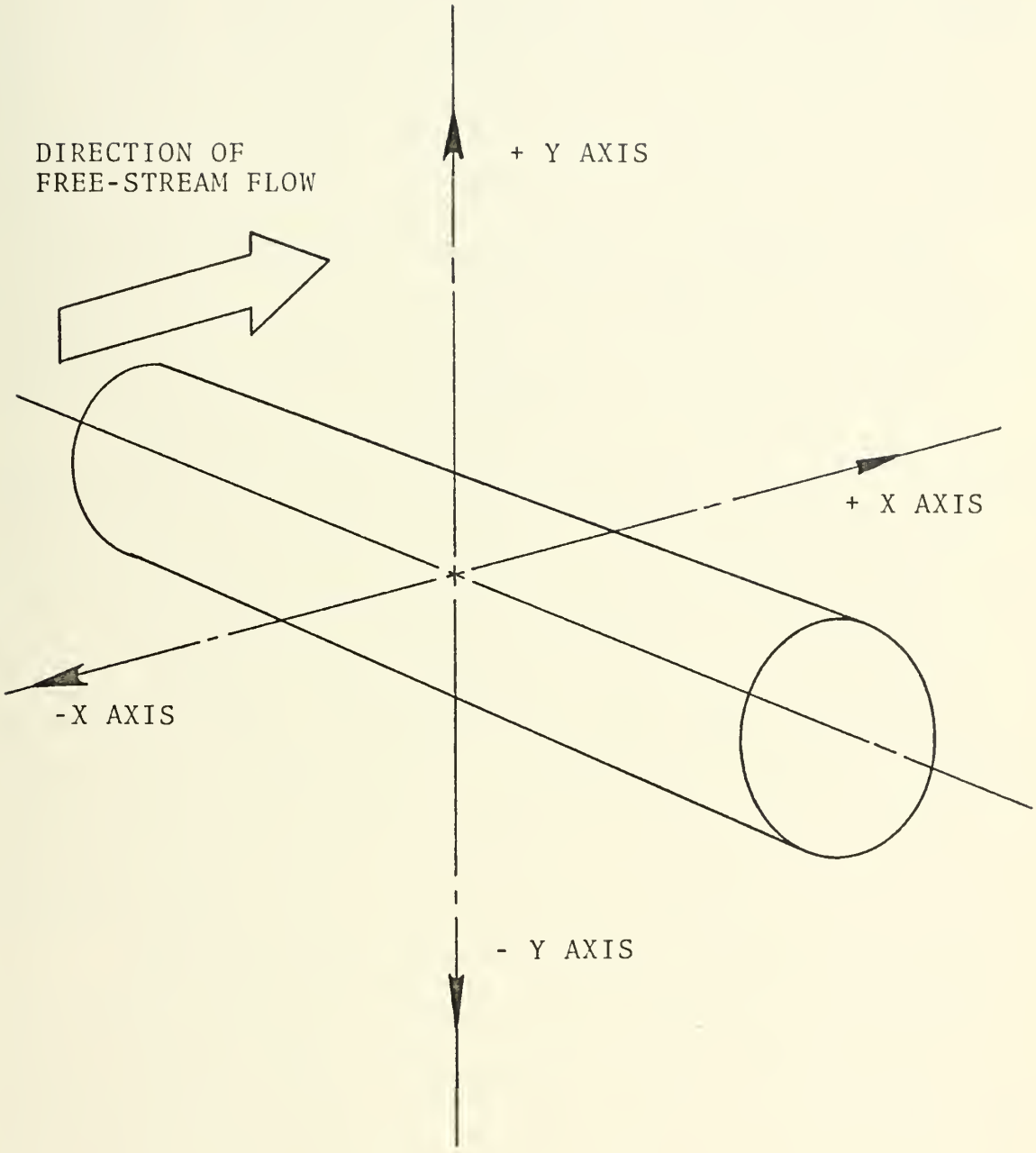

Figure 6: DEFINITION OF COORDINATE AXES

of the 3/4 inch circular cylinder. The cylinder was placed in the tunnel for the purposes of calibration of the hot-film sensor. The pressure difference between forward stagnation pressure and tunnel static pressure was measured to determine tunnel mean velocity. This method of calibration was used in preference to a Pitot tube, since it was found in previous experiments that the pressure anomaly common to dilute, high molecular weight solutions could be circumvented by using a velocity probe with a large radius [Ref. 2].

The turbulence intensity of the flow field was measured for five mean tunnel velocities: 6.3 fps; 9.9 fps; 12.4 fps; 14.5 fps; and 18.5 fps. The hot-film sensor was moved transversely across the flow field. Measurements of the D. C. component and the RMS of the A. C. component of the sensor signal, corresponding to the mean component of velocity and the fluctuating component of velocity, respectively, were recorded at intervals of 0.25 in the transverse direction, from +2.5 inches to -1.25 inches.

The turbulence intensity of the tunnel flow field with dilute polymer solution was determined in a similar manner, at the same sensor locations, for the range of degradation states of the solution from 80% to 0% PDR. The tunnel was then emptied, flushed, and the same procedure was repeated with the sensor extending through the bottom of the test section.

6. Measurement of Turbulence Intensity of the Flow Field behind the One-Inch Cylinder

The turbulence intensity profiles of water flow and polymer solution flow were measured in the wake and outside the wake of the one-inch diameter cylinder for Reynolds Numbers of 80,000, 100,000, 120,000, and 140,000. Traverses of the flow field were made with the hot-film sensor at X-axis positions of +1.0 $\frac{X}{DIAM}$ and +1.5 $\frac{X}{DIAM}$. These positions were chosen for several reasons. It was found in preliminary runs that a sensor position further downstream provided little interpretable data due to tunnel wall interference with the wake. It was also determined that at the closest position of +1.0 X/DIAM, the presence of the sensor and its support displayed no measurable interference with the pressure signal on the surface of the cylinder with the port having been rotated 120° from the forward stagnation point. The signal was the same with the sensor in the flow field as without it, at all transverse positions of the sensor. There was further reason to believe that the region immediately behind the cylinder would be of primary interest, because the apparent reduction in drag is essentially a surface effect.

Water data were obtained prior to the polymer solution data. The sensor was initially placed at a transverse position of +2.5 Y/DIAM. The tunnel was then turned on and off intermittently to allow the air trapped inside the tunnel to diffuse out via the head tank. After the entrapped air

was removed, the desired tunnel free stream velocity was obtained from previous calculations. These calculations included solid blockage and wake effects. When the desired pressure difference between static and stagnation pressure on the cylinder surface was obtained, the traverse of the flow field was made. The D. C. level and the RMS level of the fluctuating component of sensor bridge output voltage was recorded, as the sensor was moved from the initial transverse position of +2.5 Y/DIAM to 0 Y/DIAM in intervals of .25 Y/DIAM. The sensor bridge output signal was also amplified and recorded on an instrumentation tape recorder. After each Reynolds Number run, the sensor was moved back to the initial position. Free stream velocity was then changed for the next traverse.

Besides recording the described voltages, the point at which high frequency velocity spikes were first observed on the sensor oscilloscope trace was also recorded. Using the definition of wake width suggested by Bloor [Ref. 15], these observations provided a constant monitor of any macroscopic changes occurring in the wake region.

Polymer solution data were obtained in a similar manner. With the polymer solution flow, however, another variable was present due to the degradability of the solution, namely, the PDR. Thus, a series of tests were made from an initially high PDR of approximately 80% to no measurable PDR of 0%. A sample was drawn from the tunnel prior to each Reynolds Number run and tested in the rheometer. There were

four Reynolds Number runs to each test, and as many as fifteen tests before the solution registered 0% PDR.

7. Measurement of the Microscale of Turbulence

The microscale of turbulence of the water flow and the polymer solution flow behind the one-inch diameter cylinder was determined for Reynolds Numbers of 80,000, 100,000, 120,000, and 140,000. Traverses of the flow field were made at an X-axis position of +1.5 X/DIAM for the previously described transverse positions. The measurements were made simultaneously with the previously described turbulence intensity measurements. The sensor bridge output voltage was differentiated to obtain the required information. The differentiated signal was monitored and recorded on the instrumentation tape recorder.

8. Frequency Spectrum Measurements

The frequency spectrum of the sensor signal was obtained for the flow of water and the flow of dilute polymer solution about the one-inch diameter circular cylinder. Spectra were obtained for flow Reynolds Numbers of 80,000, 100,000, 120,000, and 140,000. The taped signals obtained from the sensor at an X-axis position of +1.5 X/DIAM and the transverse positions of +2.0 Y/DIAM, +1.5 Y/DIAM, +1.0 Y/DIAM, +0.875 Y/DIAM, and +0.75 Y/DIAM were band-pass filtered through six frequency bands. These frequency bands were 2-15 cps, 15-25 cps, 25-35 cps, 35-45 cps, 45-75 cps, and 75-125 cps. The RMS value of each filtered signal was determined for water and a range of polymer solution degradation states.

III. PRESENTATION OF DATA

A. EVALUATION OF EXPERIMENTAL ERRORS

The accuracy of the entire experiment hinged upon the reliability of three measurements. These primary measurements were: (1) the stagnation pressure-static pressure differential; (2) the D. C. voltage across the sensor and (3) the R.M.S. of the A. C. voltage across the sensor.

The strip chart recorder on which the pressure differential was measured was read to $\pm$0.2 mm. The worst expected error due to this reading was calculated to be 4%. However, when transforming this reading to actual velocity, the error reduced to 2% due to the parabolic relationship between pressure and velocity.

The error involved in the measurement of D. C. voltage across the sensor was estimated to be 2%. The error in measurement of the R.M.S. of the A. C. voltage across the sensor was estimated to be 5%. Combining these three errors, the maximum error in turbulence intensity was found to be 6%. This maximum error applies only to the center of the wake region. Outside the wake region, the R.M.S. readings were much more accurate, manifesting an estimated error of 2%. D. C. voltage error was reduced to 0.5%. Outside the wake region, the total estimated error was 3%.

The maximum error in the microscale of the turbulence measurements was found to be 15%. This relatively high error

possibility was generated by the necessity to square the D. C. voltage signal twice. The addition of a second R.M.S. voltage, that is, the R.M.S. of the differentiated sensor signal, also increased the maximum error of this quantity.

B. TURBULENCE INTENSITY OF TUNNEL UPSTREAM FLOW FIELD

The turbulence intensity of the upstream flow field was measured at the location -3.5 X/DIAM, in front of the 0.75-inch cylinder. A traverse of the flow field at this location yielded the turbulence intensity profile shown in Fig. 7. Figure 7 presents the profiles for five test section velocities. It is shown that the maximum intensities occurred on the minimum velocity profile, and, generally, the intensity decreased as test section velocity increased. This was the case because the measured D. C. voltage was inversely proportional to the fourth root of mean velocity. The R.M.S. values of the A. C. voltage across the sensor were essentially constant at all five flow rates.

The non-uniformity of the profiles was caused by the non-uniform D. C. voltage level across the sensor. The entrance region to the test section was greatly influenced by the three flow straighteners, previously described. A non-uniform D. C. level was measured because the flow field at this location was still in the process of being straightened. The flow field was found to be completely uniform (within experimental error) at a position of 0 X/DIAM. Thus, the profiles shown in Fig. 7 are the worst observed in the test

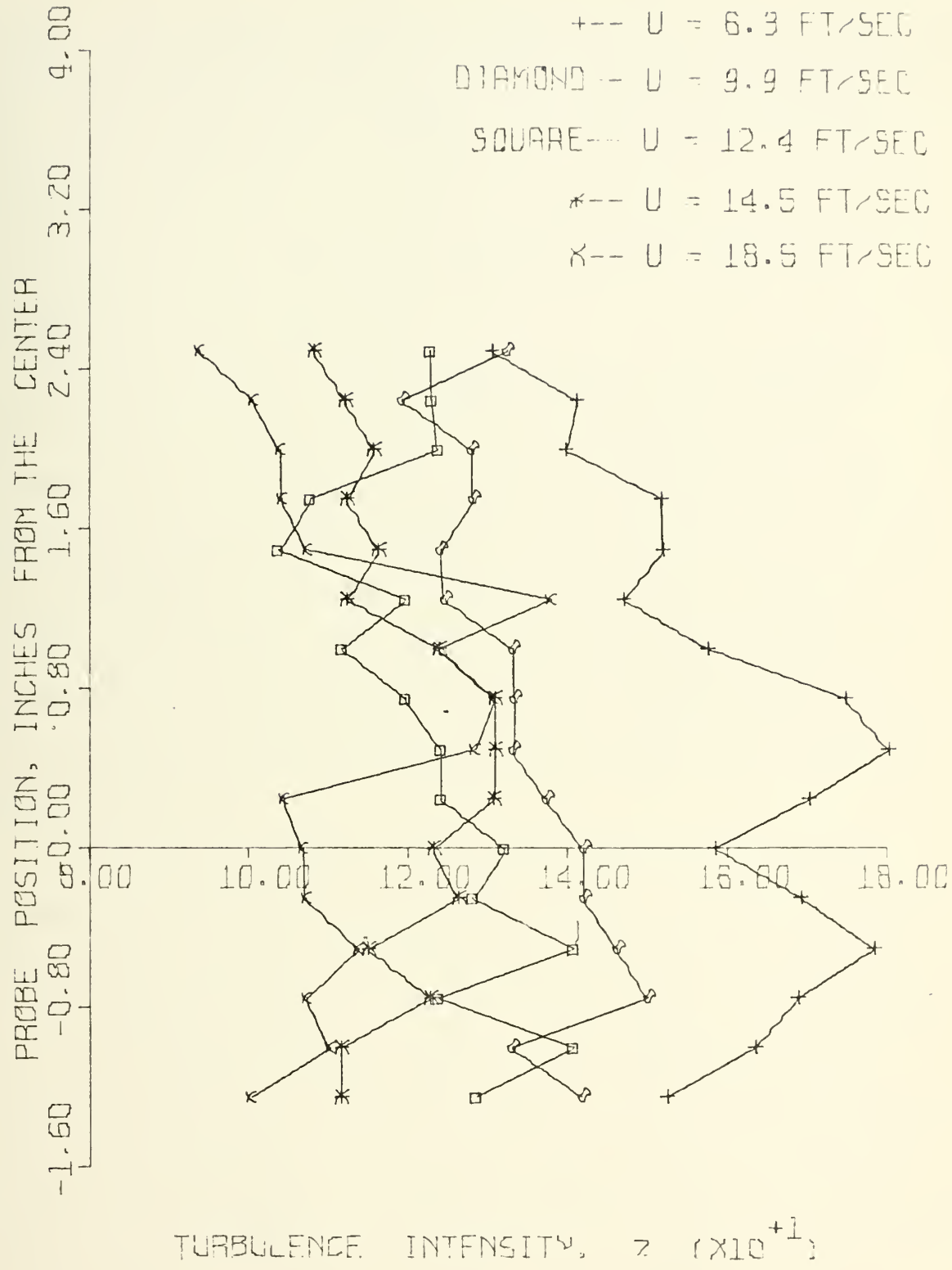

Figure 7: TURBULENCE INTENSITY PROFILE FOR TAP WATER AT X/DIAM = -3.5 FOR VARIOUS TEST SECTION VELOCITIES

section. The maximum turbulence intensity was found to be 1.8%, the minimum was found to be 0.9%, at the entrance. At the center of the test section, the turbulence intensity was found to be 1.5%.

C. MEASUREMENT OF TURBULENCE INTENSITY OF THE FLOW FIELD BEHIND ONE-INCH CYLINDER

The data obtained from the comprehensive investigation of the turbulence intensity of the flow field behind the one-inch cylinder is presented in Figs. 8 through 62. The turbulence intensity was measured at the location +1.0 X/DIAM and +1.5 X/DIAM, for Reynolds Numbers of 80,000, 100,000, 120,000, and 140,000. The turbulence intensity profiles were obtained for tap water and a range of degradations of 25 WPPM polymer solution with particular emphasis on the PDR range of 20% to 0%.

Figures 8 through 13 show the turbulence intensity profiles for tap water and 25 WPPM polymer solutions at 50% PDR, 14% PDR, 11% PDR, 7% PDR, 3% PDR, and 0% PDR, respectively, at a Reynolds Number of 80,000. The intensity characteristics of the polymer solution flow in the region outside the wake were found to be nearly identical to water flow turbulence intensity measurements. There was a small amount of suppression of the turbulence in the region +1.5 Y/DIAM to +0.75 Y/DIAM, at this X-position of +1.0 X/DIAM. This suppression was greatest at a PDR of 50% and decreased to no suppression at a PDR of 0%.

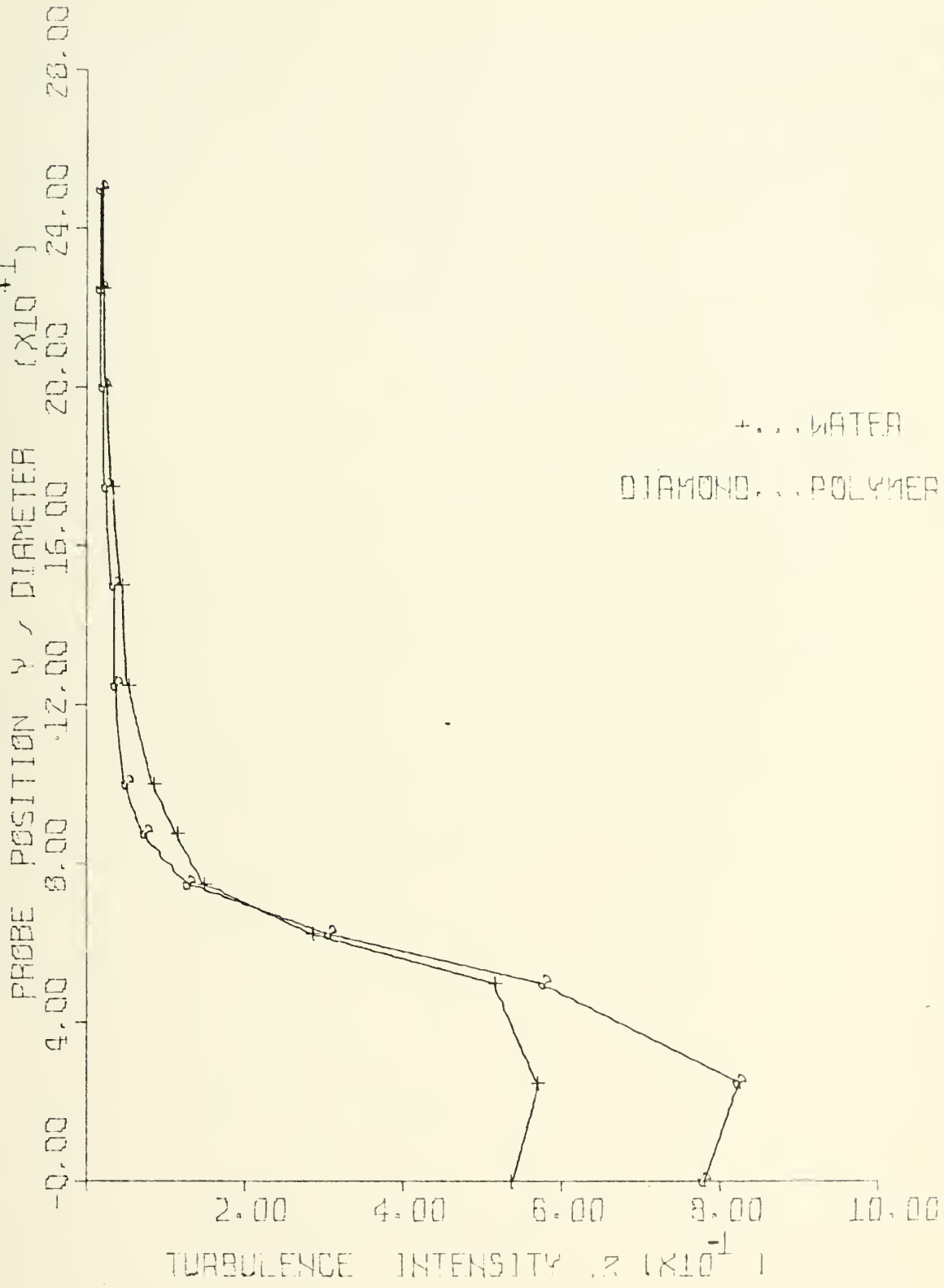

Figure 8: TURBULENCE INTENSITY PROFILES FOR TAP WATER AND 25 WPPM POLYMER SOLUTION, 50% PDR; RE No = 80,000; X/DIAM = +1.0

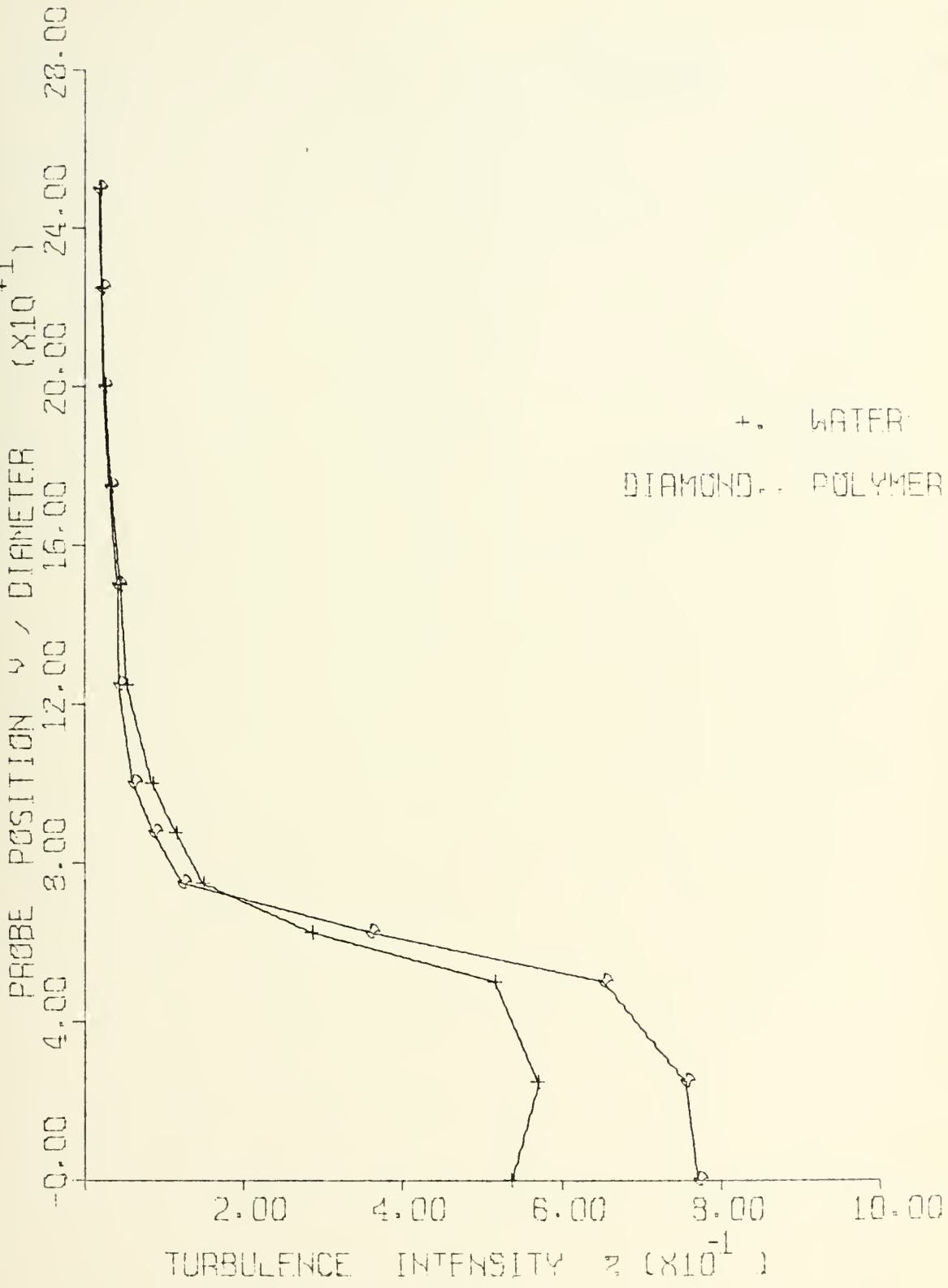

Figure 9: TURBULENCE INTENSITY PROFILES FOR TAP WATER AND 25 WPPM POLYMER SOLUTION, 14% PDR, RE No = 80,000; X/DIAM = +1.0

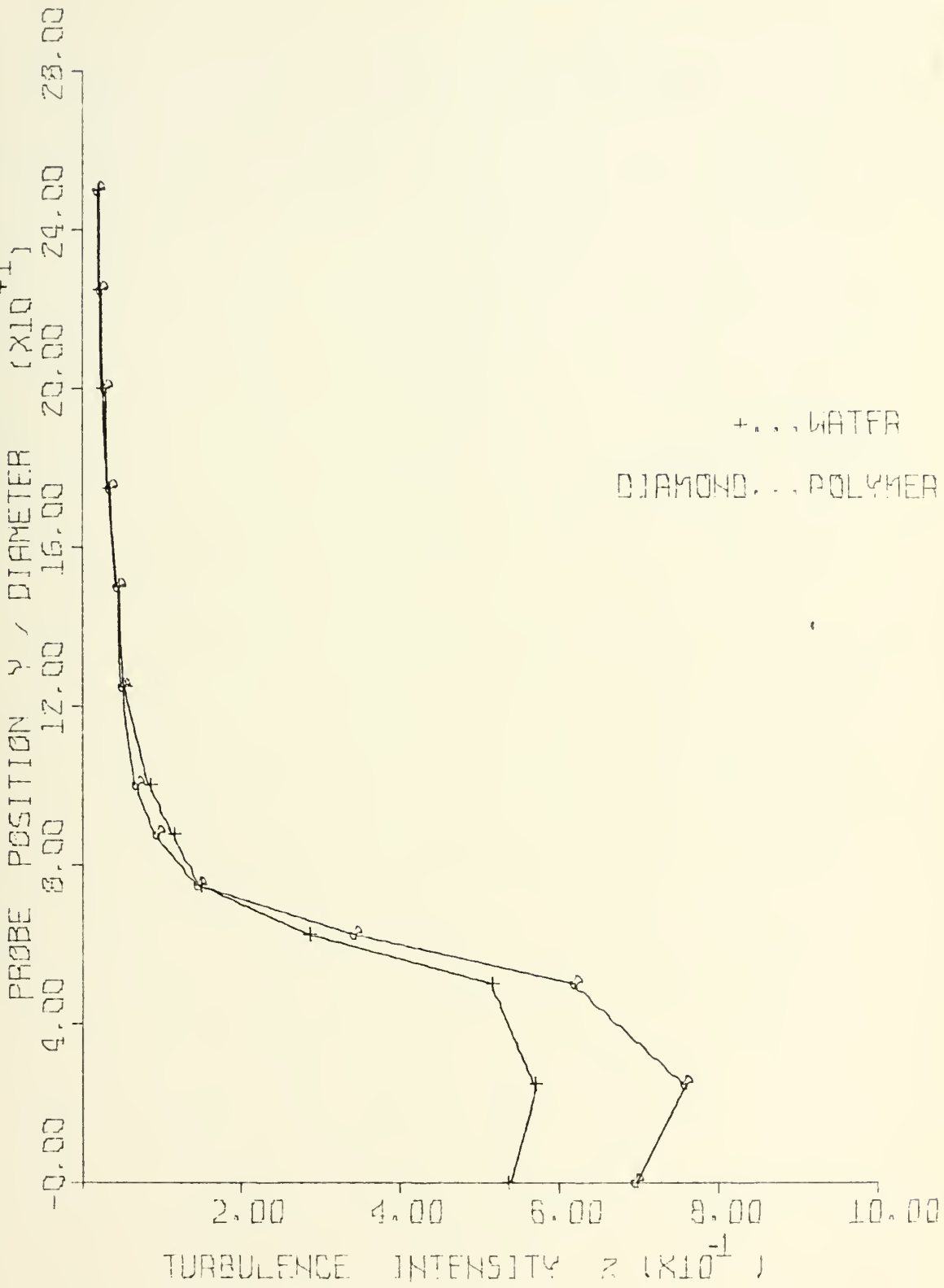

Figure 10: TURBULENCE INTENSITY PROFILES FOR TAP WATER AND 25 WPPM POLYMER SOLUTION, 11% PDR, RE No = 80,000; X/DIAM = +1.0

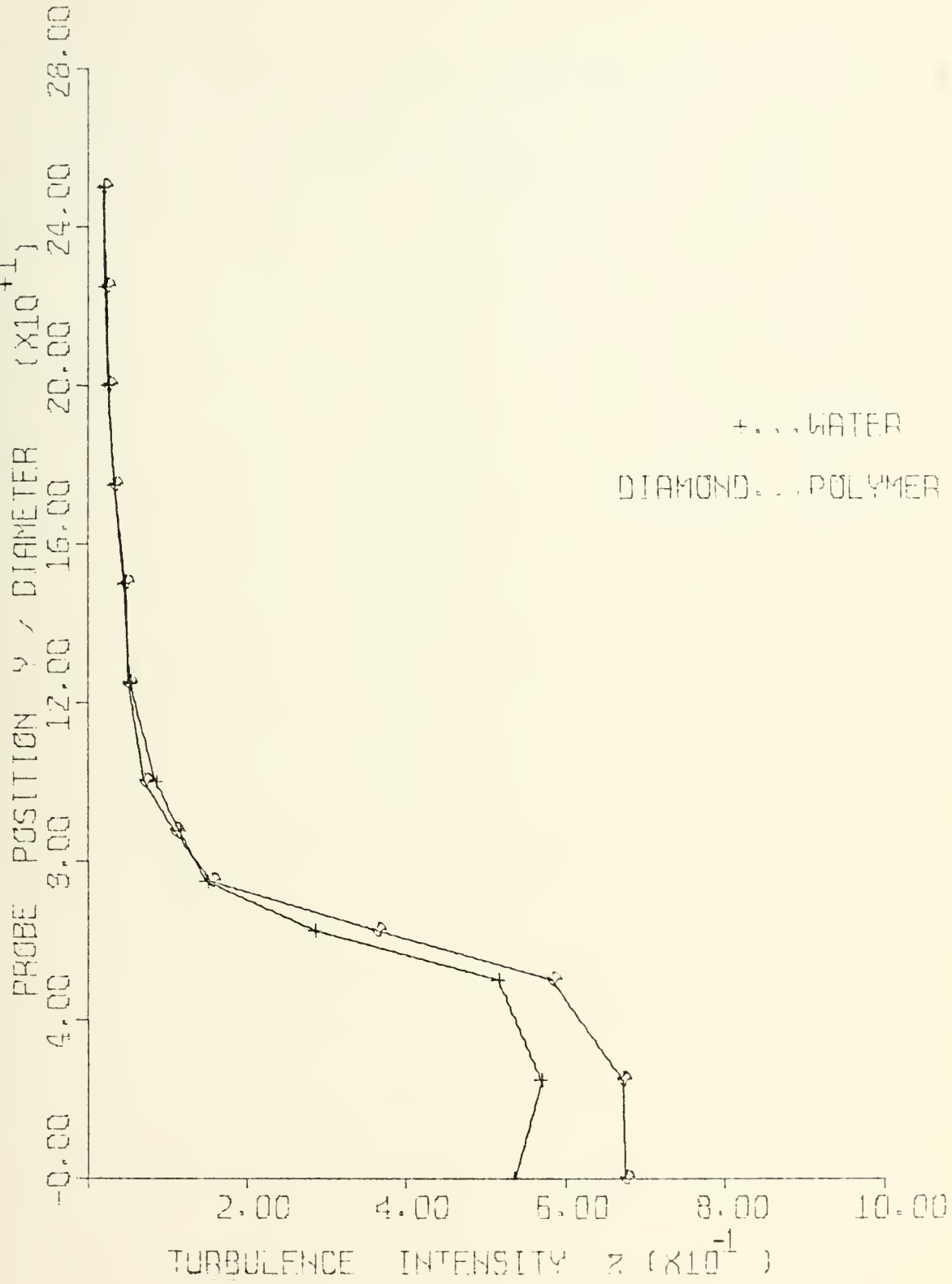

Figure 11: TURBULENCE INTENSITY PROFILES FOR TAP WATER AND 25 WPPM POLYMER SOLUTION, 7% PDR, RE No = 80,000; X/DIAM = + 1.0

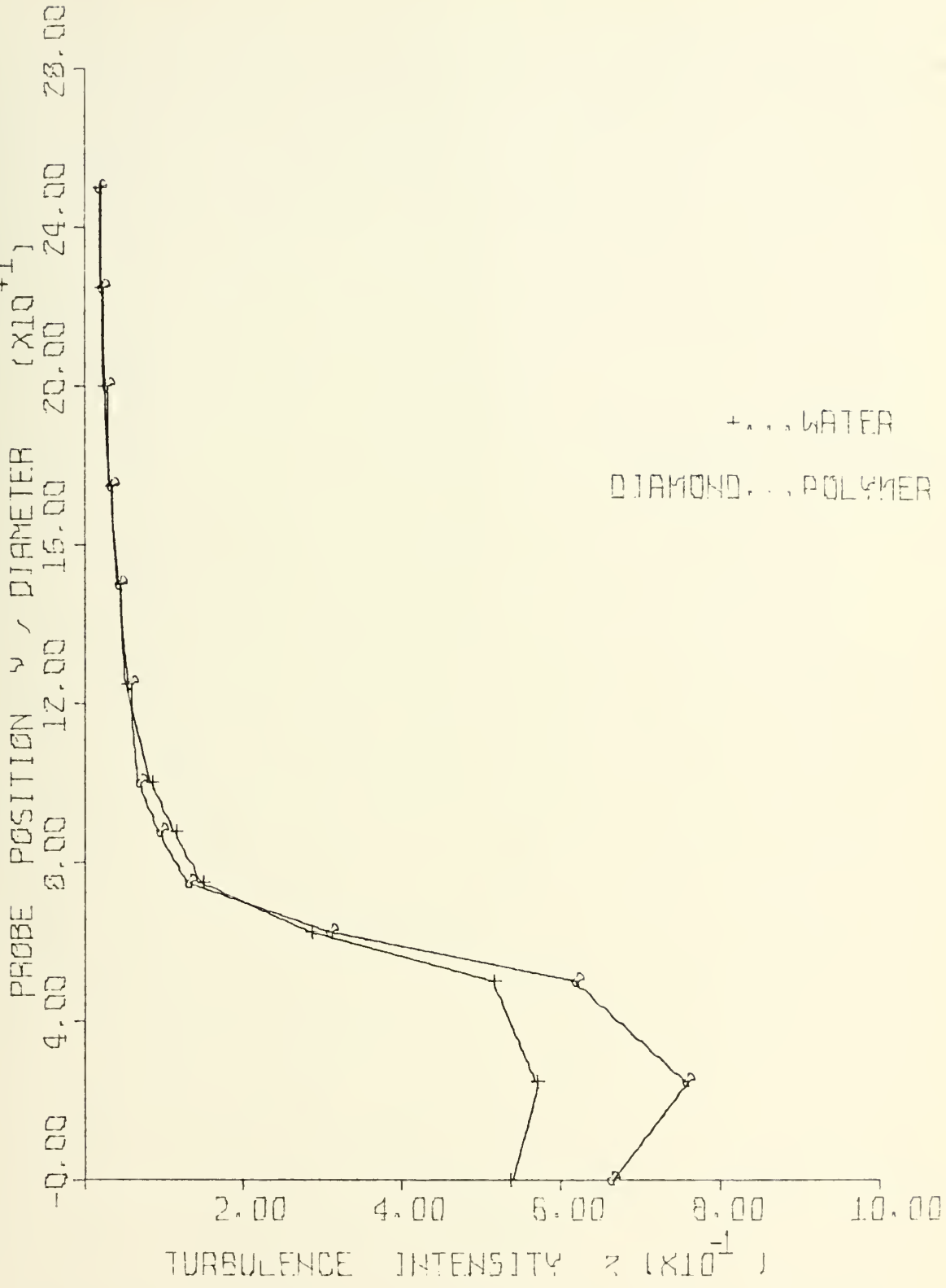

Figure 12: TURBULENCE INTENSITY PROFILES FOR TAP WATER AND 25 WPPM POLYMER SOLUTION, 3% PDR, RE No = 80,000; X/DIAM = +1.0

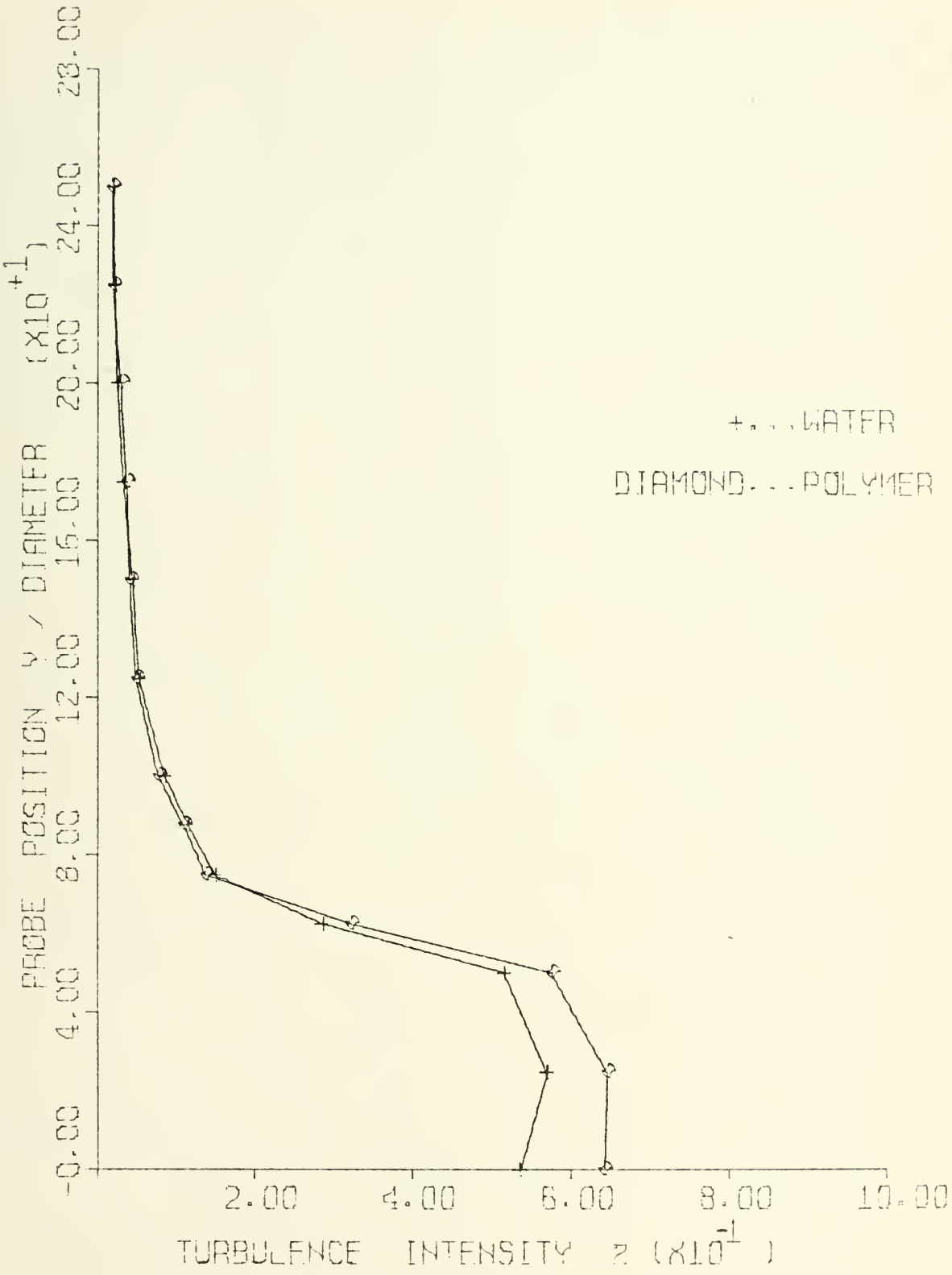

Figure 13: TURBULENCE INTENSITY PROFILES FOR TAP WATER AND 25 WPPM POLYMER SOLUTION, 0% PDR, RE No = 80,000; X/DIAM = +1.0

A marked difference in turbulence intensity was observed inside the wake at this Reynolds Number and X-coordinate of +1.0 X/DIAM. At a PDR of 50%, the turbulence intensity was found to be 40% greater than that observed in water flow measurements. This increase of turbulence intensity inside the wake region progressively decreased with PDR. At 0% PDR, the difference had diminished to 10%.

The turbulence intensity profiles of water and polymer solution at a Reynolds Number of 100,000 and an X-coordinate of +1.0 X/DIAM are presented in Figs. 14 through 19. The polymer solution profiles presented in these figures are for degradation states of 47% PDR, 14% PDR, 11% PDR, 7% PDR, 3% PDR, and 0% PDR, respectively. A significant suppression of turbulence intensity was observed outside the wake region, diminishing to no suppression at 0% PDR. Maximum suppression occurred at a PDR of 14%. At this PDR and Reynolds Number, the turbulence intensity in the region close to the wake (+1.0 Y/DIAM to +0.75 Y/DIAM) was half as great as for water flow. This indicated a reduction in the width of the wake. This reduction is further substantiated by the high-frequency velocity spike observations to be presented later.

As observed at the lower Reynolds Number of 80,000, the turbulence intensity in the wake region was found to be greater for polymer solution than for water. The maximum difference was observed at 14% PDR. At this degradation state, the turbulence intensity was found to be 90% greater for

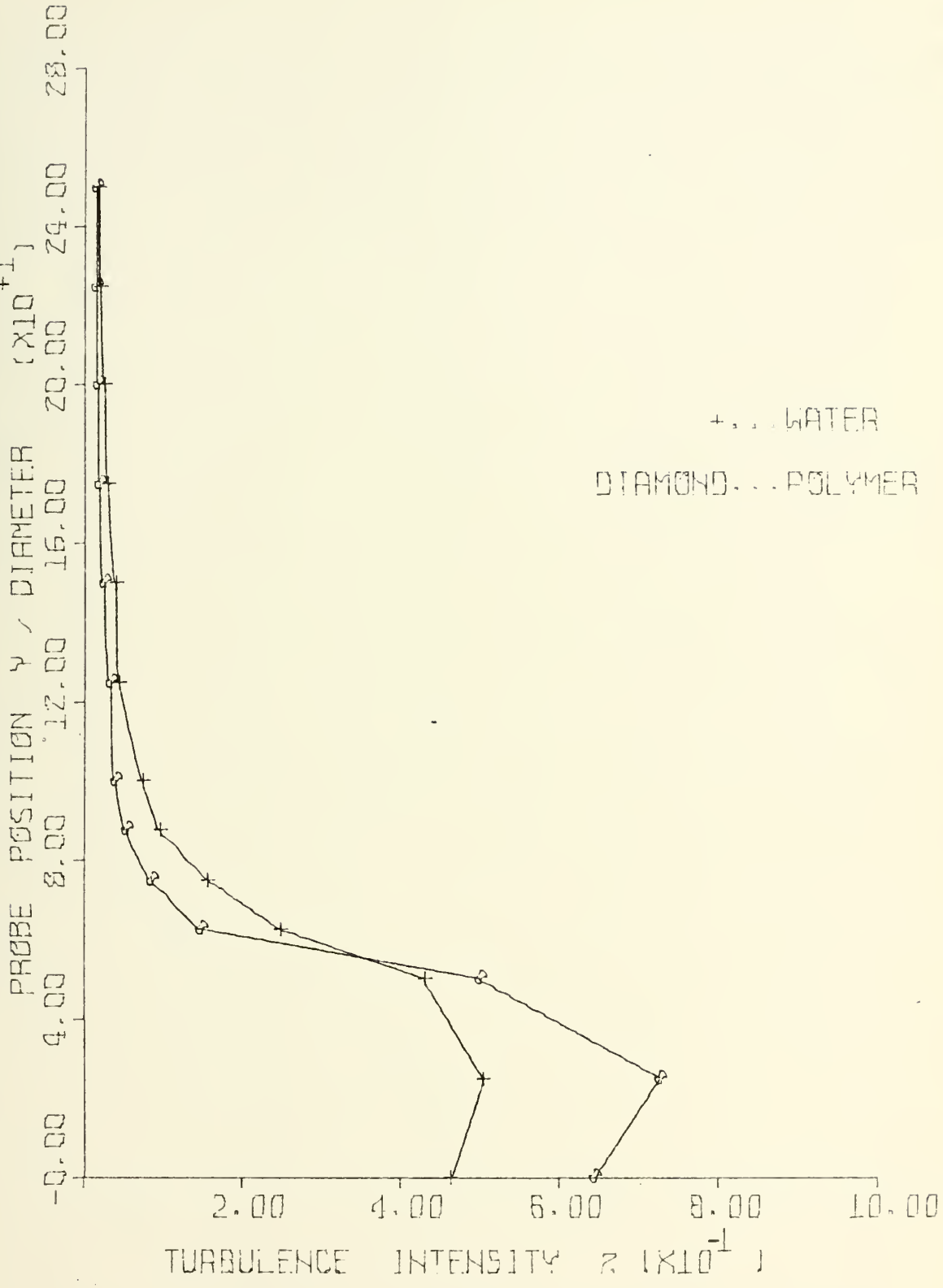

Figure 14: TURBULENCE INTENSITY PROFILES FOR TAP WATER AND 25 WPPM POLYMER SOLUTION, 47% PDR; RE No = 100,000; X/DIAM = +1.0

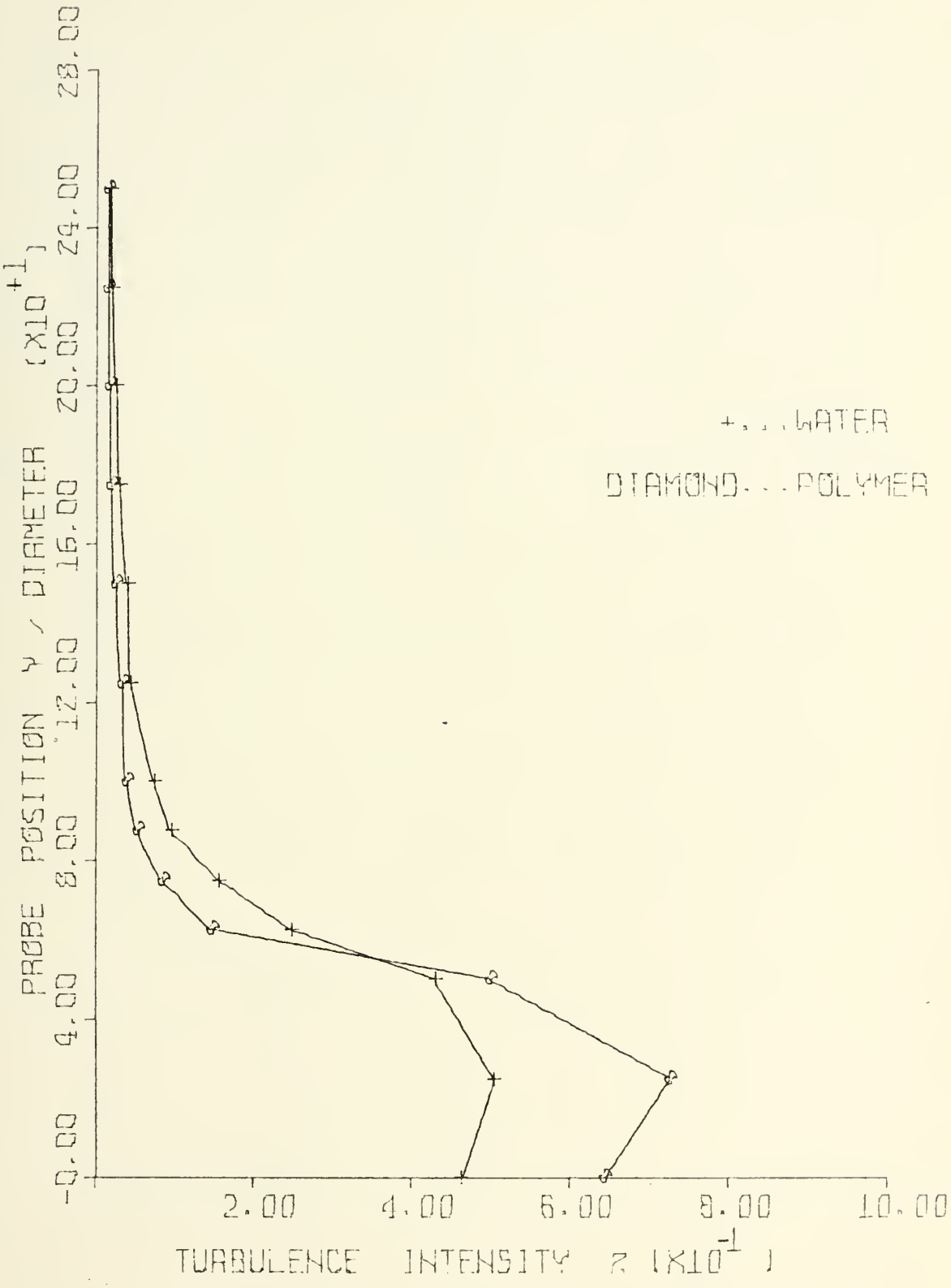

Figure 14: TURBULENCE INTENSITY PROFILES FOR TAP WATER AND 25 WPPM POLYMER SOLUTION, 47% PDR; RE No = 100,000; X/DIAM = +1.0

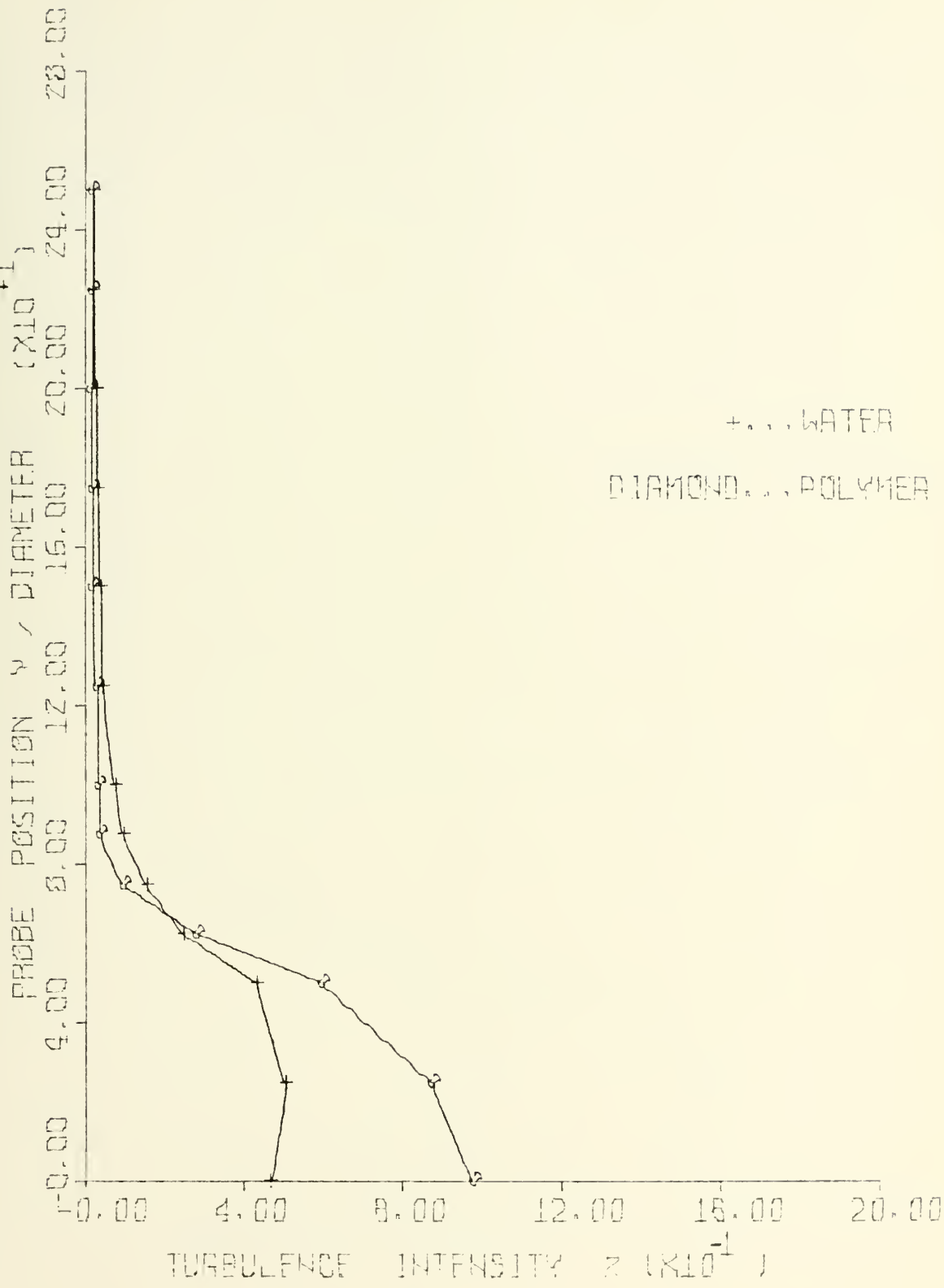

Figure 15: TURBULENCE INTENSITY PROFILES FOR TAP WATER AND 25 WPPM POLYMER SOLUTION, 14% PDR; RE No = 100,000; X/DIAM = +1.0

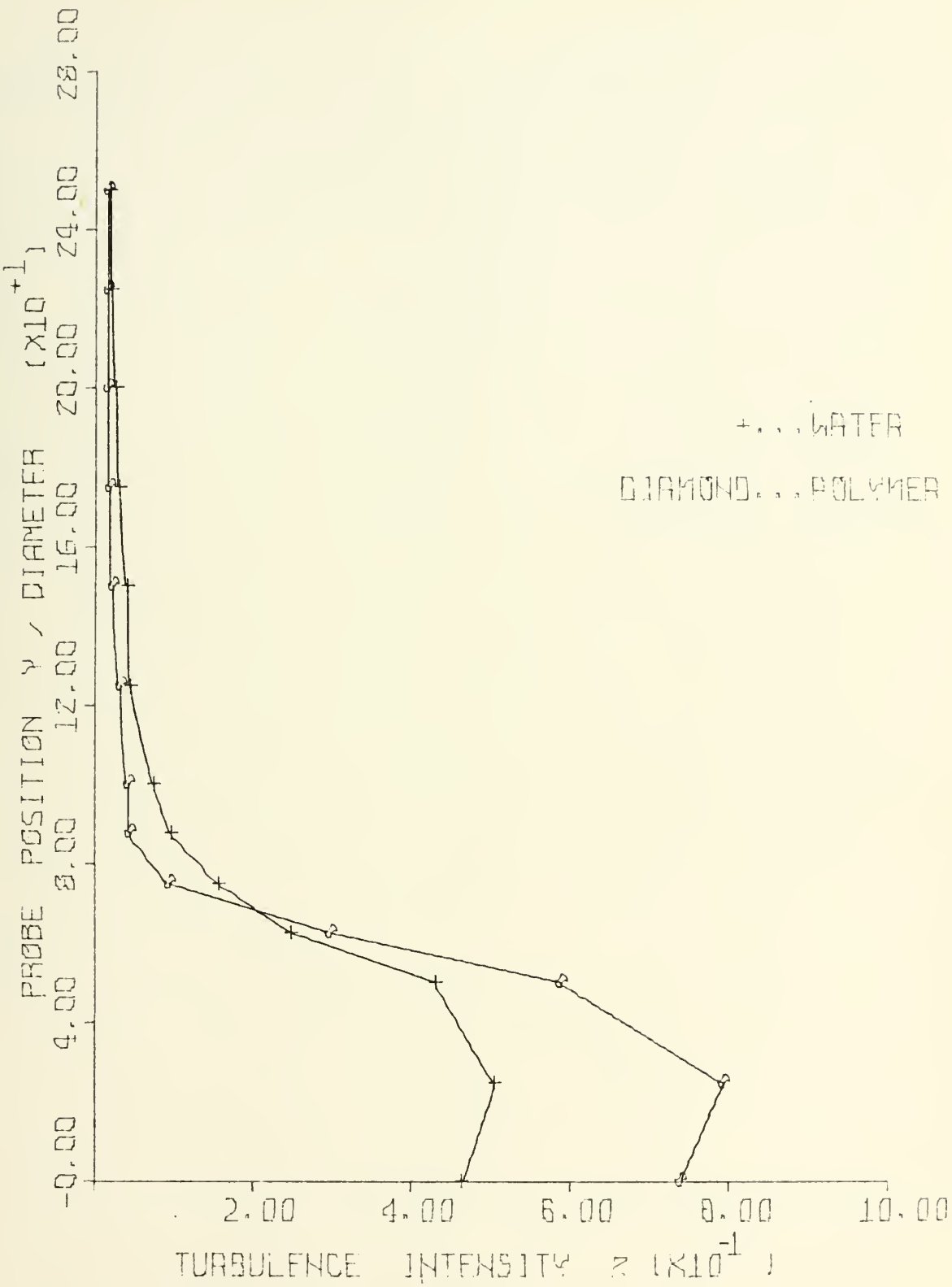

Figure 16: TURBULENCE INTENSITY PROFILES FOR TAP WATER AND 25 WPPM POLYMER SOLUTION, 11% PDR, RE No = 100,000; X/DIAM = +1.0

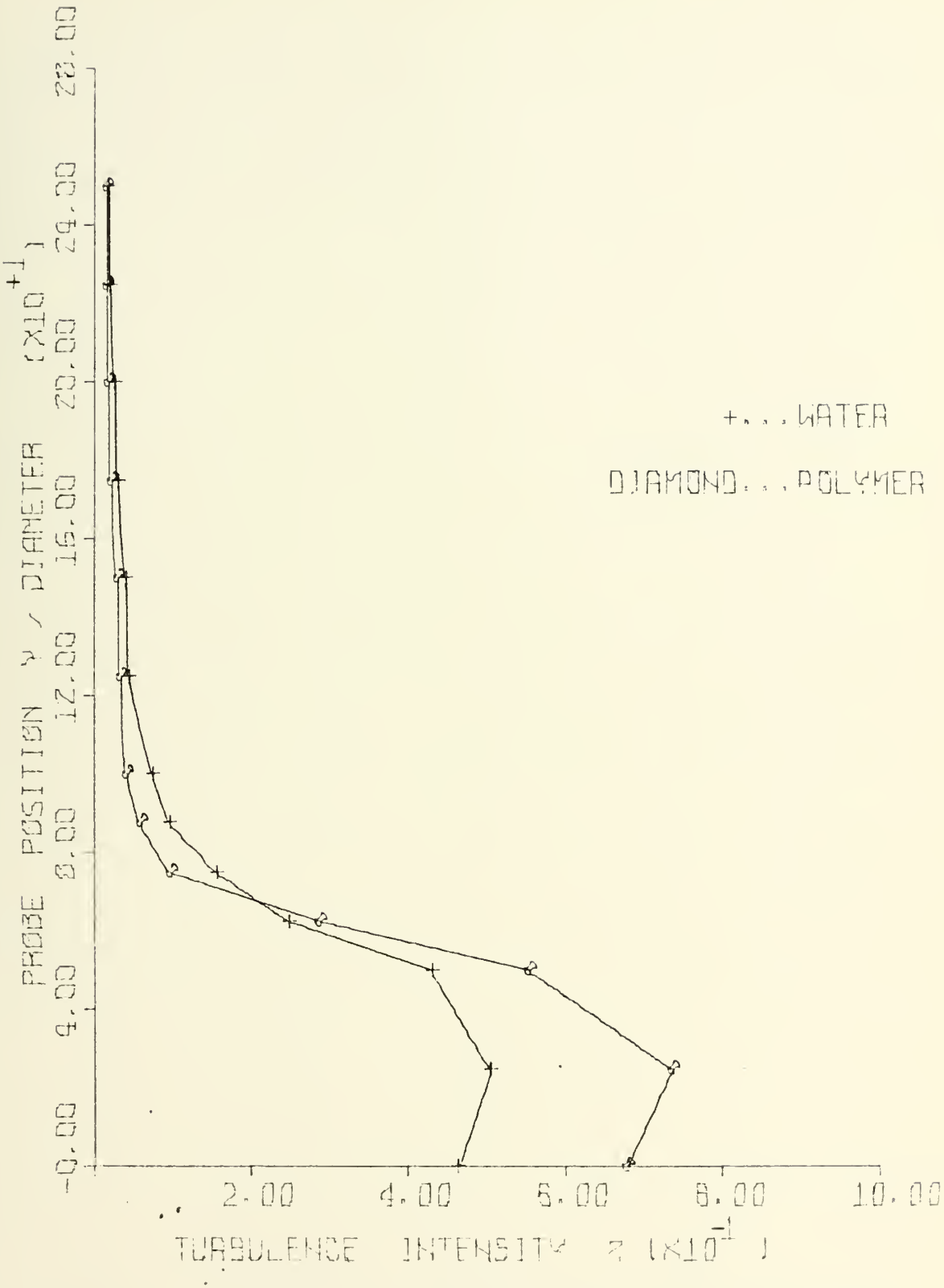

Figure 17: TURBULENCE INTENSITY PROFILES FOR TAP WATER AND 25 WPPM POLYMER SOLUTION, 7% PDR; RE No = 100,000; X/DIAM = +1.0

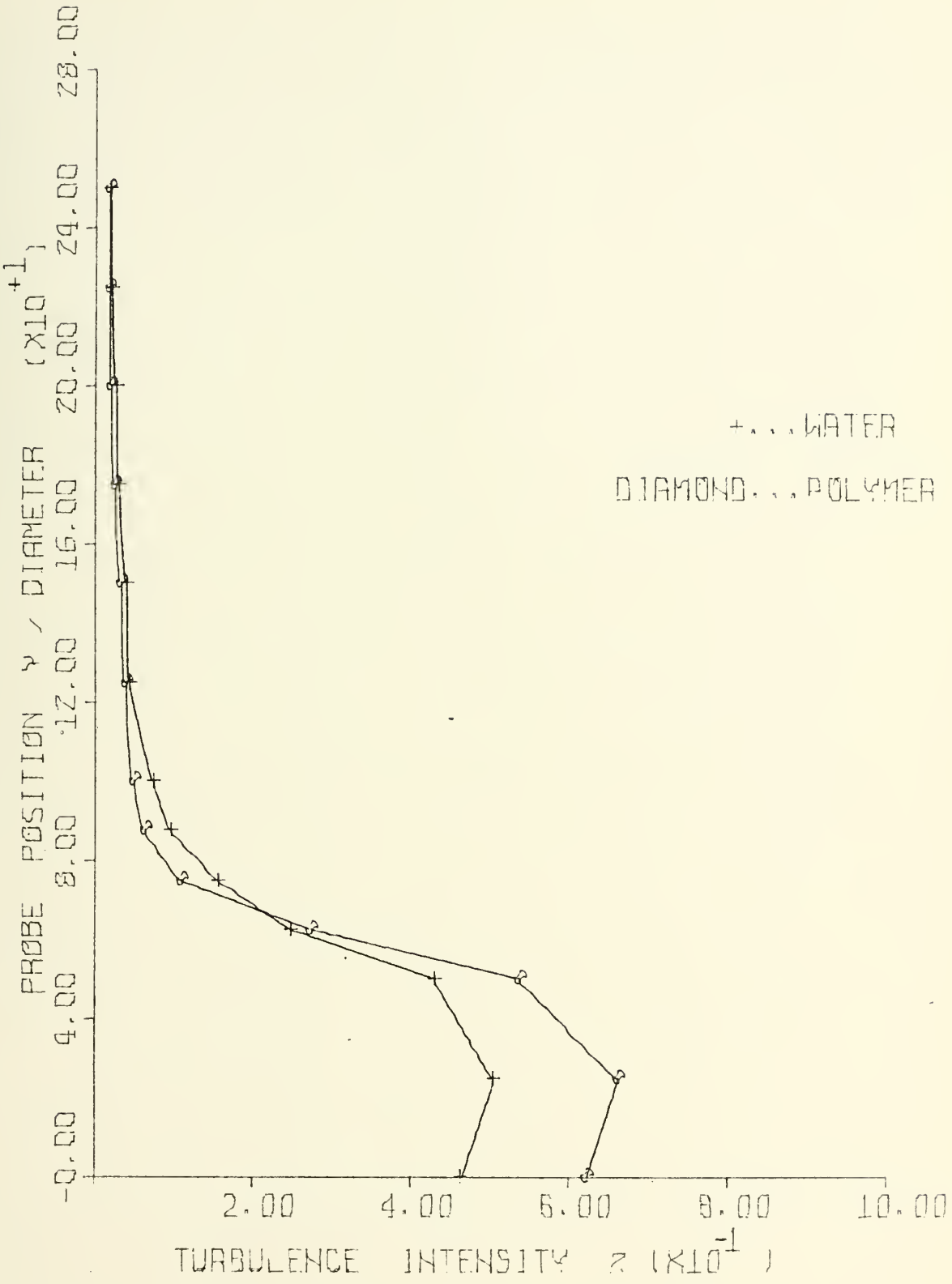

Figure 18: TURBULENCE INTENSITY PROFILES FOR TAP WATER AND 25 WPPM POLYMER SOLUTION, 3% PDR; RE No = 100,000; X/DIAM = +1.0

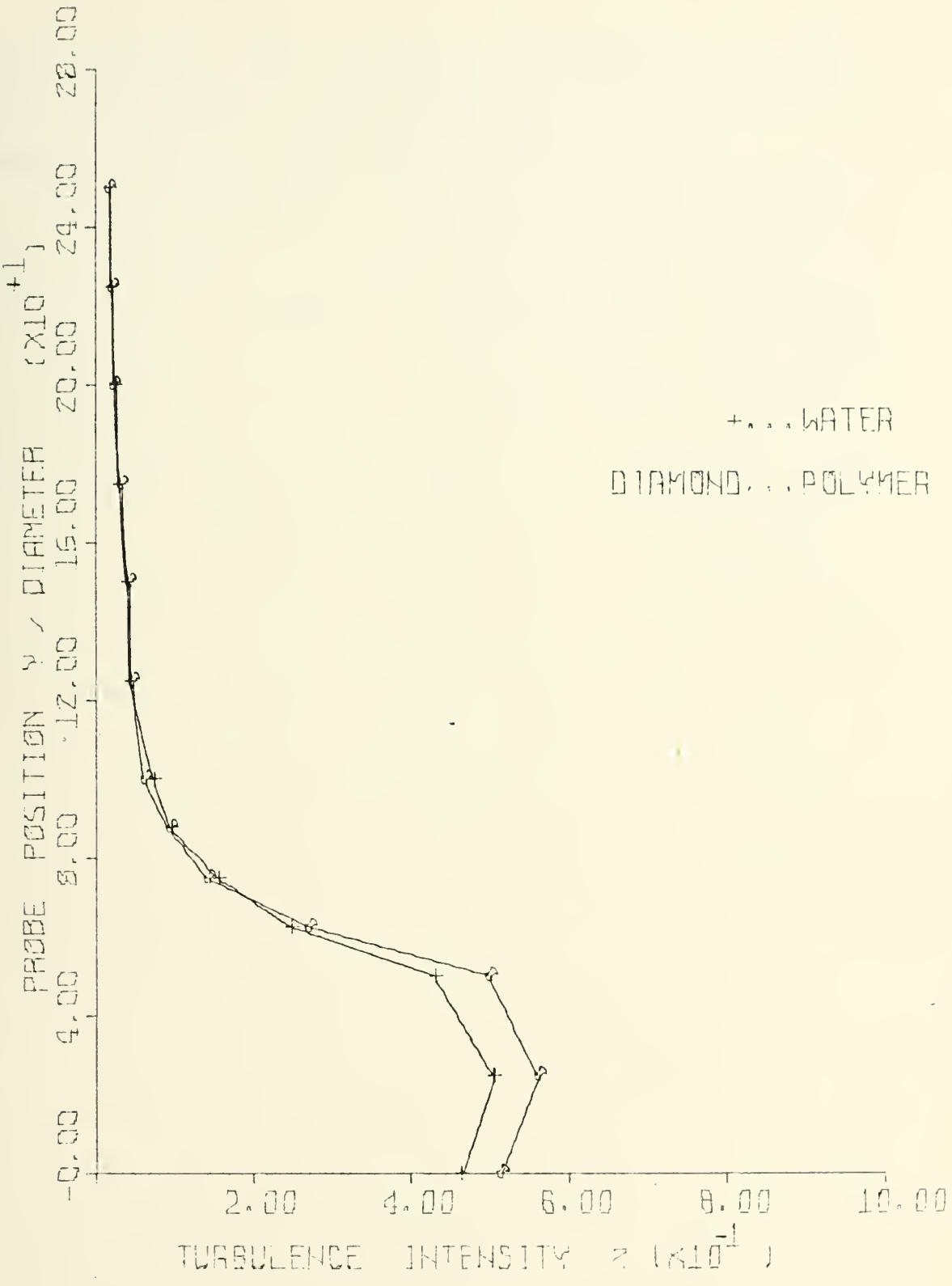

Figure 19: TURBULENCE INTENSITY PROFILES FOR TAP WATER AND 25 WPPM POLYMER SOLUTION, 0% PDR; RE No = 100,000; X/DIAM = +1.0

polymer solution. The difference decreased with PDR. at 0% PDR, the polymer solution registered a 10% increase in turbulence intensity over that observed in water.

The turbulence intensity profiles for water and polymer solution at a Reynolds Number of 120,000 and an X-coordinate of +1.0 X/DIAM are presented in Figs. 20 through 25. The polymer solution profiles presented in these figures are for degradation states of 45% PDR, 14% PDR, 10% PDR, 7% PDR, 3% PDR, and 0% PDR, respectively. Extremely large reductions in turbulence intensity were observed outside the wake region at this Reynolds Number, which indicated a suppression of the wake. The maximum suppression of turbulence intensity outside the wake region occurred at a PDR of 10%. In the region of +1.25 Y/DIAM to +0.50 Y/DIAM, the turbulence intensity was diminished to 33% of the value observed in water flow. The difference progressively increased from that observed at 45% PDR to the maximum and then decreased to that observed at 0% PDR. At 0% PDR, the turbulence intensity had attained 74% of the value observed with water flow.

A great increase of turbulence intensity was observed in the wake at this Reynolds Number. At 45% PDR, the intensity inside the wake was 42% greater than that observed in water flow. A maximum was observed at a PDR of 14%. At this degradation state, the increase was 180% at the center of the wake. The difference progressively diminished with PDR. Large differences were still observed at 3% PDR. At 0% PDR, the difference was 36%.

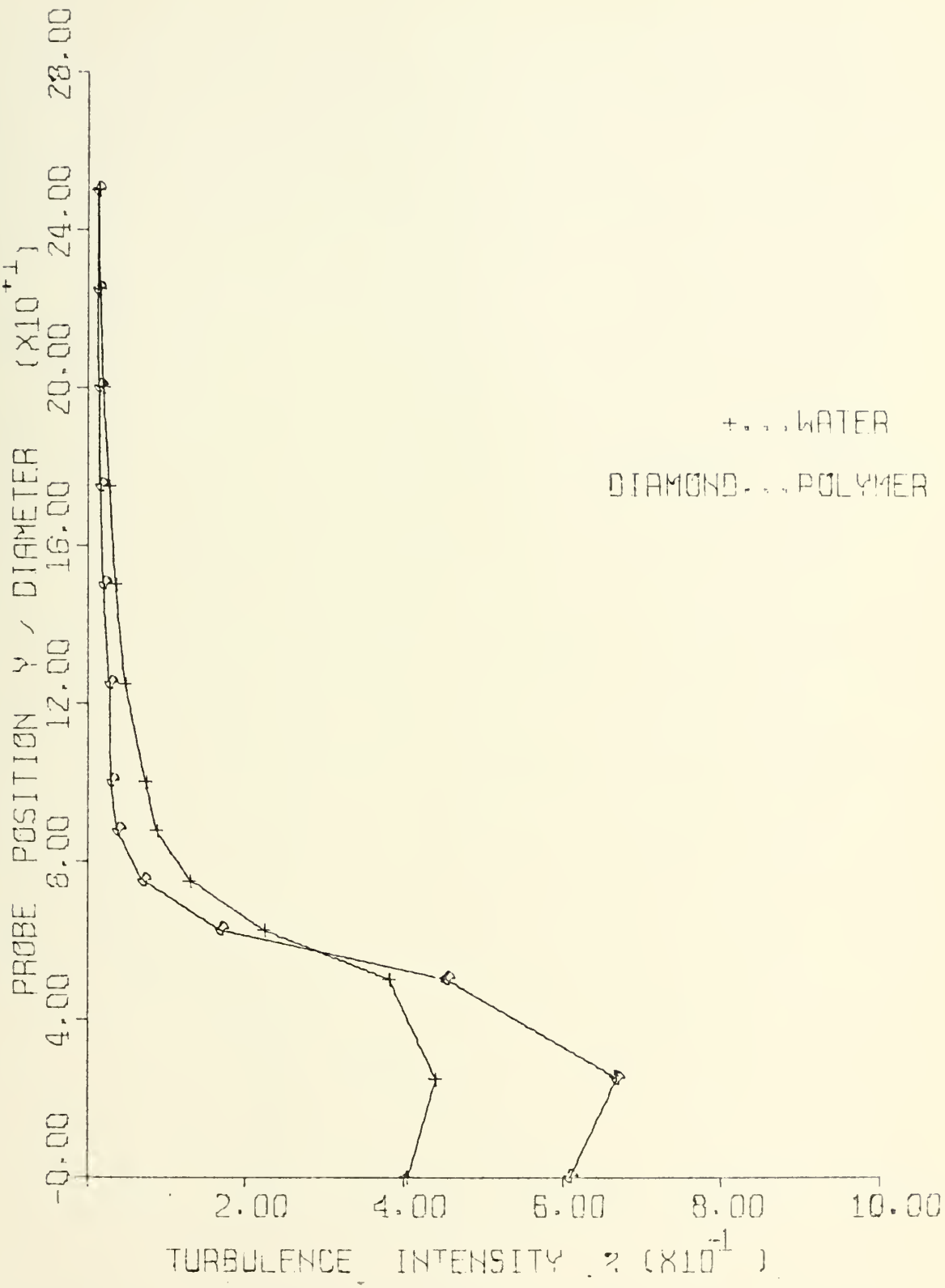

Figure 20: TURBULENCE INTENSITY PROFILES FOR TAP WATER AND 25 WPPM POLYMER SOLUTION, 45% PDR; RE No = 120,000; X/DIAM = +1.0

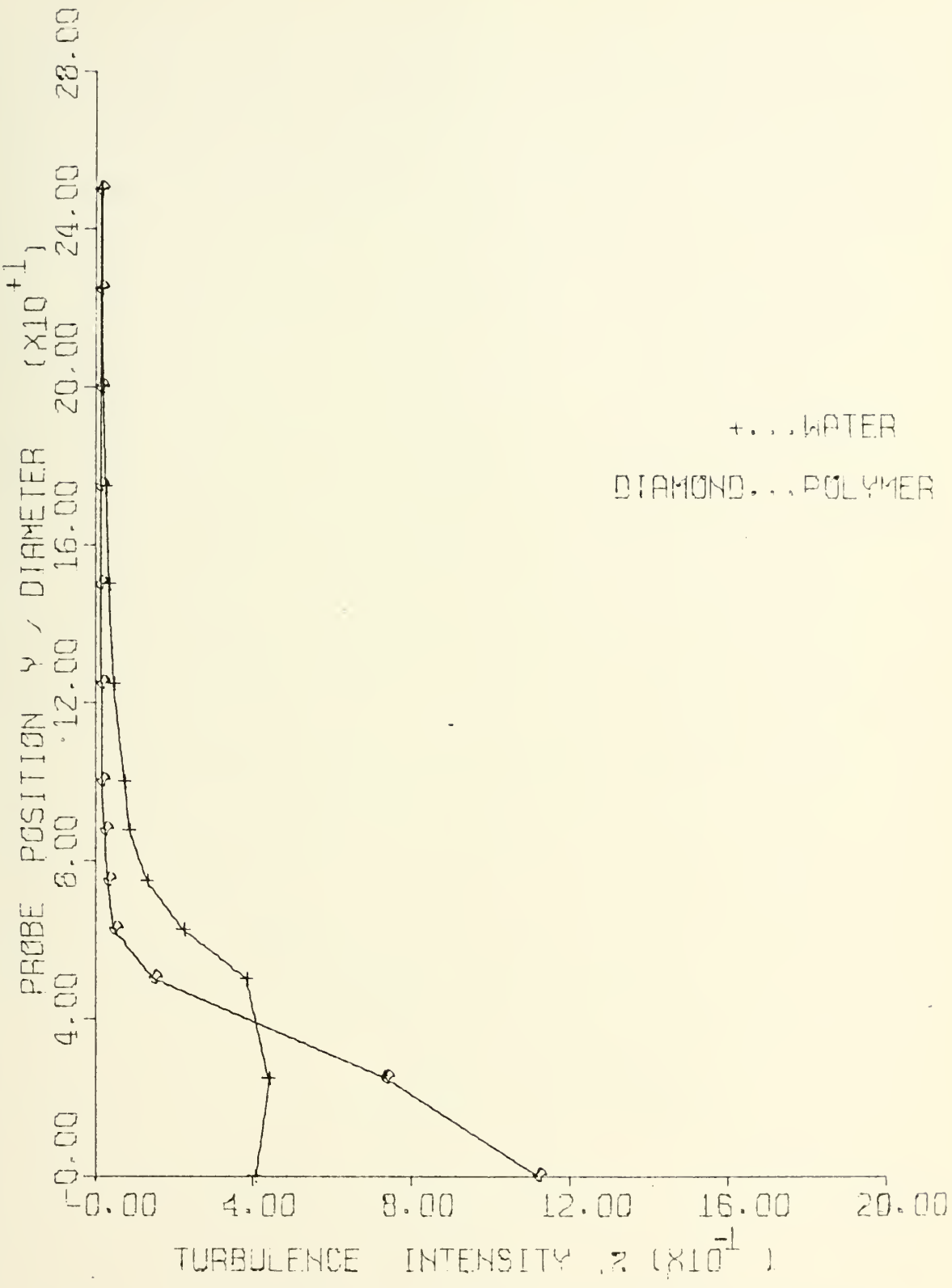

Figure 21: TURBULENCE INTENSITY PROFILES FOR TAP WATER AND 25 WPPM POLYMER SOLUTION, 14% PDR; RE No = 120,000; X/DIAM = +1.0

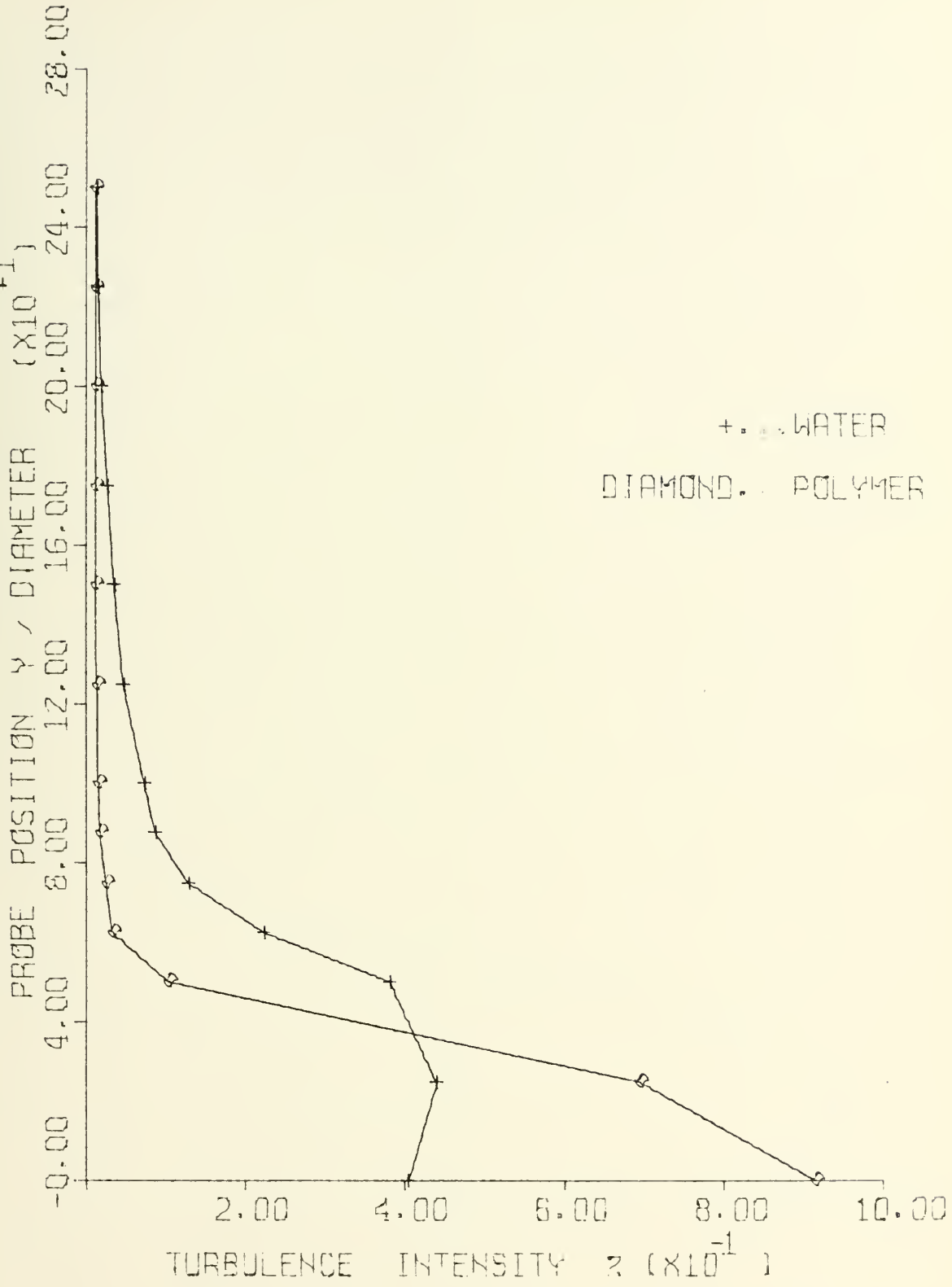

Figure 22: TURBULENCE INTENSITY PROFILES FOR TAP WATER AND 25 WPPM POLYMER SOLUTION, 10% PDR; RE No = 120,000; X/DIAM = +1.0

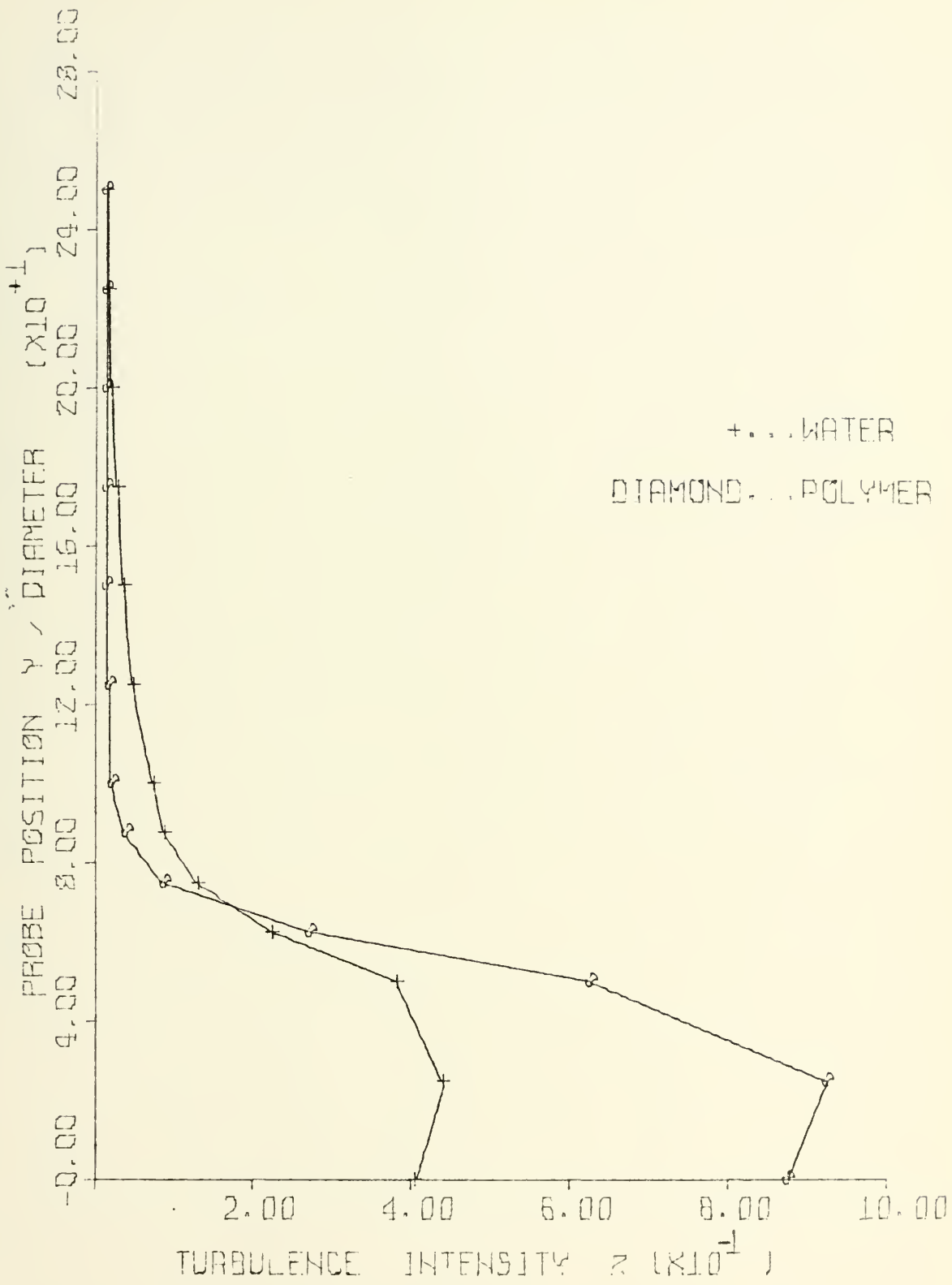

Figure 23: TURBULENCE INTENSITY PROFILES FOR TAP WATER AND 25 WPPM POLYMER SOLUTION, 7% PDR; RE No = 120,000; X/DIAM = +1.0

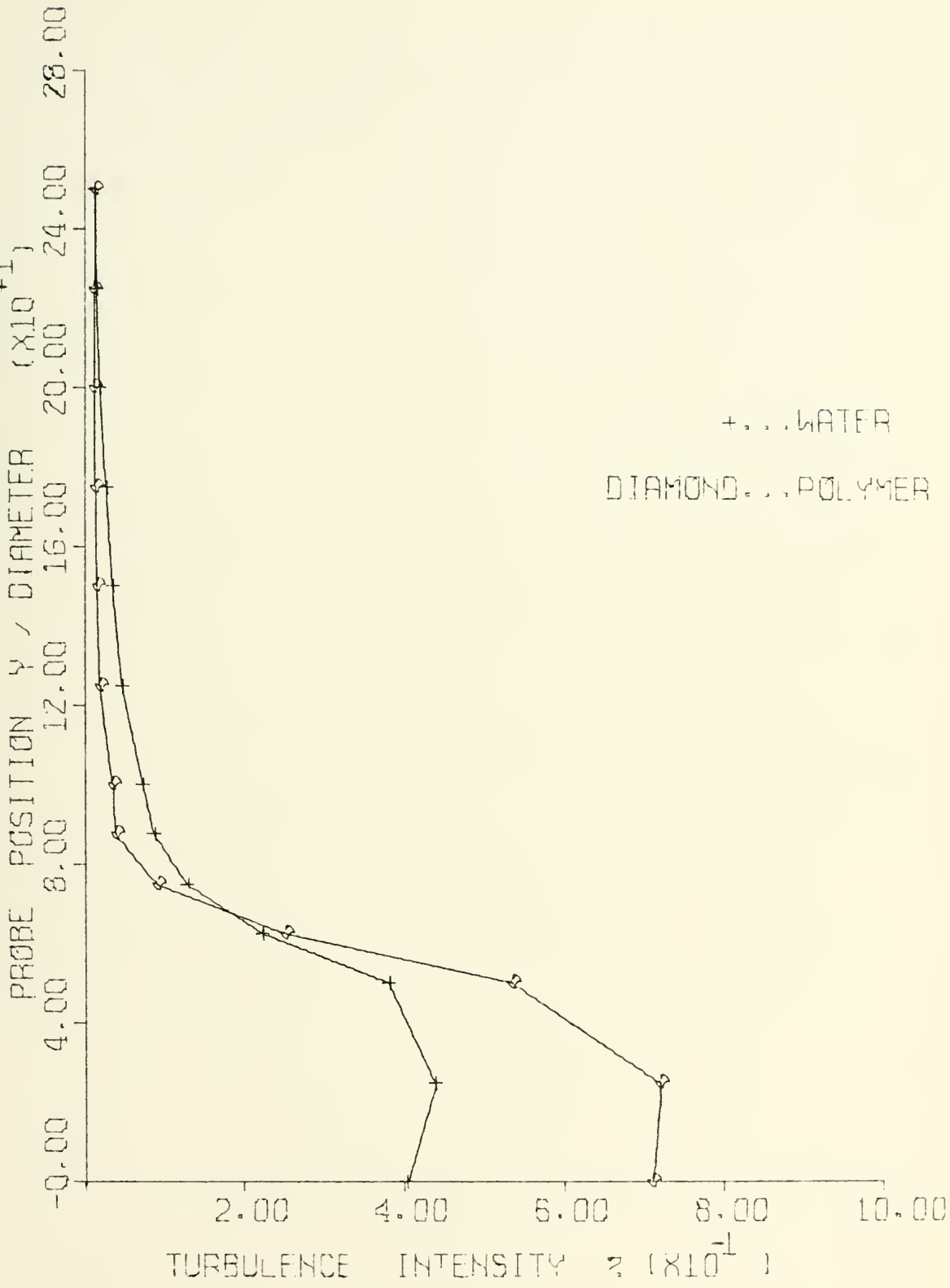

Figure 24: TURBULENCE INTENSITY PROFILES FOR TAP WATER AND 25 WPPM POLYMER SOLUTION, 3% PDR; RE No = 120,000; X/DIAM = +1.0

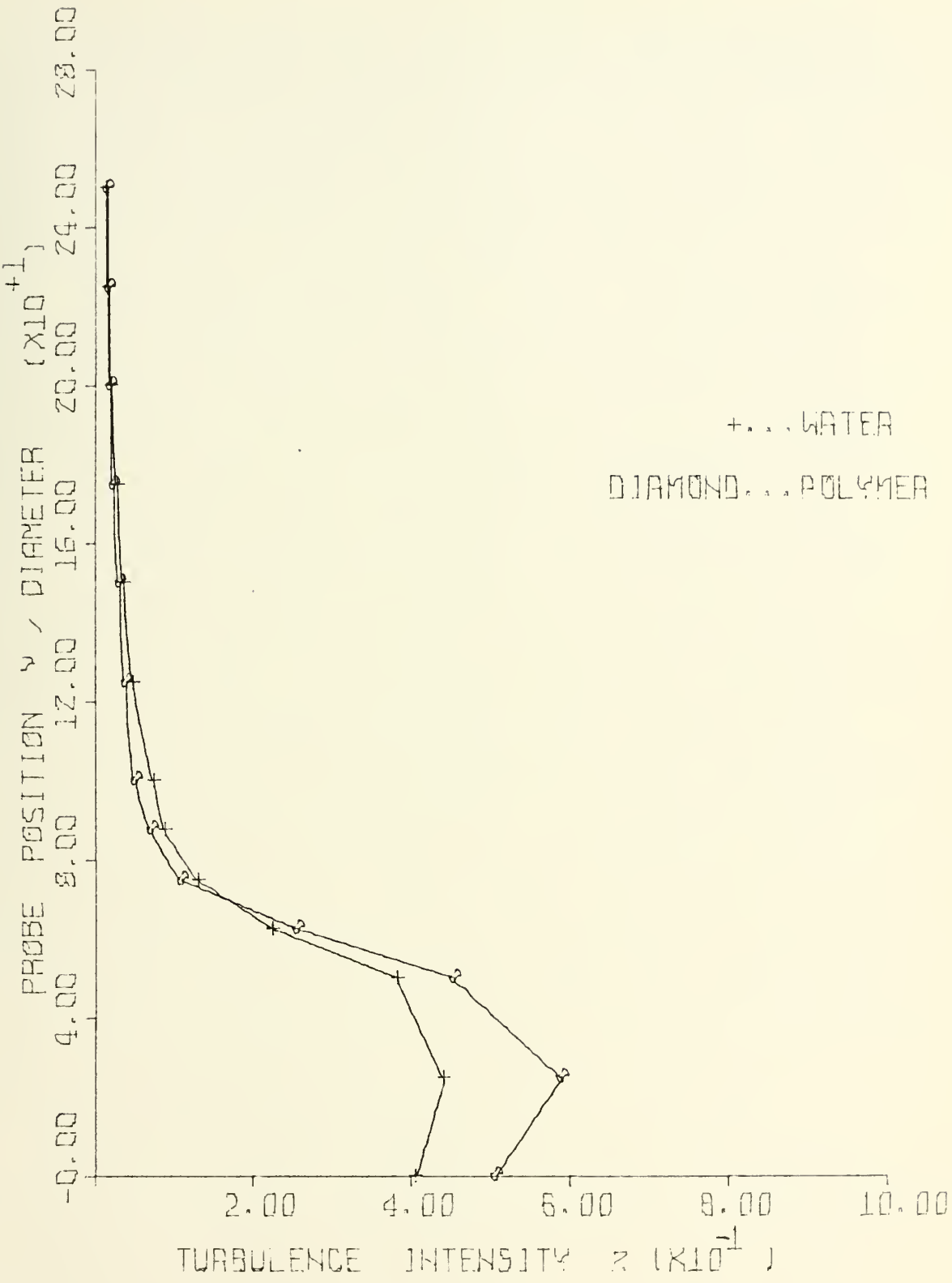

Figure 25: TURBULENCE INTENSITY PROFILES FOR TAP WATER AND 25 WPPM POLYMER SOLUTION, 0% PDR; RE No = 120,000; X/DIAM = +1.0

The turbulence intensity profiles for water and polymer solution at a Reynolds Number of 140,000 and an X-coordinate of +1.0 X/DIAM are presented in Figs. 26 through 31. The polymer solution profiles presented in these figures are for degradation states of 43% PDR, 14% PDR, 10% PDR, 7% PDR, 3% PDR, and 0% PDR, respectively. Again, extremely large reductions in turbulence intensity were observed outside the wake region. The maximum suppression was observed at a PDR of 7%. At this PDR, the turbulence intensity was 18% of that observed in water flow in the region +1.0 Y/DIAM to +0.50 Y/DIAM, indicating a large suppression of the wake. The turbulence intensity in this region then progressively increased with PDR. At 0% PDR, the turbulence intensity was 71% of the value observed with water flow in this region.

The turbulence intensities inside the wake region again increased in polymer solution flow. The maximum increase was observed at 14% PDR. The increase was found to be 140% over that observed in water flow at the center of the wake. The difference again diminished with PDR, with large differences still being observed at 3% PDR. At 0% PDR, the differences had decreased to 35% at the center of the wake.

Turbulence intensity profiles were also measured at the position +1.5 X/DIAM. Water data and polymer solution data are presented in the same manner as for previous profiles.

Turbulence intensity profiles for water and polymer solution at an X-coordinate of +1.5 X/DIAM and a Reynolds Number of 80,000 are presented in Figs. 32 through 37. The

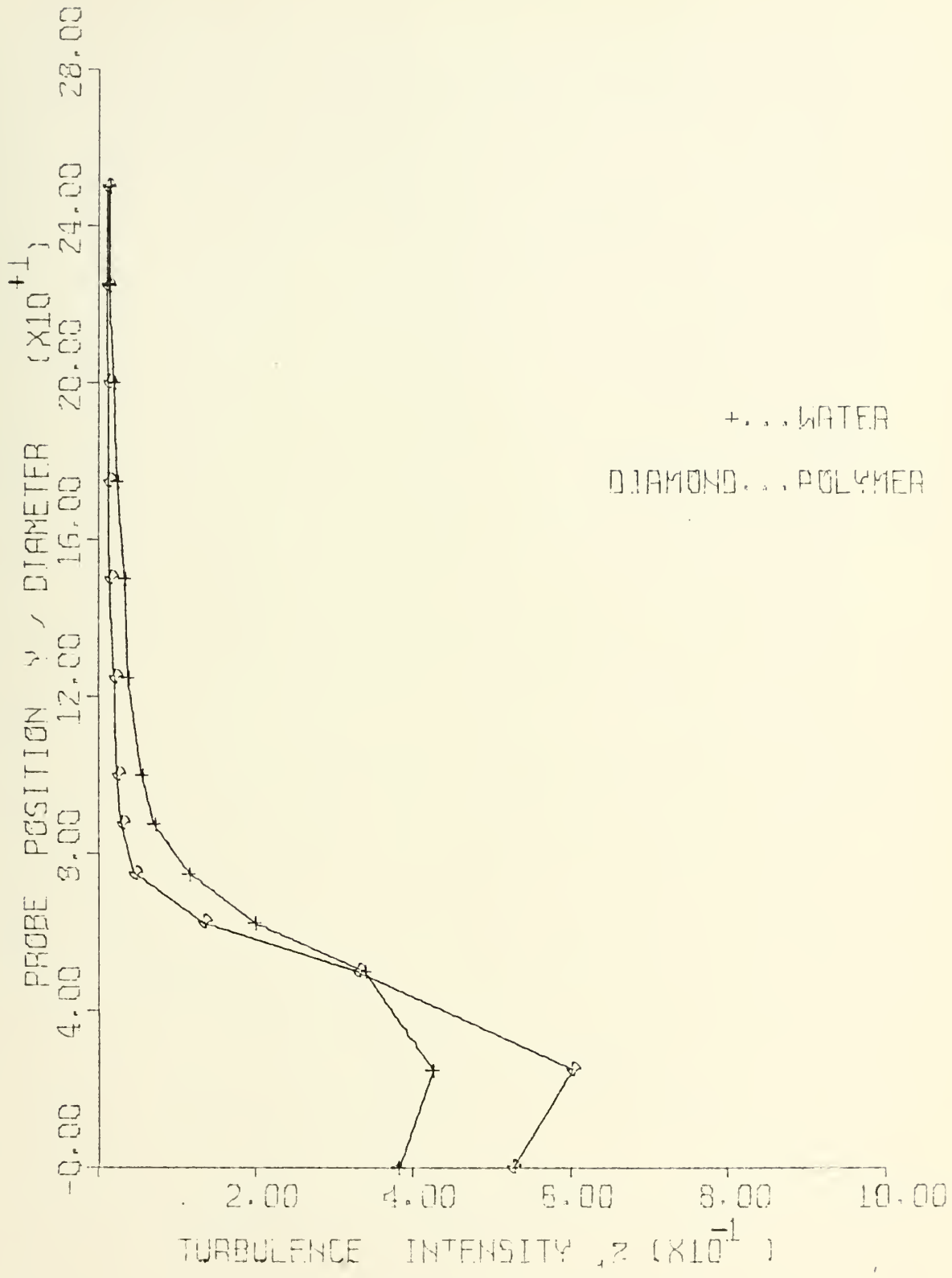

Figure 26: TURBULENCE INTENSITY PROFILES FOR TAP WATER AND 25 WPPM POLYMER SOLUTION, 43% PDR; RE No = 140,000; X/DIAM = +1.0

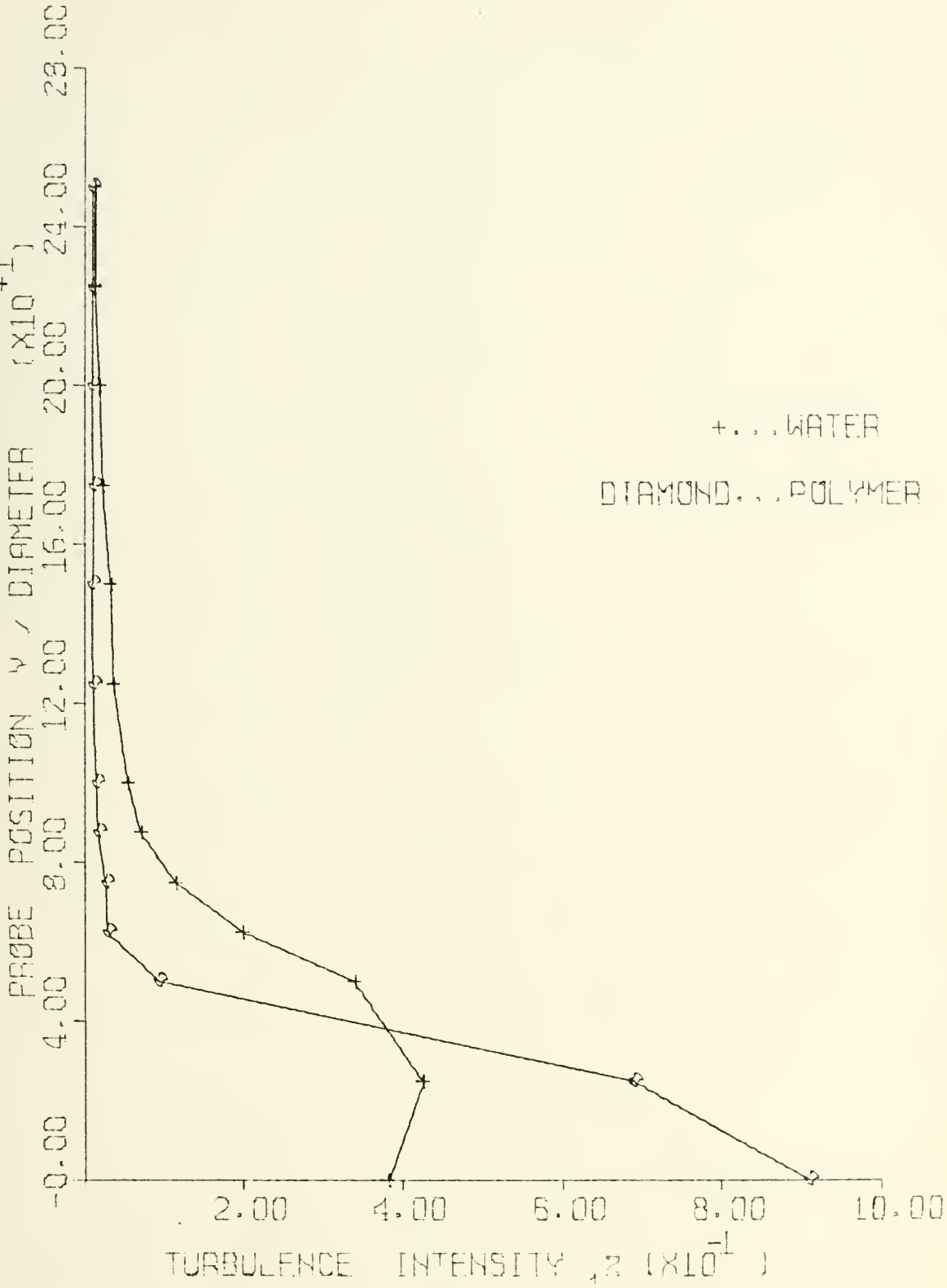

Figure 27: TURBULENCE INTENSITY PROFILES FOR TAP WATER AND 25 WPPM POLYMER SOLUTION, 14% PDR; RE No = 140,000; X/DIAM = +1.0

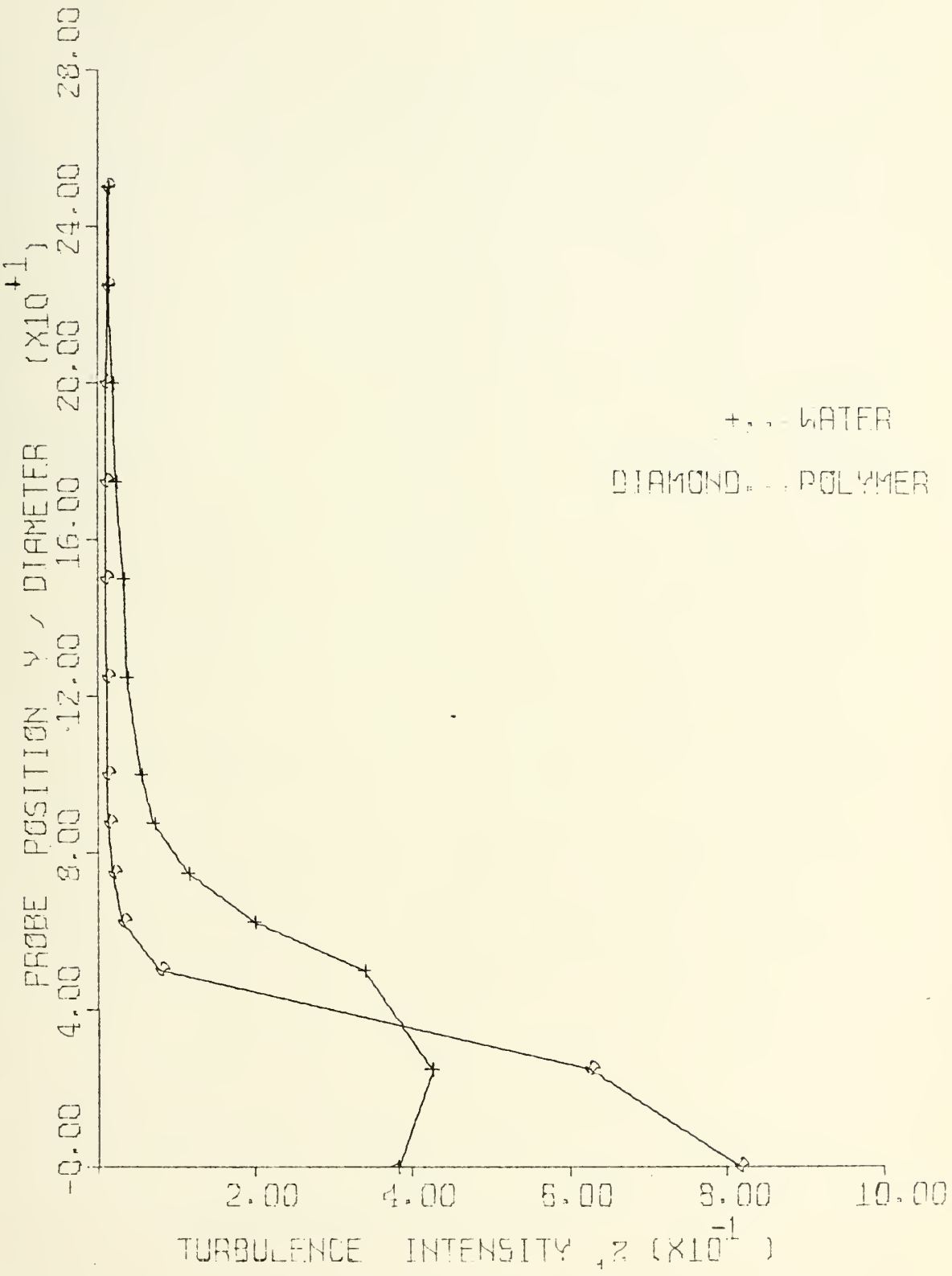

Figure 28: TURBULENCE INTENSITY PROFILES FOR TAP WATER AND 25 WPPM POLYMER SOLUTION, 10% PDR; RE No = 140,000; X/DIAM = +1.0

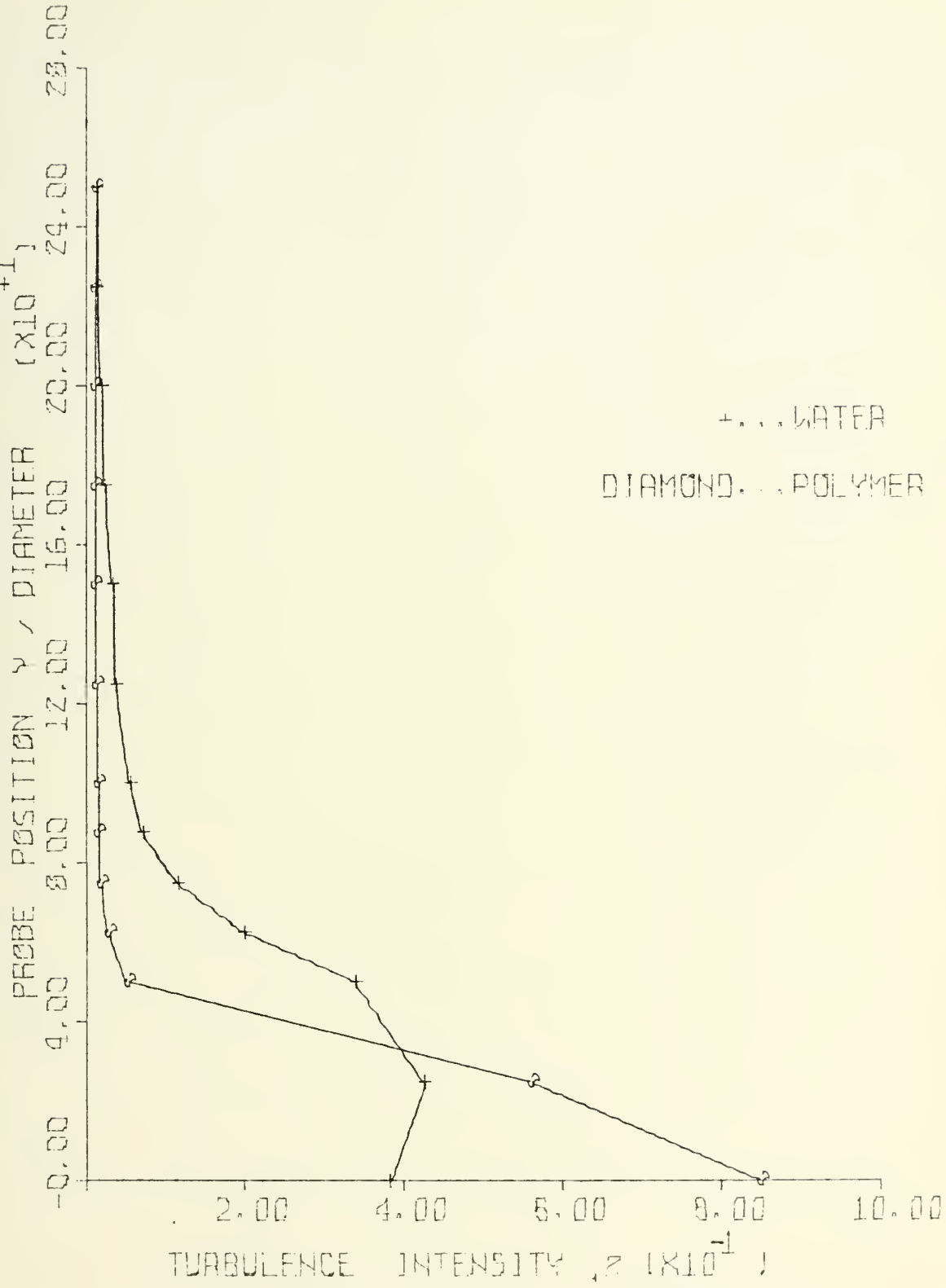

Figure 29: TURBULENCE INTENSITY PROFILES FOR TAP WATER AND 25 WPPM POLYMER SOLUTION, 7% PDR; RE No = 140,000; X/DIAM = +1.0

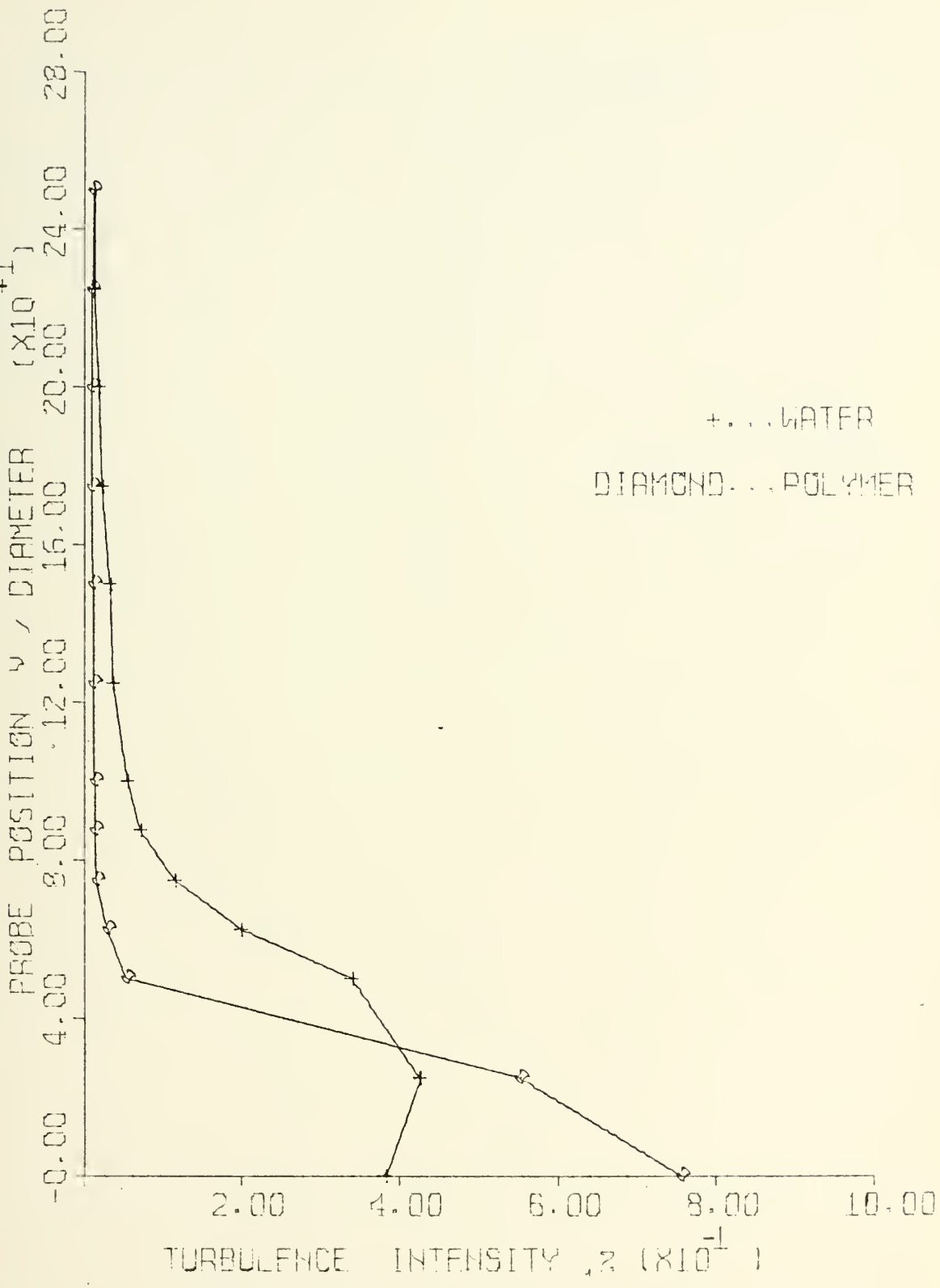

Figure 30: TURBULENCE INTENSITY PROFILES FOR TAP WATER AND 25 WPPM POLYMER SOLUTION, 3% PDR; RE No = 140,000; X/DIAM = +1.0

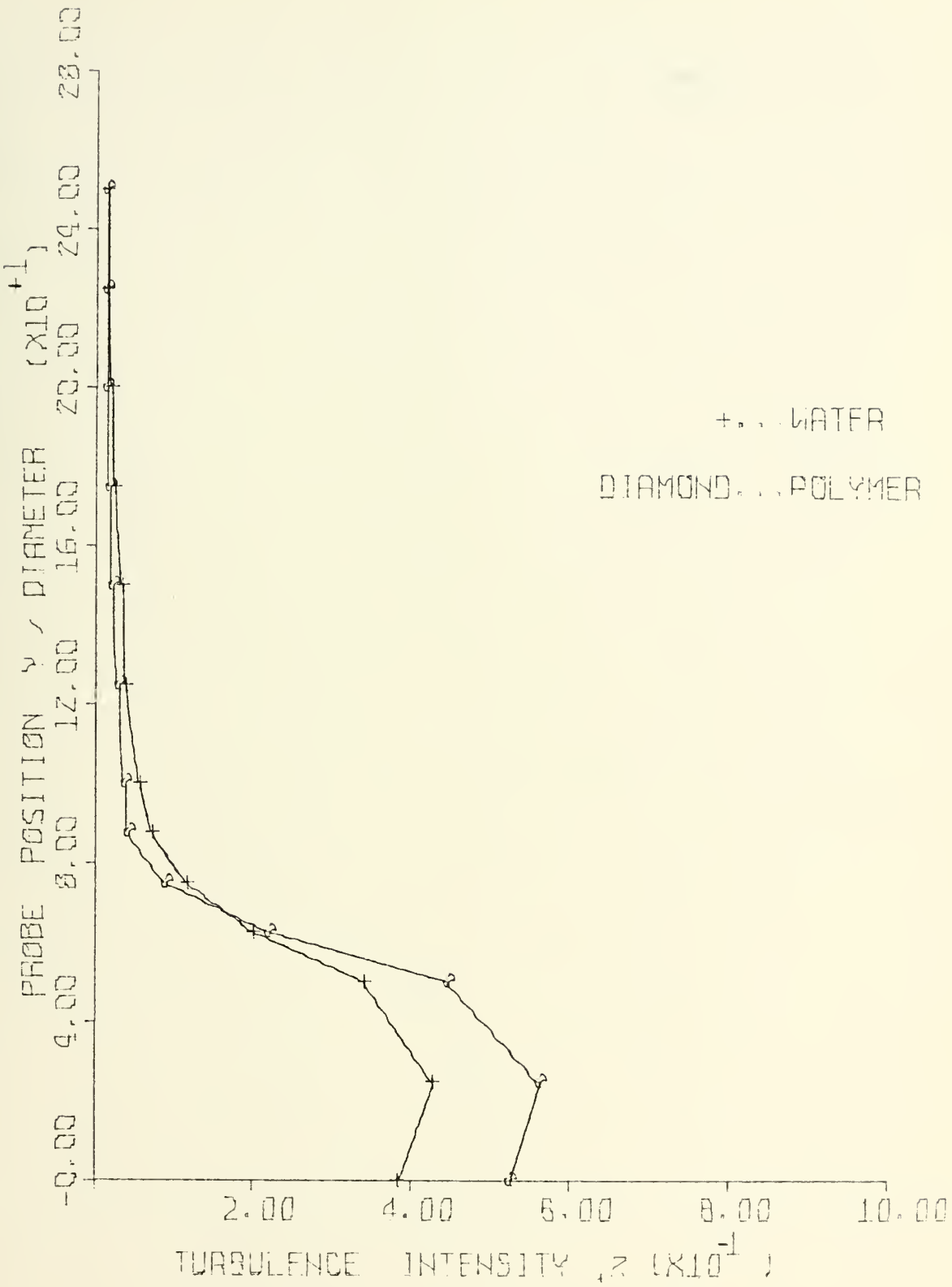

Figure 31: TURBULENCE INTENSITY PROFILES FOR TAP WATER AND 25 WPPM POLYMER SOLUTION, 0% PDR; RE No = 140,000; X/DIAM = +1.0

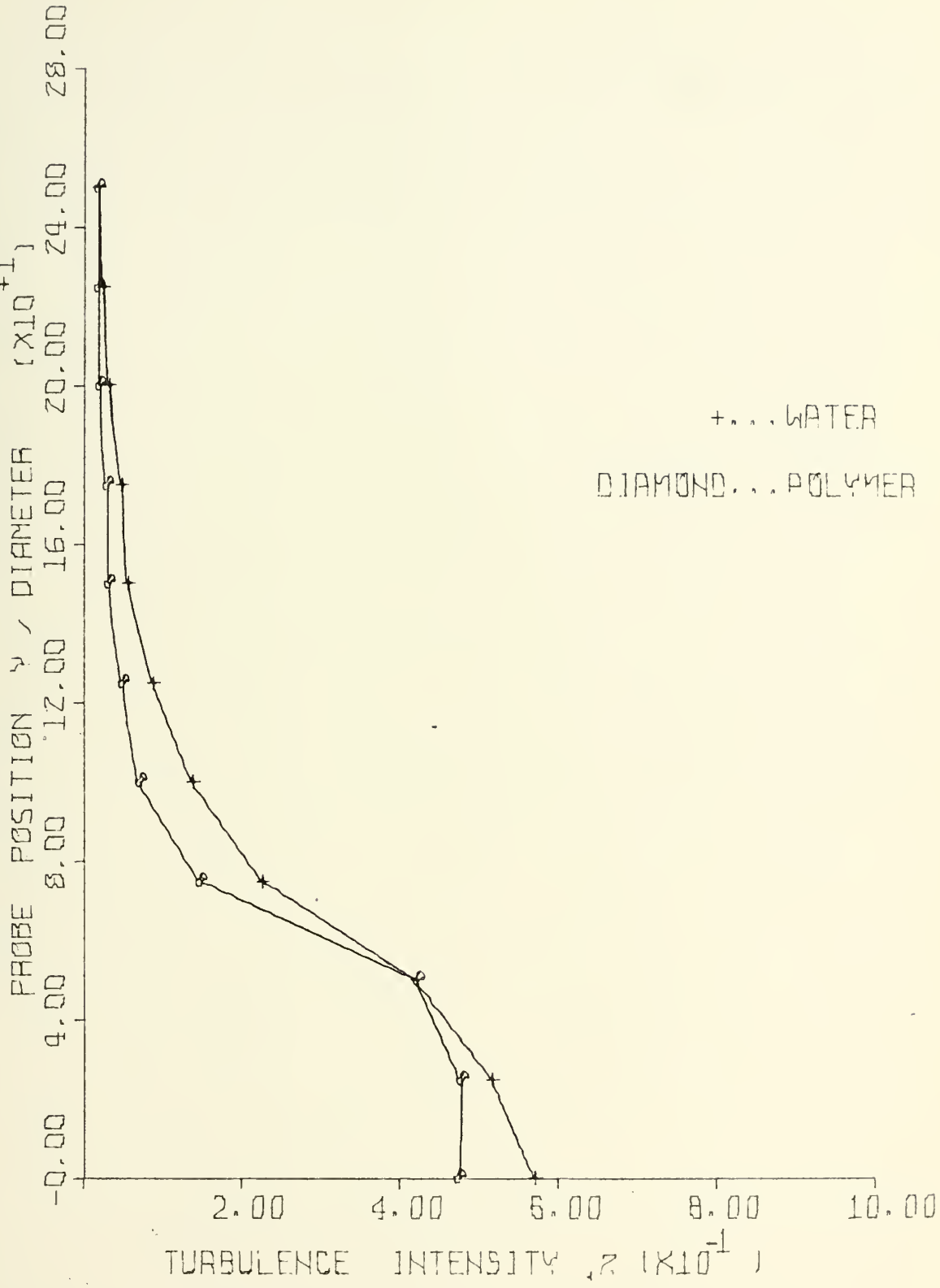

Figure 32: TURBULENCE INTENSITY PROFILES FOR TAP WATER AND 25 WPPM POLYMER SOLUTION, 20% PDR; RE No = 80,000; X/DIAM = +1.5

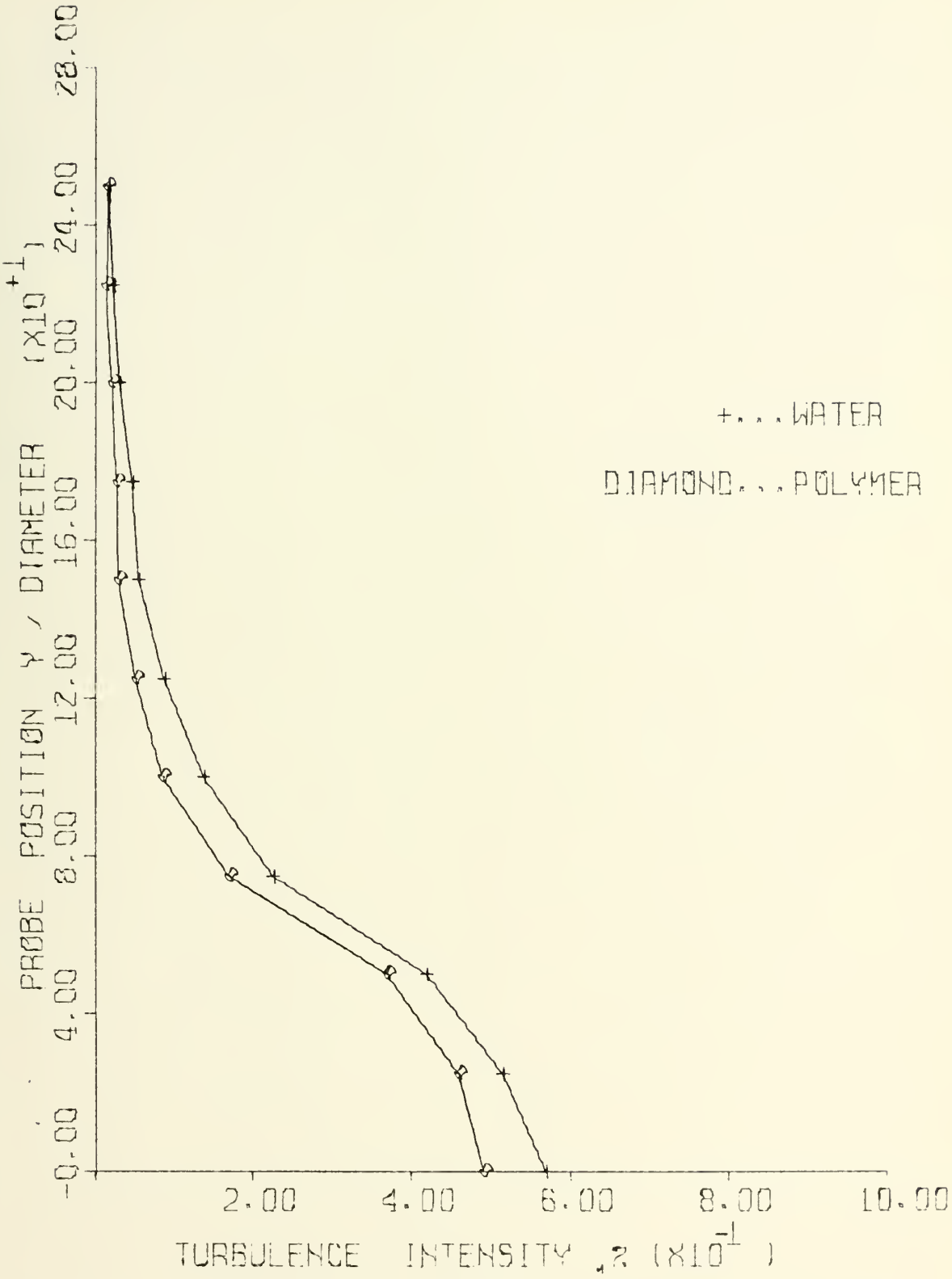

Figure 33: TURBULENCE INTENSITY PROFILES FOR TAP WATER AND 25 WPPM POLYMER SOLUTION, 14% PDR; RE No = 80,000; X/DIAM = +1.5

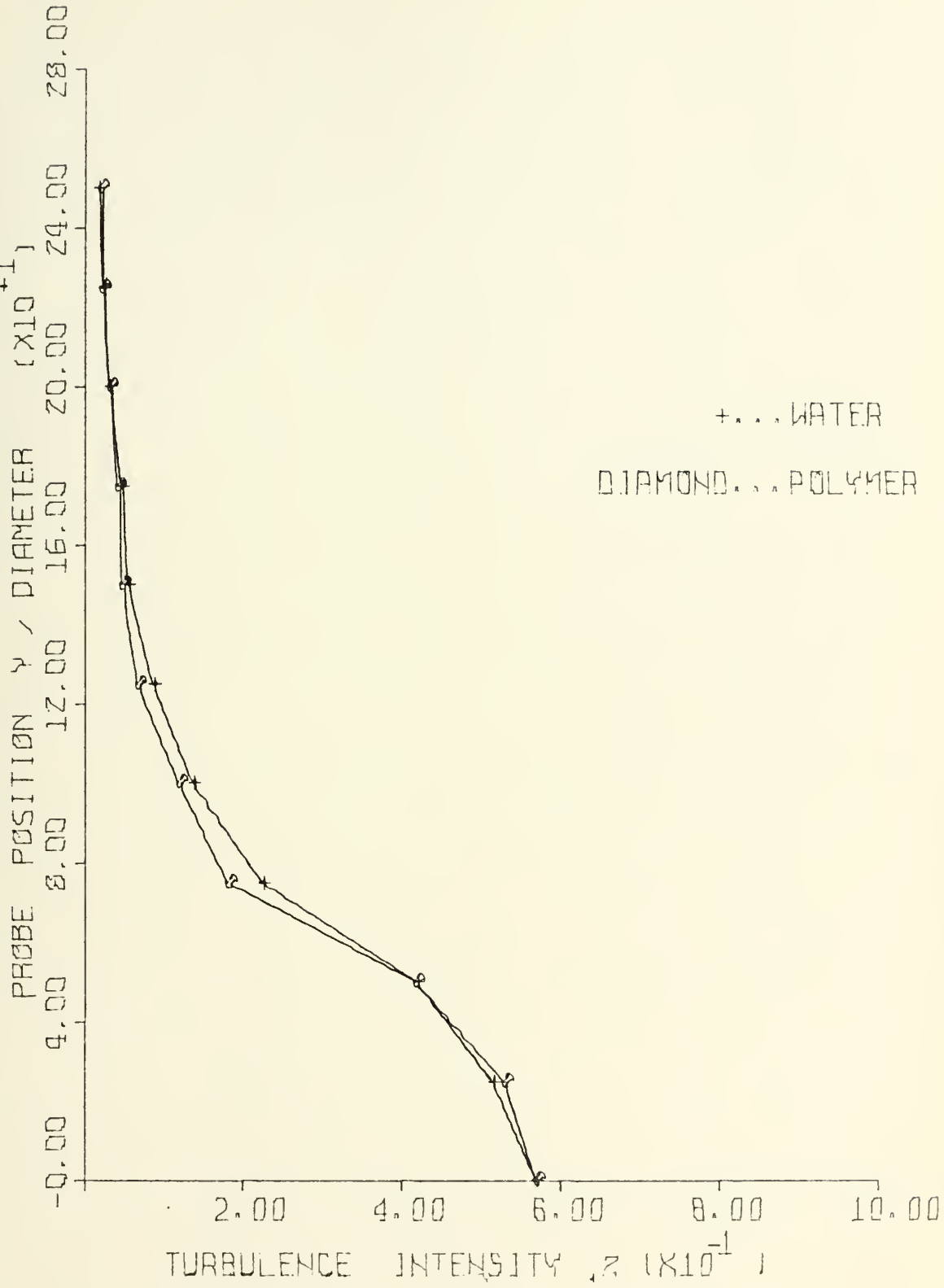

Figure 34: TURBULENCE INTENSITY PROFILES FOR TAP WATER AND 25 WPPM POLYMER SOLUTION, 11% PDR; RE No = 80,000; X/DIAM = +1.5

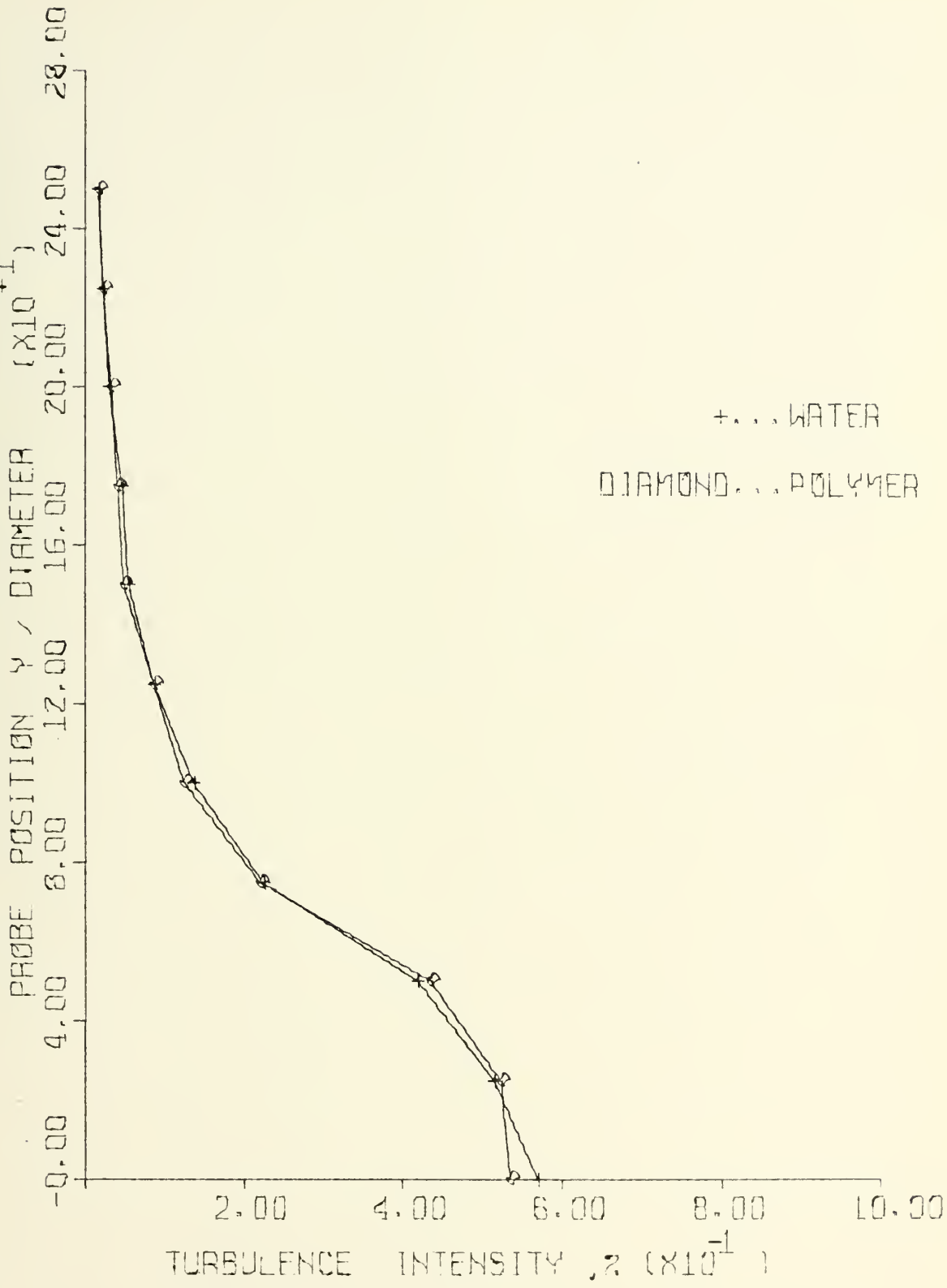

Figure 35: TURBULENCE INTENSITY PROFILES FOR TAP WATER AND 25 WPPM POLYMER SOLUTION, 6% PDR; RE No = 80,000; X/DIAM = +1.5

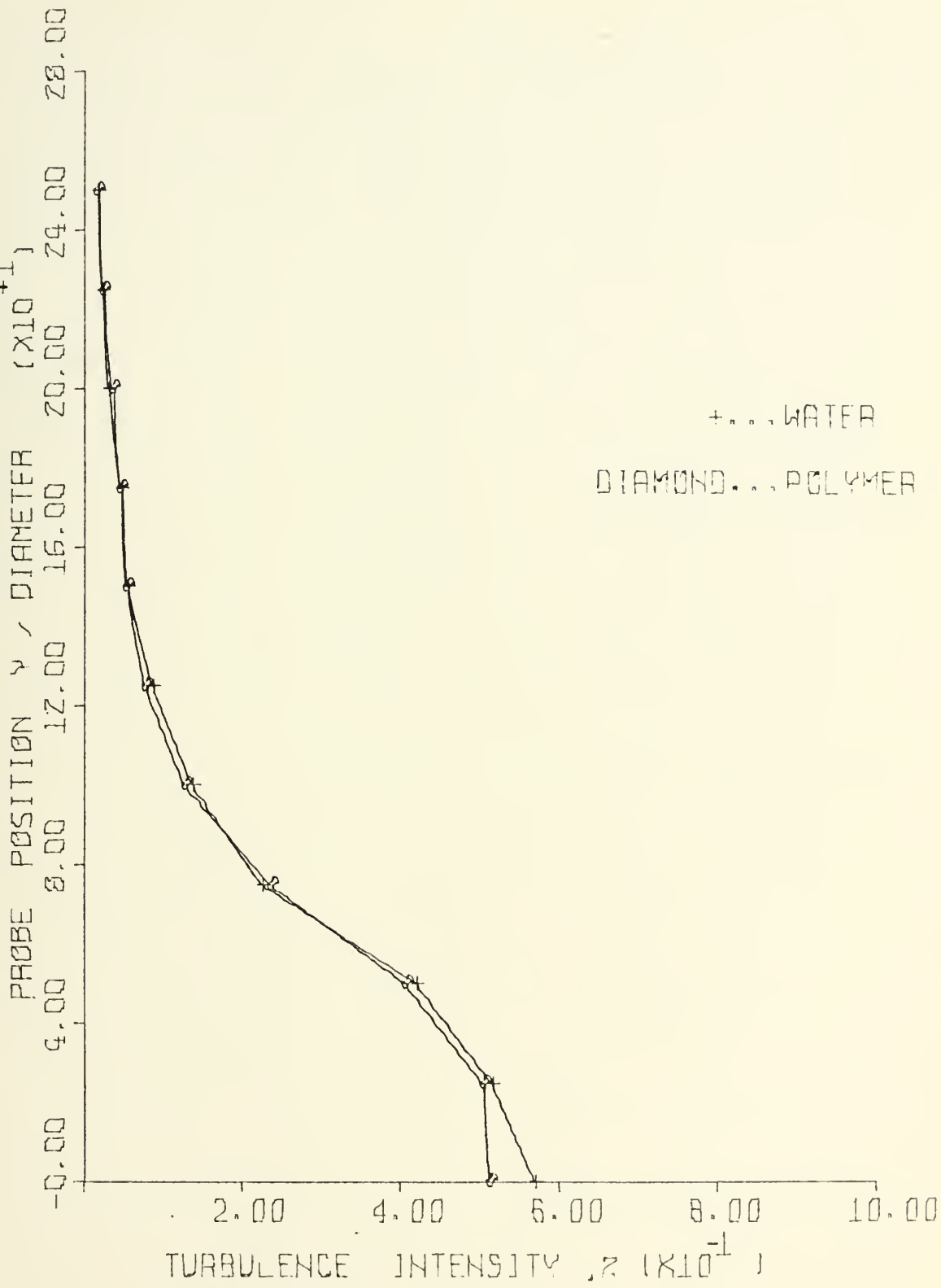

Figure 36: TURBULENCE INTENSITY PROFILES FOR TAP WATER AND 25 WPPM POLYMER SOLUTION, 3% PDR; RE No = 80,000; X/DIAM = +1.5

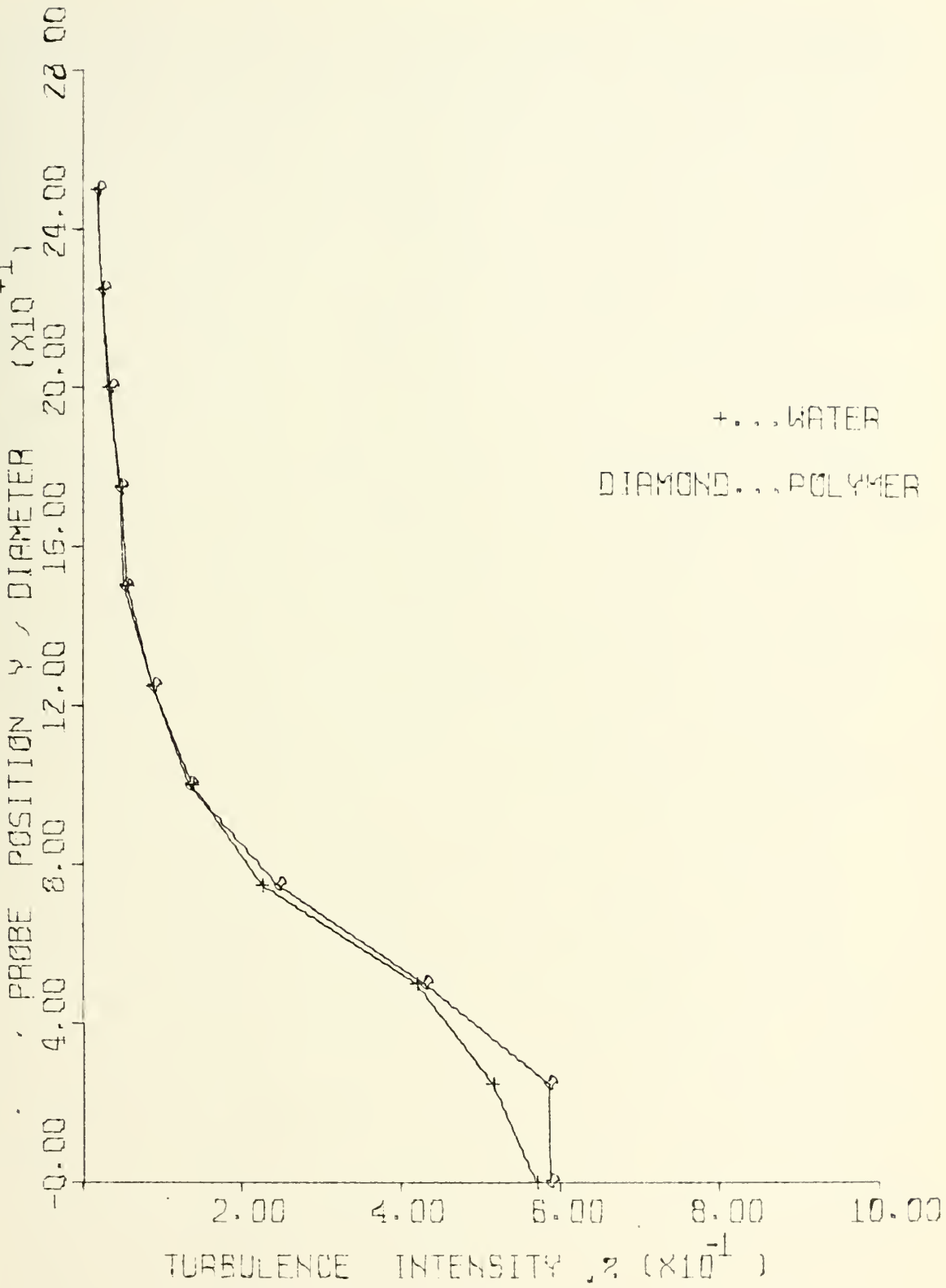

Figure 37: TURBULENCE INTENSITY PROFILES FOR TAP WATER AND 25 WPPM POLYMER SOLUTION, 0% PDR; RE No = 80,000; X/DIAM = +1.5

polymer solution profiles in these figures were for degradations states of 20% PDR, 14% PDR, 11% PDR, 6% PDR, 3% PDR, and 0% PDR, respectively. The profiles display the same characteristics as those measured at +1.0 X/DIAM, namely, a diminishing difference in turbulence intensity between water and polymer solution outside the wake region. Inside the wake region, the turbulence intensity of water was found to decrease significantly below that observed at the X-coordinate +1.0 X/DIAM. The turbulence intensity profile in the wake with polymer solution was found to be much closer to the water profile at the downstream location, +1.5 X/DIAM. The curves are essentially the same, within experimental error, for this Reynolds Number, with the exception of the 20% PDR profile.

Turbulence intensity profiles for water and polymer solution at an X-coordinate of +1.5 X/DIAM and a Reynolds Number of 100,000 are presented in Figs. 38 through 43. The polymer solution profiles in these figures were for degradation states of 20% PDR, 14% PDR, 10% PDR, 6% PDR, 3% PDR, and 0% PDR, respectively. The profiles display the same characteristics as those taken at +1.0 X/DIAM. A maximum reduction of turbulence intensity outside the wake region occurred at a PDR of 14%. Inside the wake region, however, the difference between water and polymer solution turbulence intensity was greatly diminished, reaching a maximum at 10% PDR, where the difference was 39% at the center of the wake.

Turbulence intensity profiles for water and polymer solution at an X-coordinate of +1.5 X/DIAM and a Reynolds

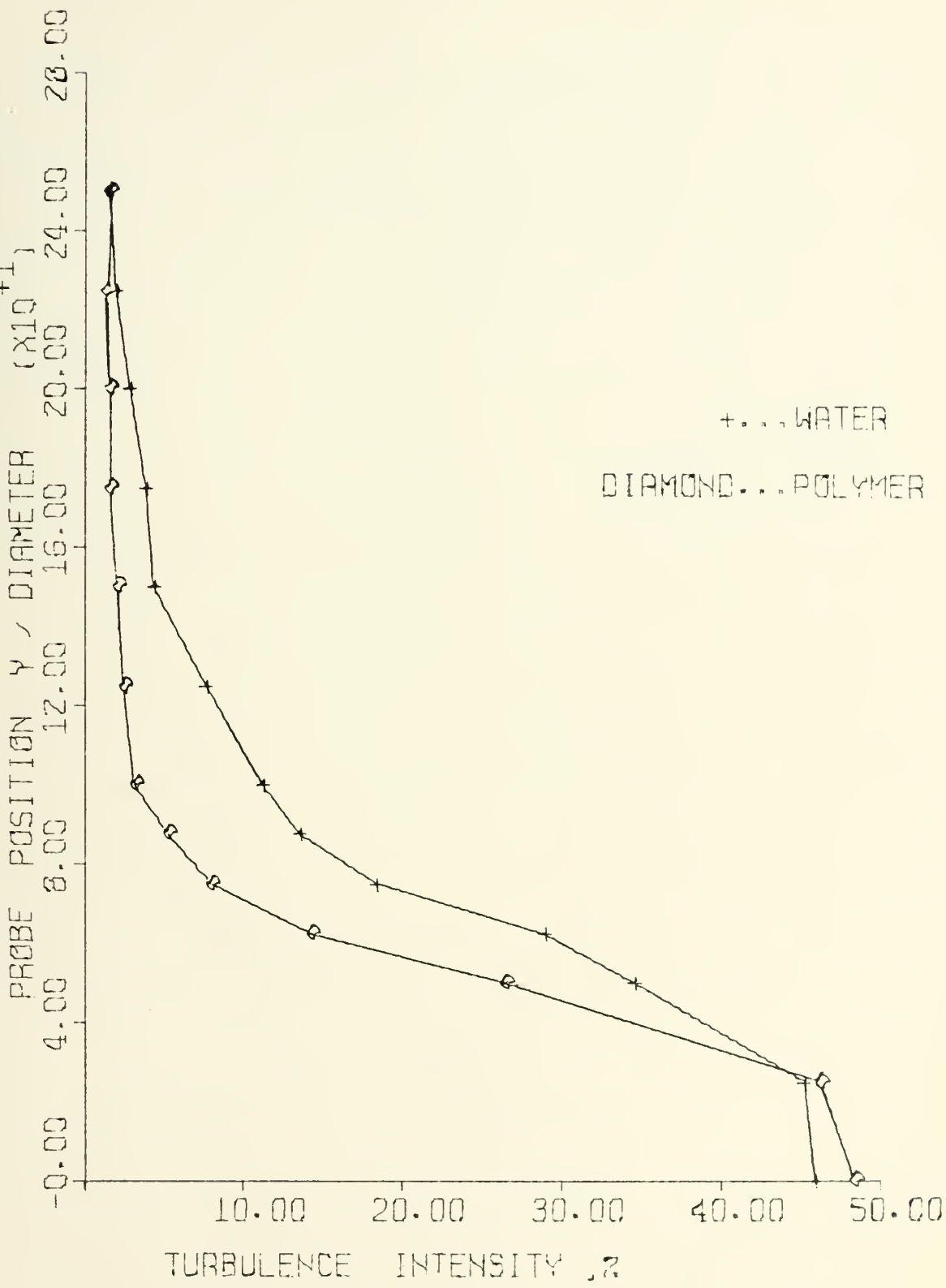

Figure 38: TURBULENCE INTENSITY PROFILES FOR TAP WATER AND 25 WPPM POLYMER SOLUTION, 20% PDR; RE No = 100,000; X/DIAM = +1.5

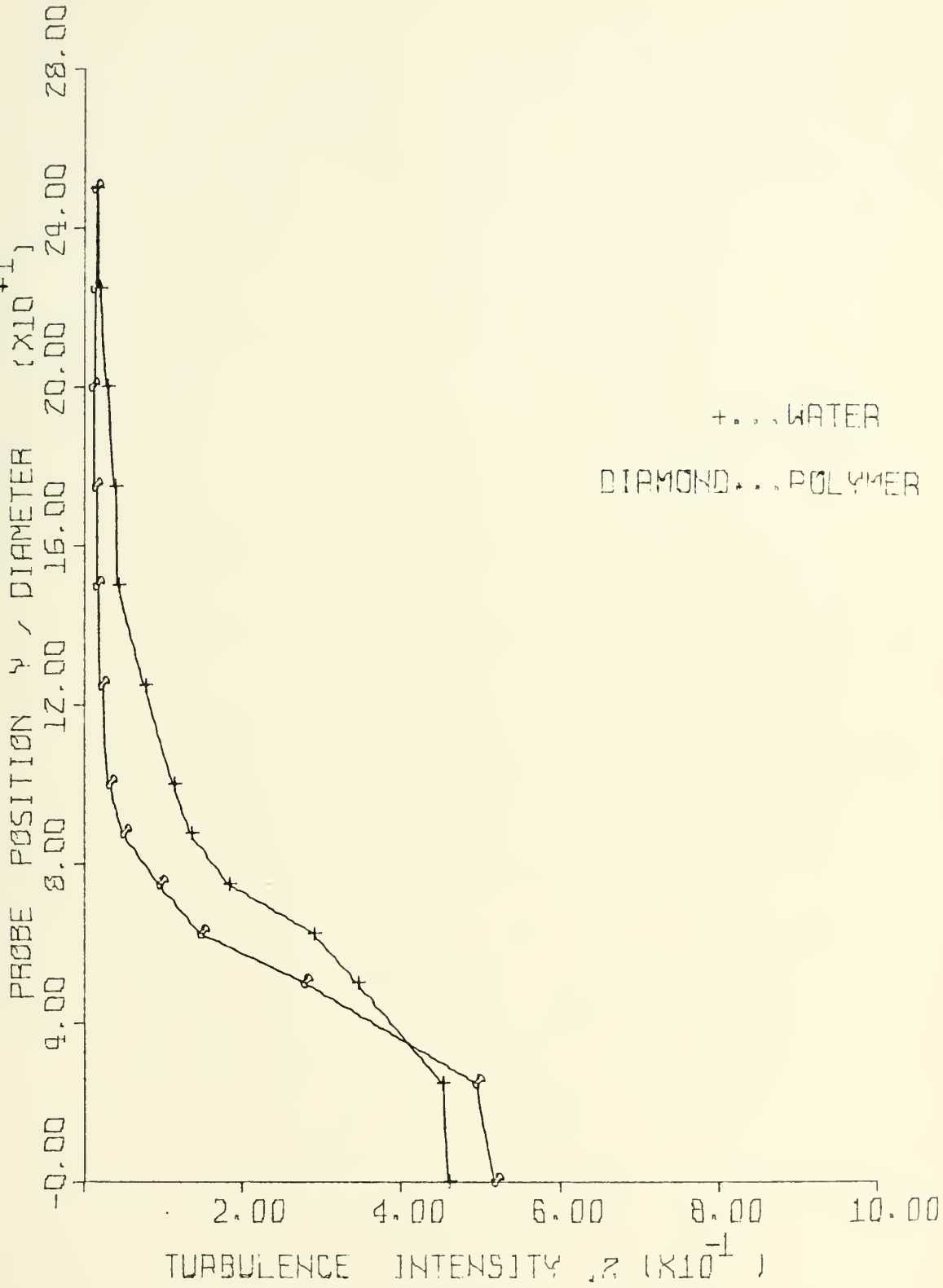

Figure 39: TURBULENCE INTENSITY PROFILES FOR TAP WATER AND 25 WPPM POLYMER SOLUTION, 14% PDR; RE No = 100,000; X/DIAM = +1.5

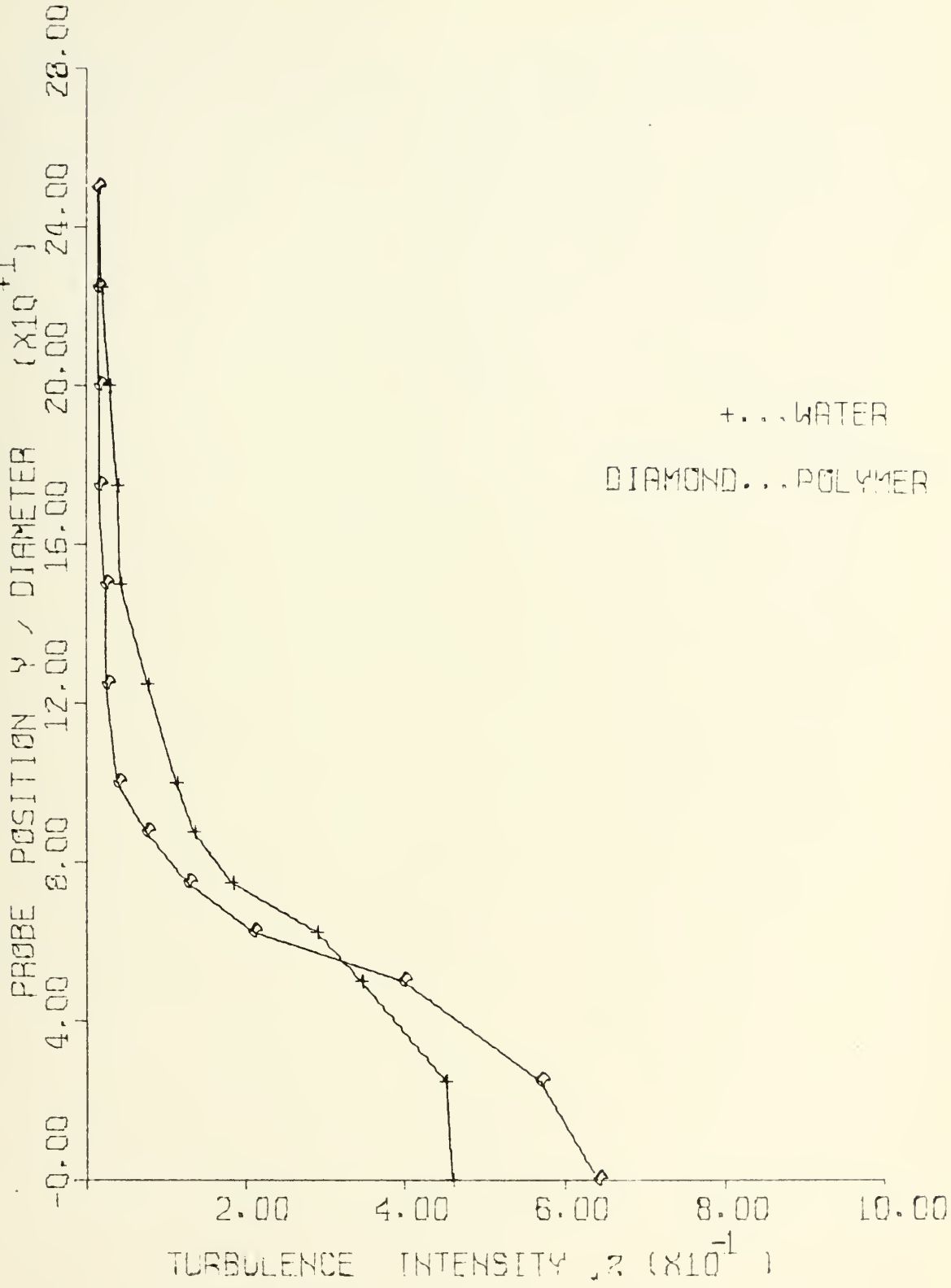

Figure 40: TURBULENCE INTENSITY PROFILES FOR TAP WATER AND 25 WPPM POLYMER SOLUTION, 10% PDR; RE No = 100,000; X/DIAM = +1.5

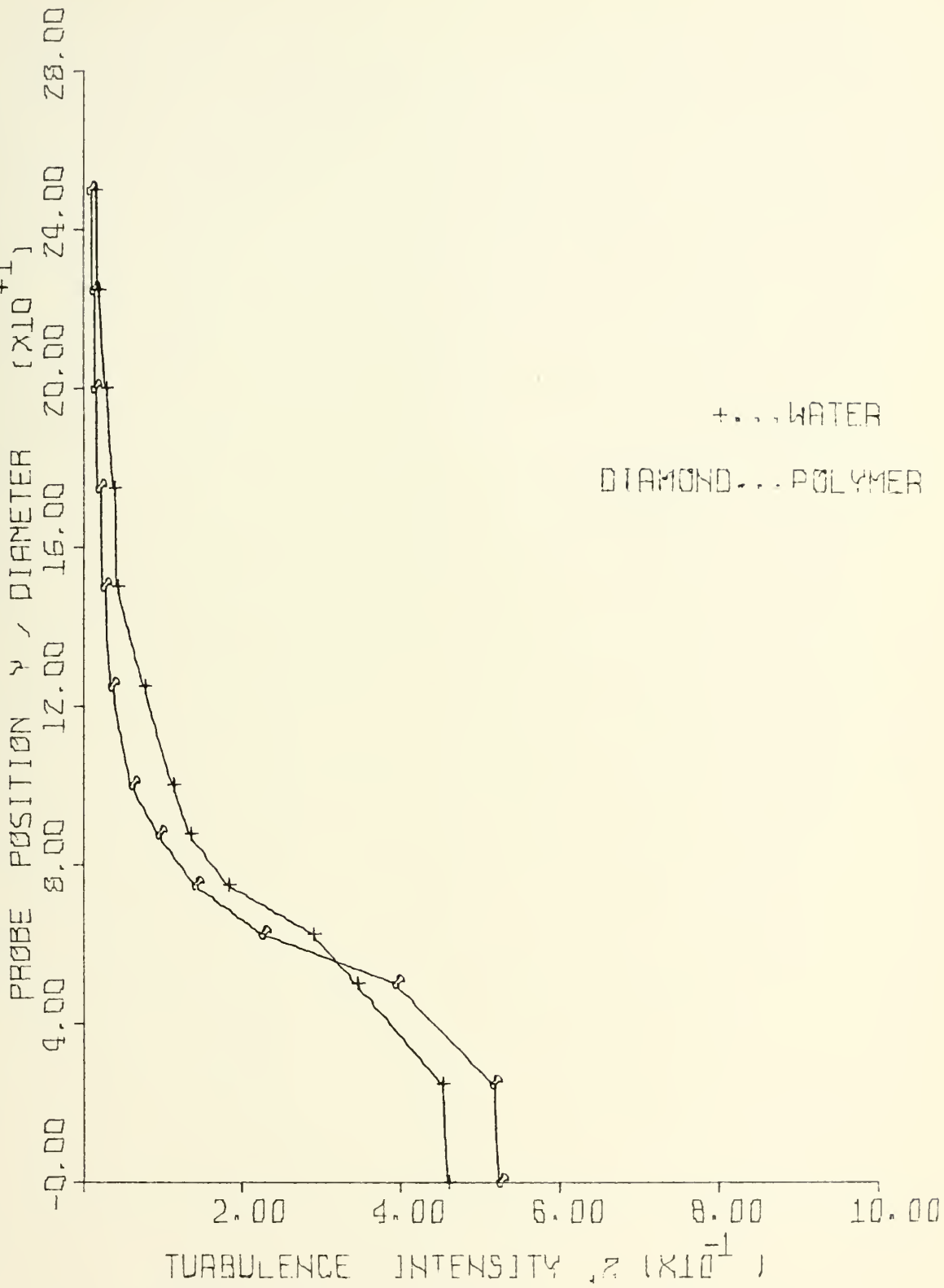

Figure 41: TURBULENCE INTENSITY PROFILES FOR TAP WATER AND 25 WPPM POLYMER SOLUTION, 6% PDR; RE No = 100,000; X/DIAM = +1.5

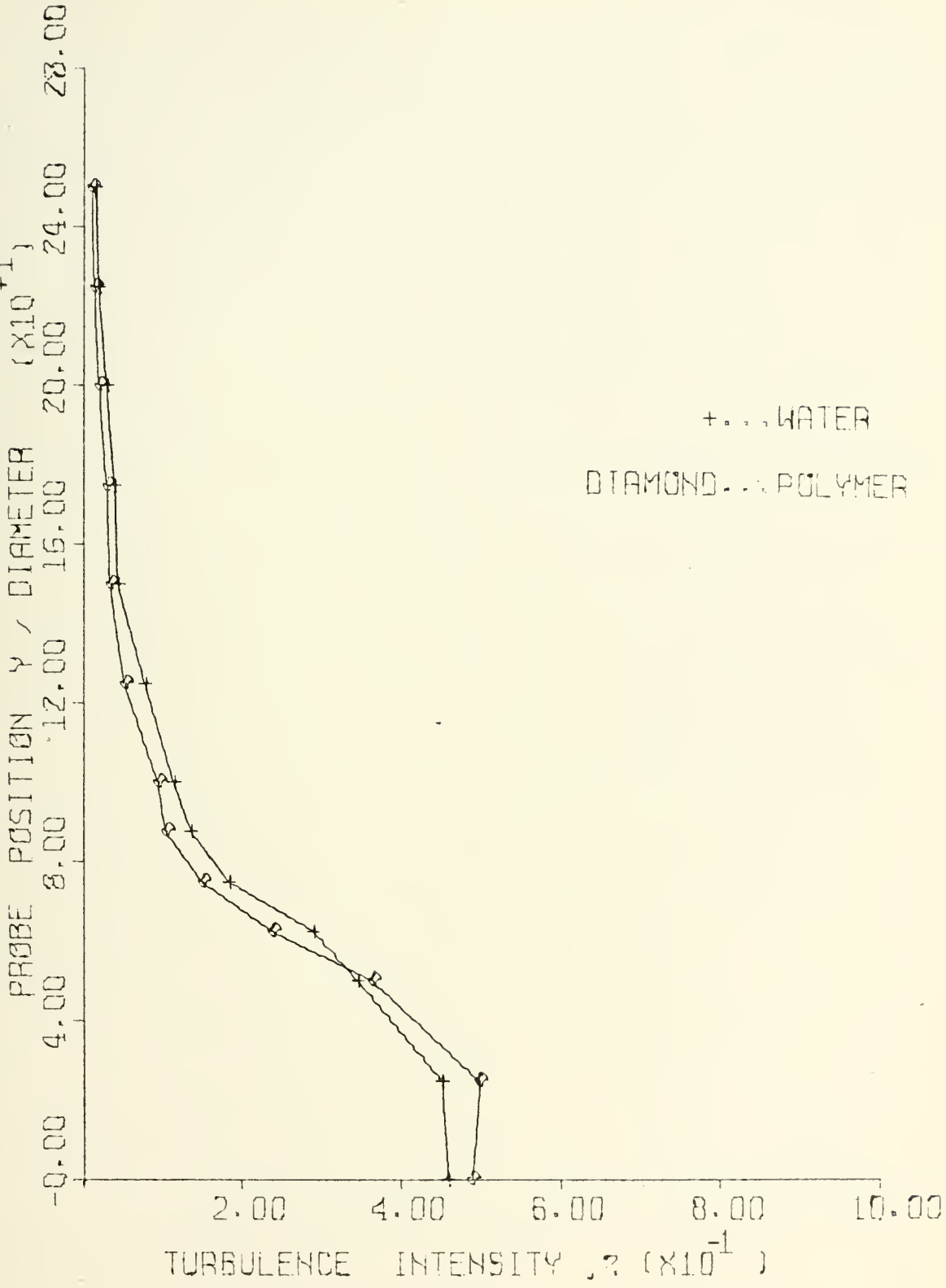

Figure 42: TURBULENCE INTENSITY PROFILES FOR TAP WATER AND 25 WPPM POLYMER SOLUTION, 3% PDR; RE No = 100,000; X/DIAM = +1.5

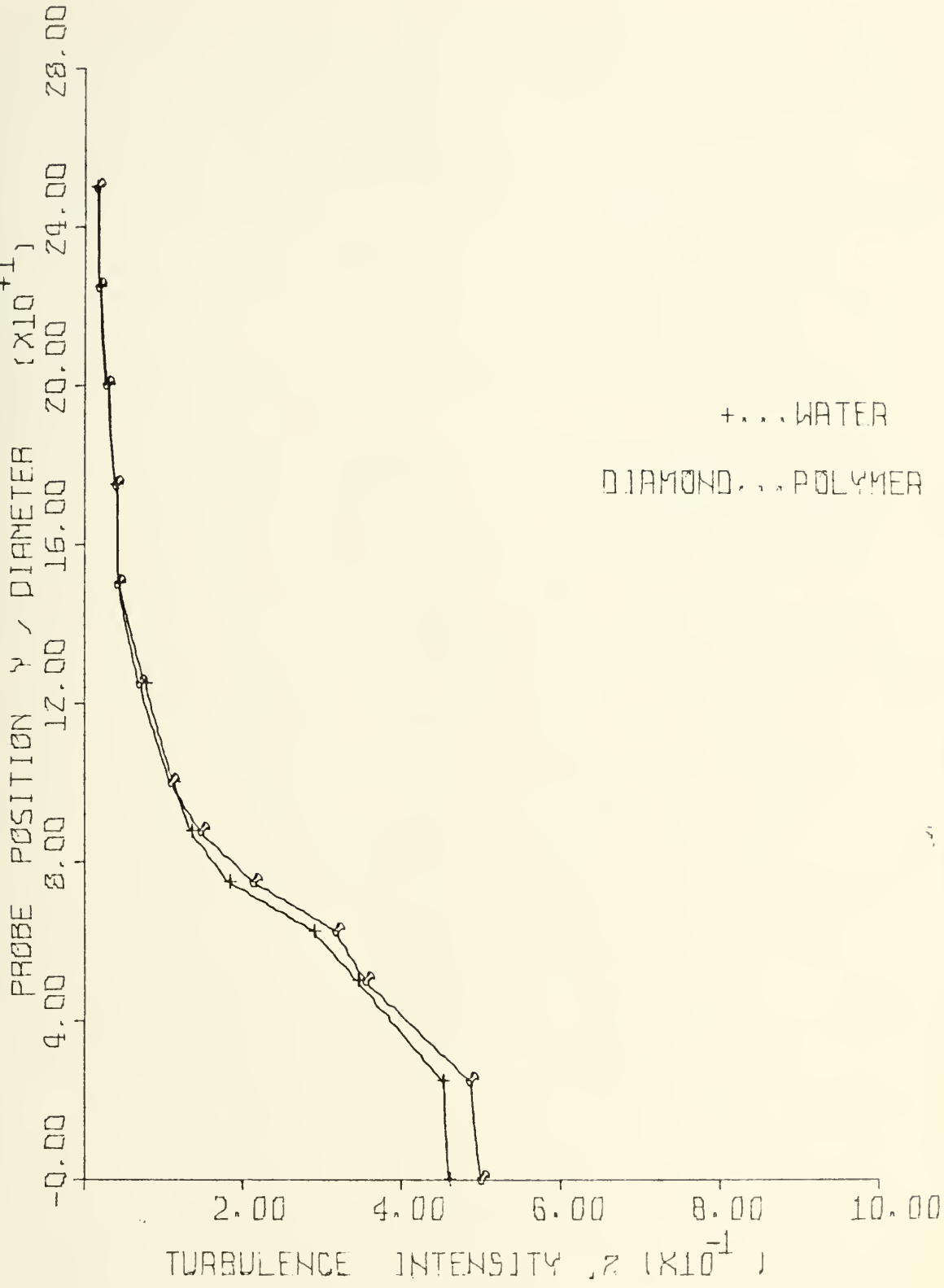

Figure 43: TURBULENCE INTENSITY PROFILES FOR TAP WATER AND 25 WPPM POLYMER SOLUTION, 0% PDR; RE No = 100,000; X/DIAM = +1.5

Number of 120,000 are presented in Figs. 44 through 49. The polymer solution profiles in these figures were for degradation states of 19% PDR, 13% PDR, 10% PDR, 6% PDR, 3% PDR, and 0% PDR, respectively. A very large reduction in turbulence intensity was observed throughout the region outside the wake. The greatest reduction was observed at a PDR of 10%, with very large reductions observed at all PDR's, with the exception of the 0% PDR.

At this downstream position, the difference between the intensities inside the wake was not as pronounced as those observed 0.5 DIAM closer to the cylinder. A maximum difference was observed at 6% PDR, where the intensity with polymer was 139% of that observed with water at the center of the wake.

Turbulence intensity profiles for water and polymer solution at an X-coordinate of +1.5 X/DIAM and a Reynolds Number of 140,000 are presented in Figs. 50 through 55. The polymer solution profiles in these figures were for degradation states of 18% PDR, 12% PDR, 9% PDR, 6% PDR, 3% PDR, and 0% PDR, respectively. Very large reductions in turbulence intensity were observed throughout the upper portion of the profile for the polymer solution flow. The maximum reduction was observed at 3% PDR, where the turbulence intensity was found to be 20% of that observed in water flow at +0.50 Y/DIAM. At this Reynolds Number, very little difference in intensities was observed in the wake itself. At 6% PDR, the maximum difference was observed. The turbulence intensity of the polymer flow was 136% of the value obtained with water flow.

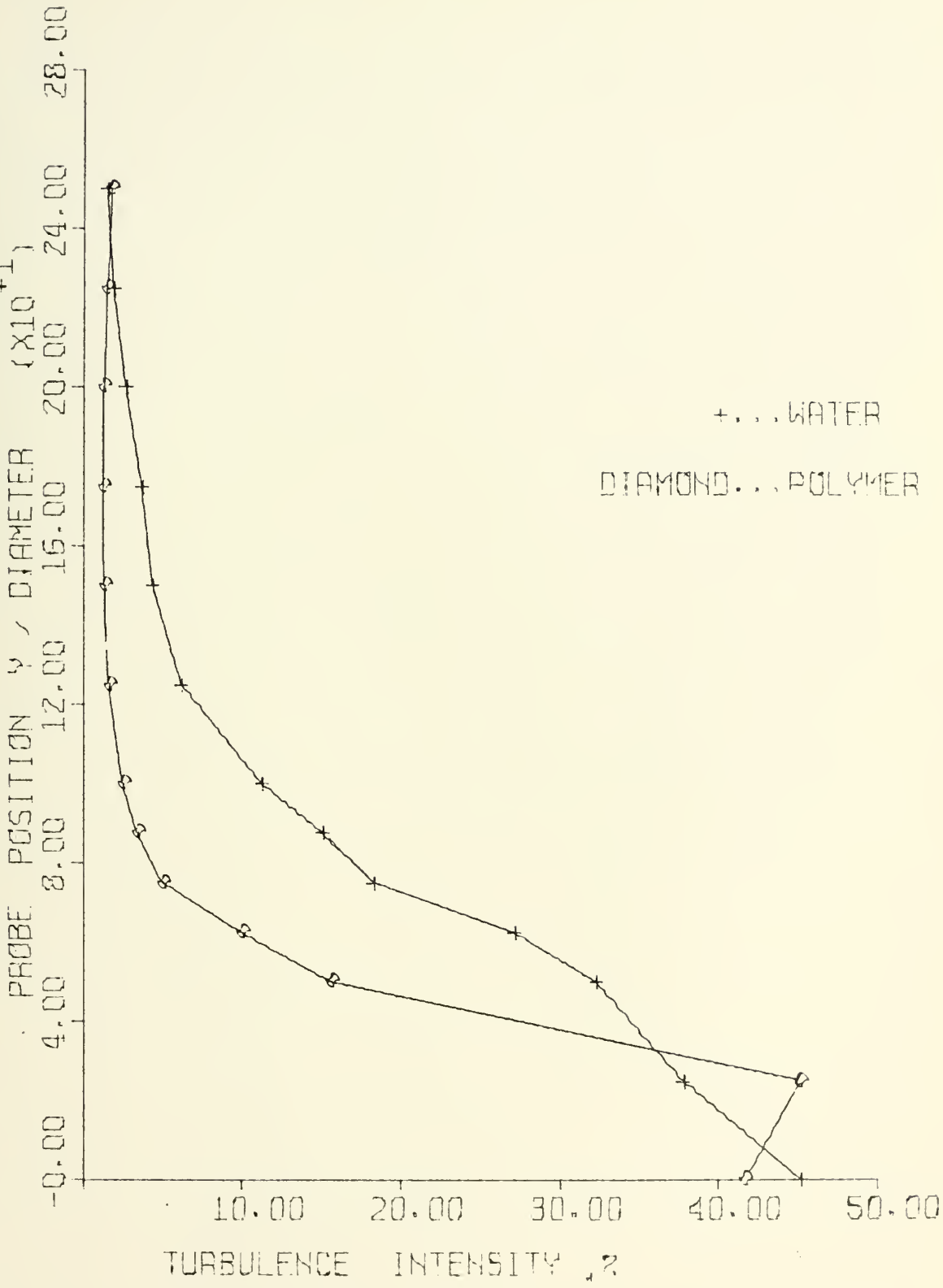

Figure 44: TURBULENCE INTENSITY PROFILES FOR TAP WATER AND 25 WPPM POLYMER SOLUTION, 19% PDR; RE No = 120,000; X/DIAM = +1.5

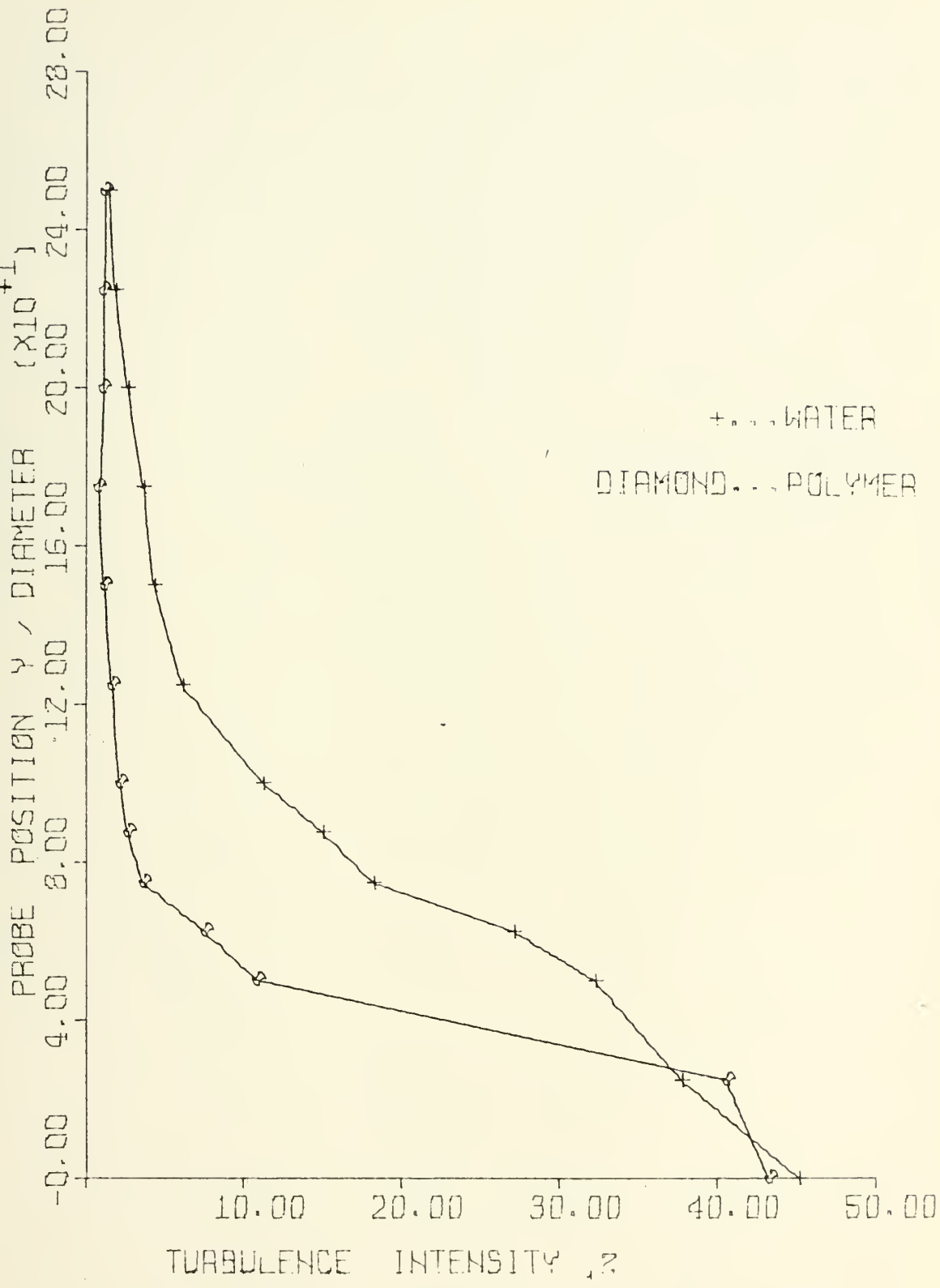

Figure 45: TURBULENCE INTENSITY PROFILES FOR TAP WATER AND 25 WPPM POLYMER SOLUTION, 13% PDR; RE No = 120,000; X/DIAM = +1.5

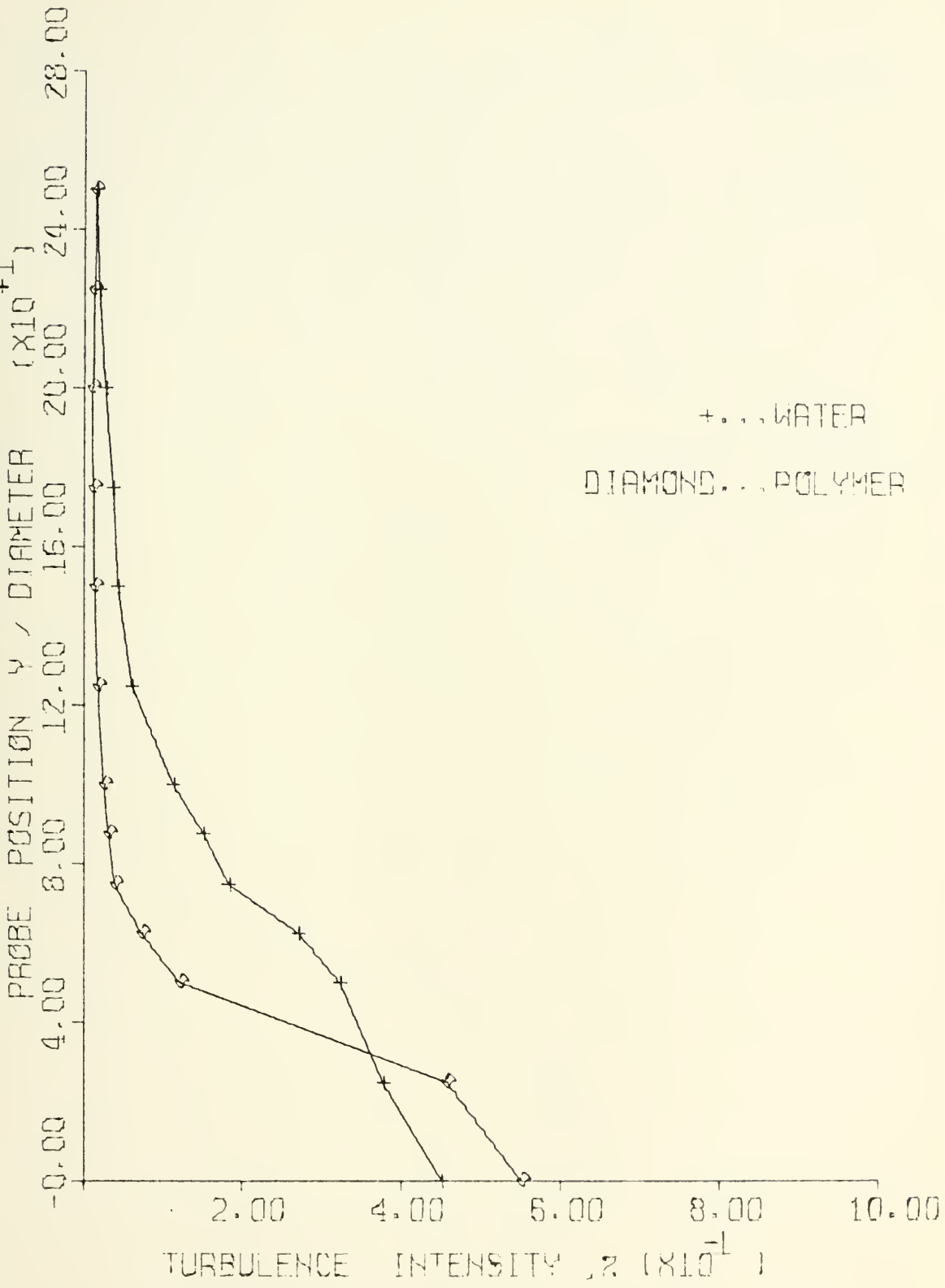

Figure 46: TURBULENCE INTENSITY PROFILES FOR TAP WATER AND 25 WPPM POLYMER SOLUTION, 10% PDR; RE No = 120,000; X/DIAM = +1.5

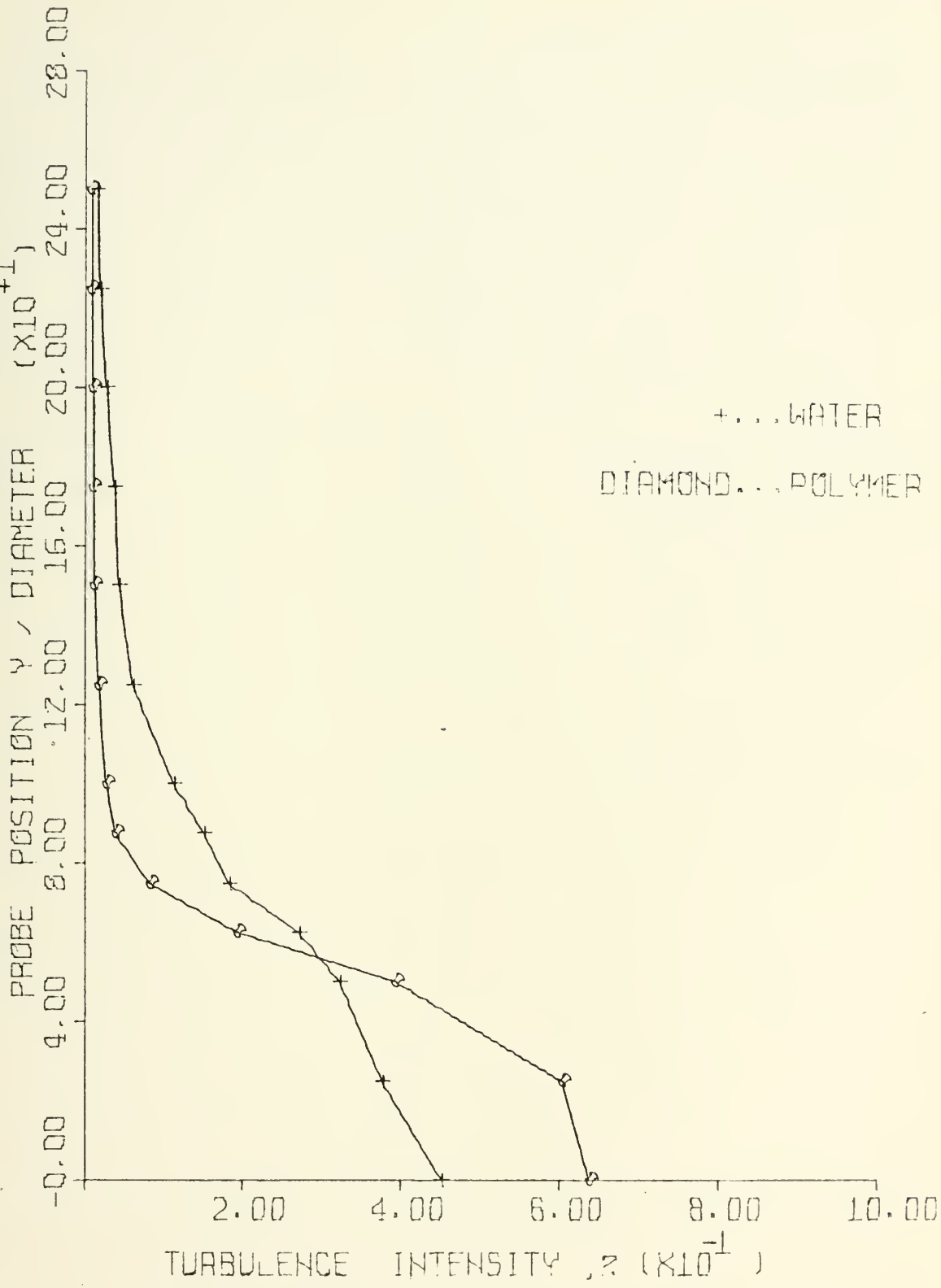

Figure 47: TURBULENCE INTENSITY PROFILES FOR TAP WATER AND 25 WPPM POLYMER SOLUTION, 6% PDR; RE No = 120,000; X/DIAM = +1.5

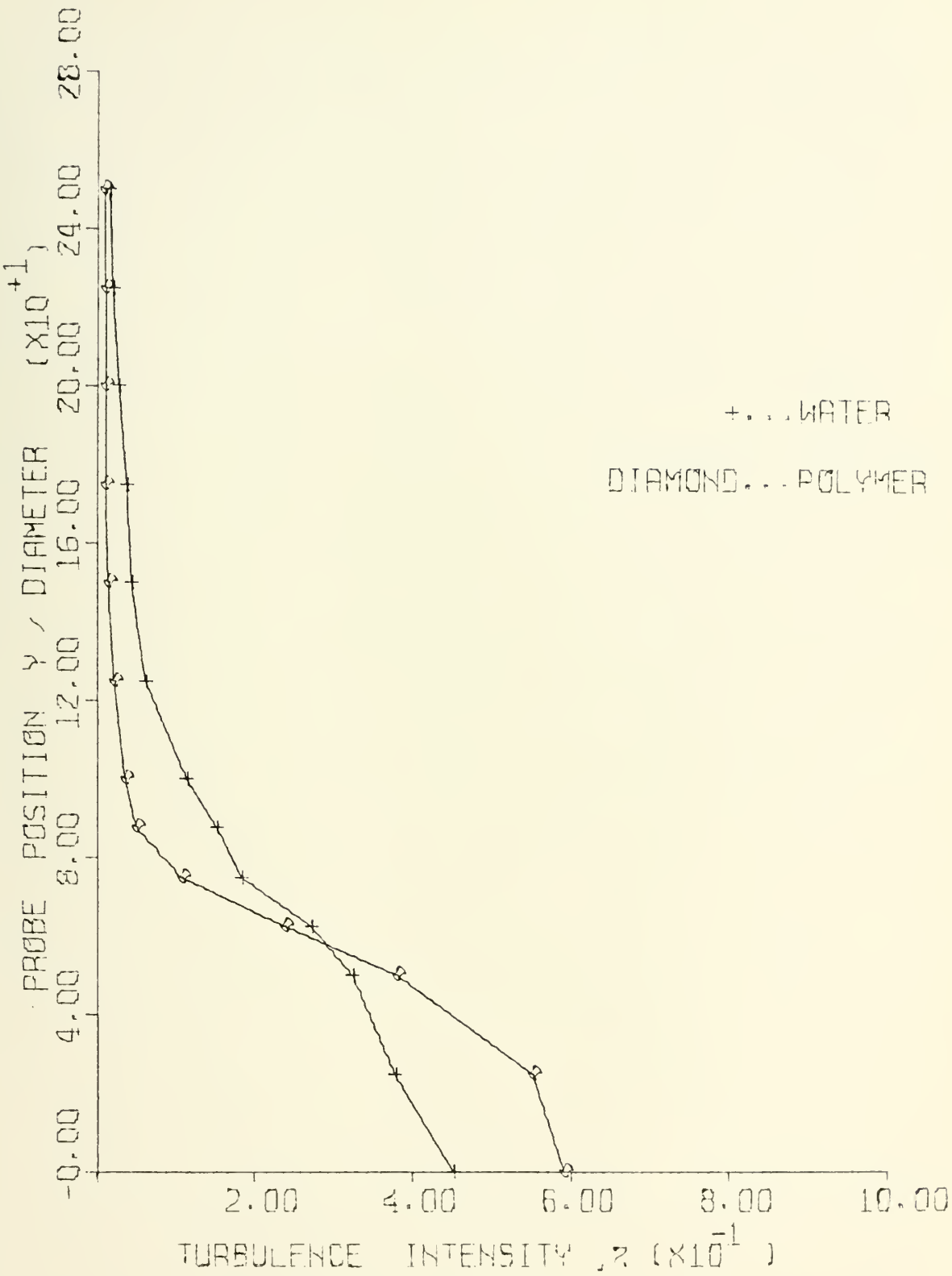

Figure 48: TURBULENCE INTENSITY PROFILES FOR TAP WATER AND 25 WPPM POLYMER SOLUTION, 3% PDR; RE No = 120,000; X/DIAM = +1.5

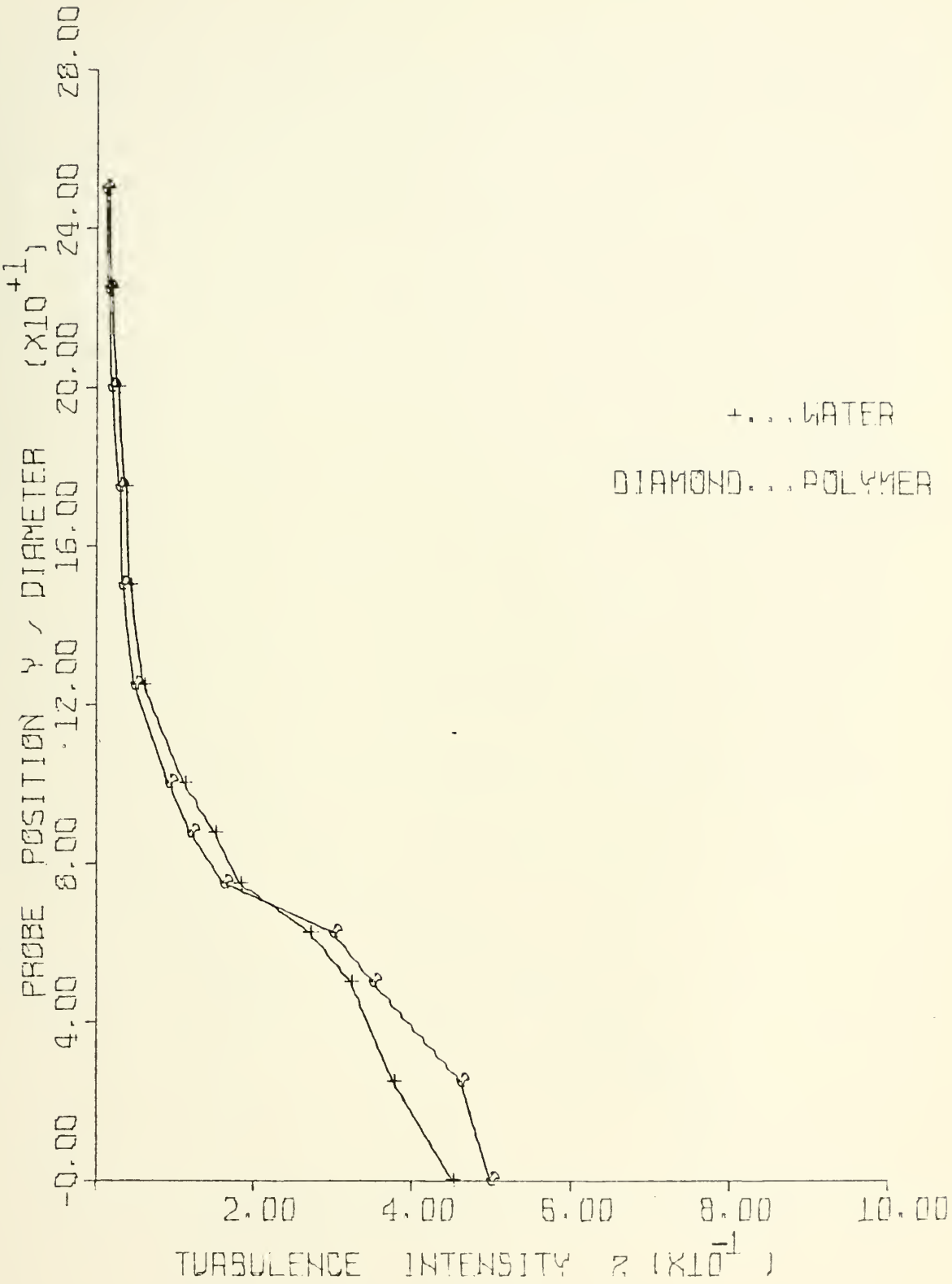

Figure 49: TURBULENCE INTENSITY PROFILES FOR TAP WATER AND 25 WPPM POLYMER SOLUTION, 0% PDR; RE No = 120,000; X/DIAM = +1.5

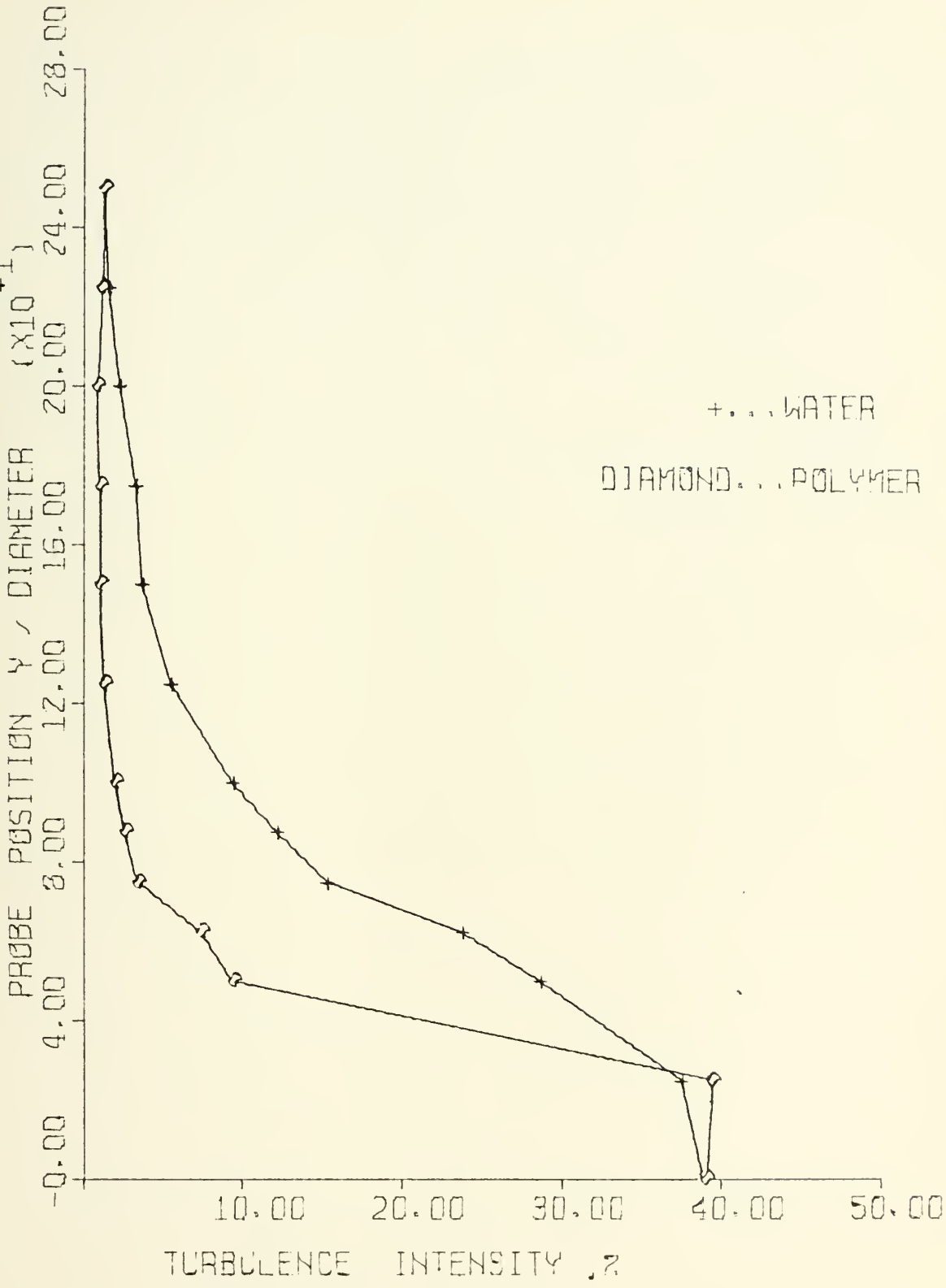

Figure 50: TURBULENCE INTENSITY PROFILES FOR TAP WATER AND 25 WPPM POLYMER SOLUTION, 18% PDR; RE No = 140,000; X/DIAM = +1.5

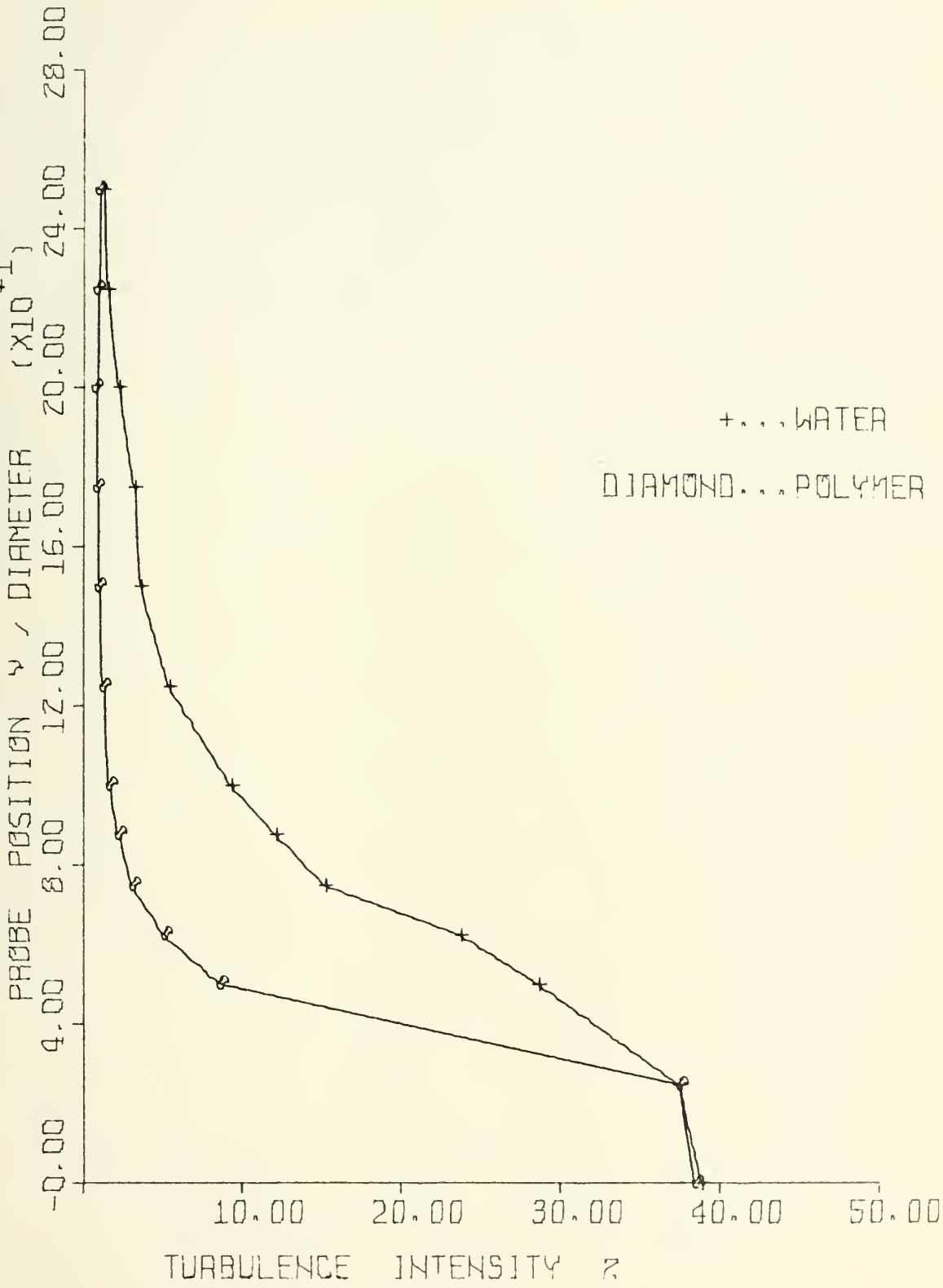

Figure 51: TURBULENCE INTENSITY PROFILES FOR TAP WATER AND 25 WPPM POLYMER SOLUTION, 12% PDR; RE No = 140,000; X/DIAM = +1.5

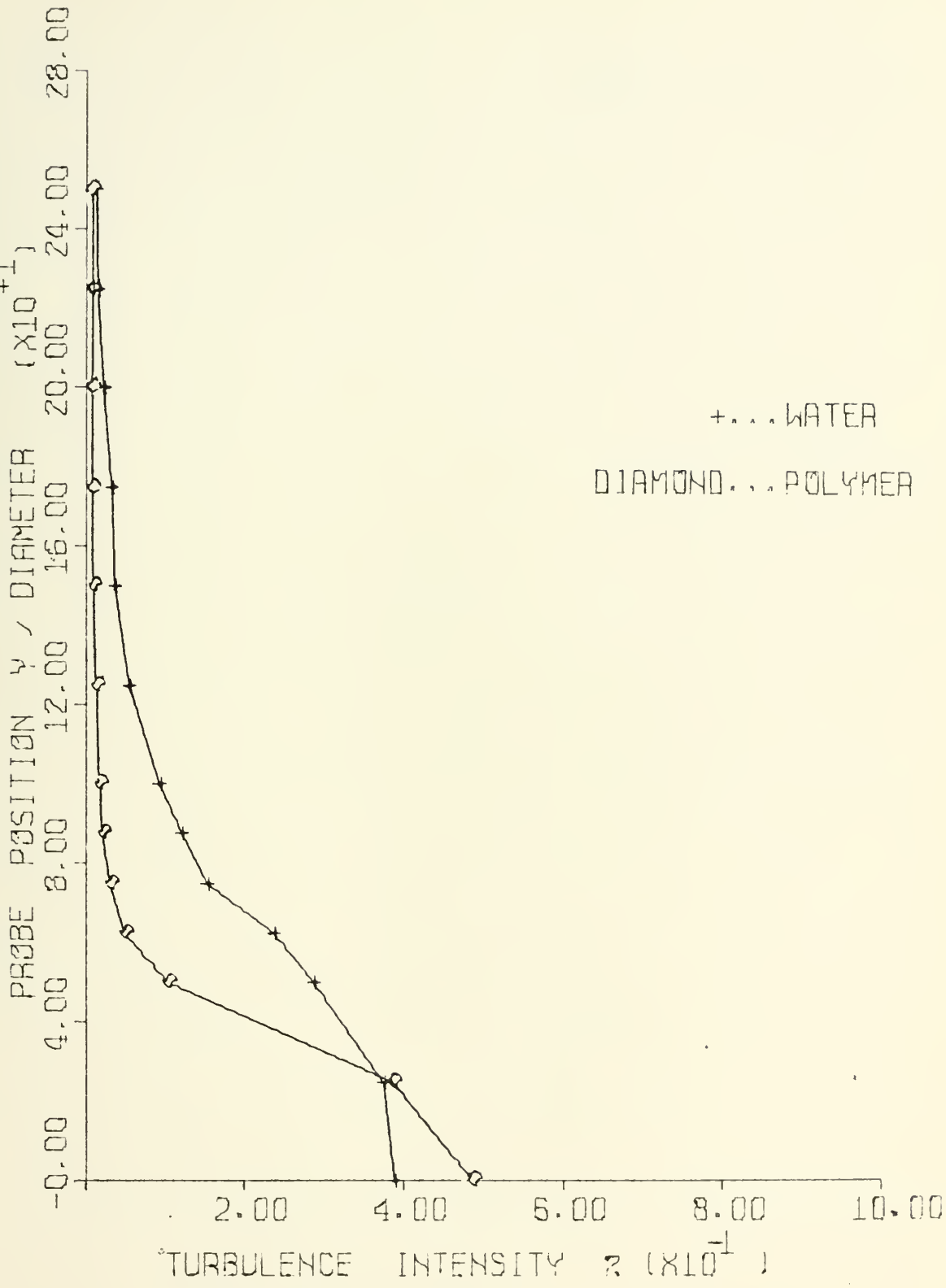

Figure 52: TURBULENCE INTENSITY PROFILES FOR TAP WATER AND 25 WPPM POLYMER SOLUTION, 9% PDR; RE No = 140,000; X/DIAM = +1.5

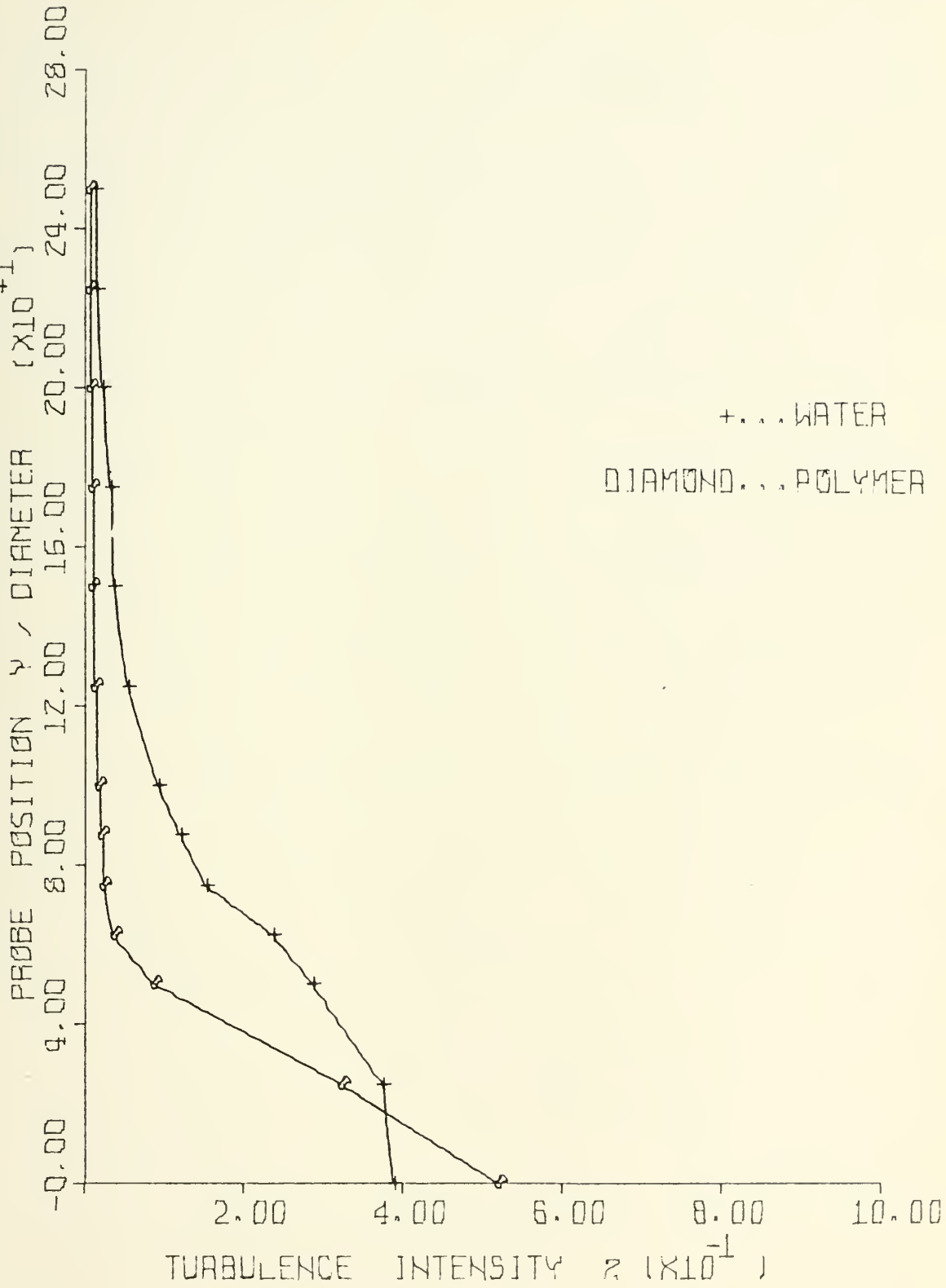

Figure 53: TURBULENCE INTENSITY PROFILES FOR TAP WATER AND 25 WPPM POLYMER SOLUTION, 6% PDR; RE No = 140,000; X/DIAM = +1.5

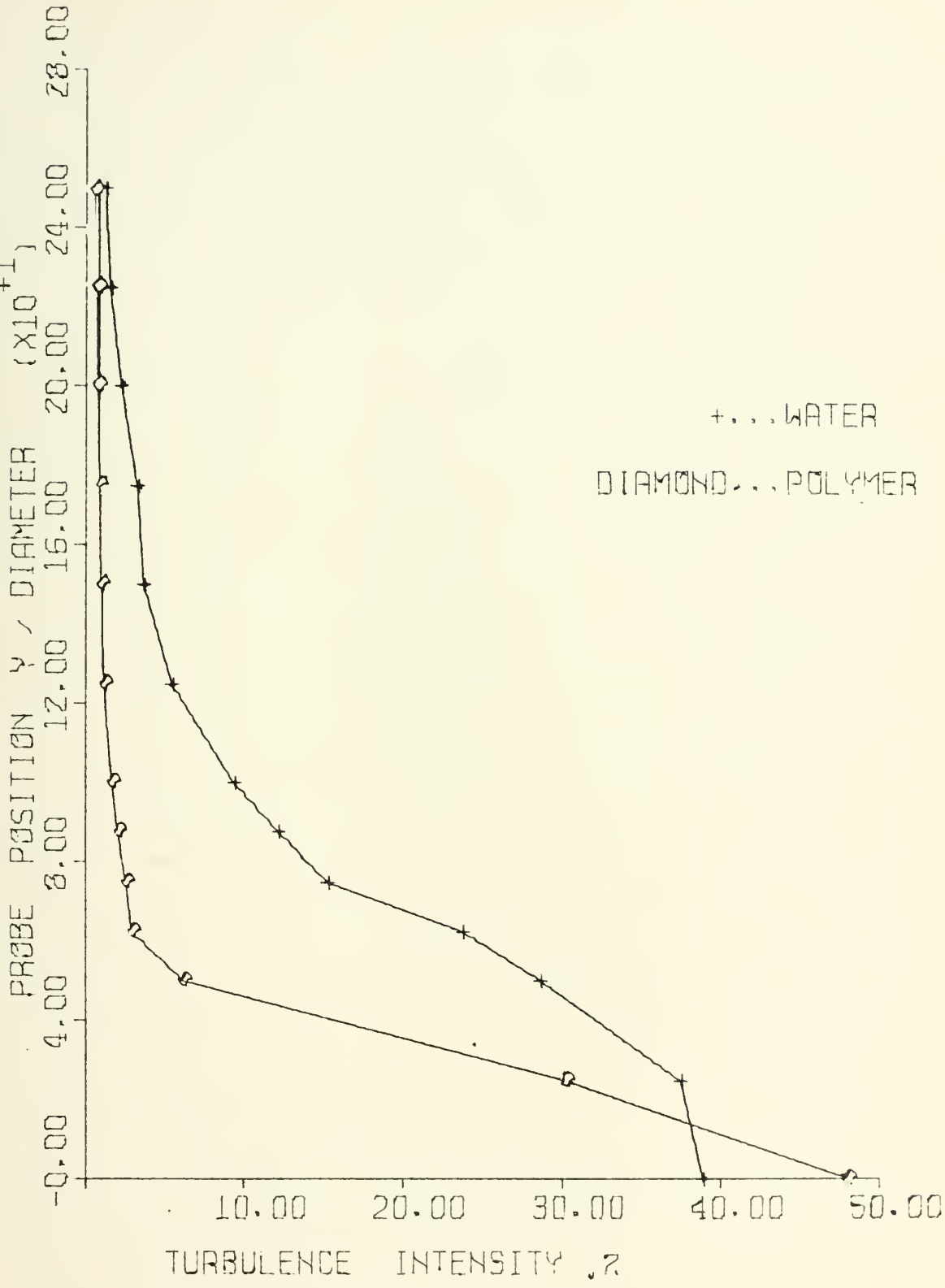

Figure 54: TURBULENCE INTENSITY PROFILES FOR TAP WATER AND 25 WPPM POLYMER SOLUTION, 3% PDR; RE No = 140,000; X/DIAM = +1.5

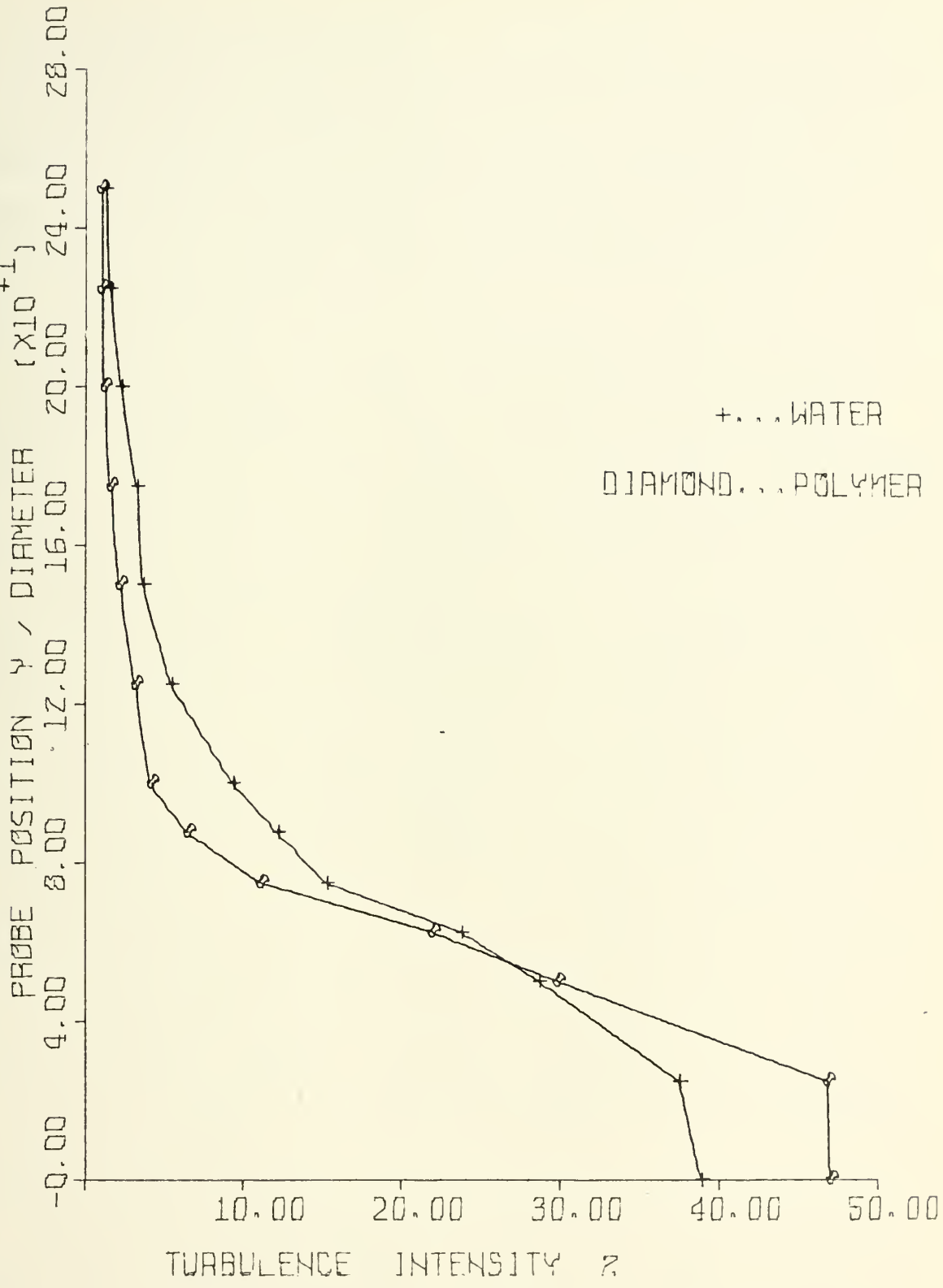

Figure 55: TURBULENCE INTENSITY PROFILES FOR TAP WATER AND 25 WPPM POLYMER SOLUTION, 0% PDR; RE No = 140,000; X/DIAM = +1.5

D. MEASUREMENT OF WAKE WIDTH

The wake width, previously defined as the transverse position in the flow field at which high-frequency velocity spikes are first observed, was obtained at +1.5 X/DIAM. This observation gave an indication of the macroscopic changes occurring in the flow field.

The wake width for polymer solution flow was obtained for the Reynolds Numbers 80,000, 100,000, 120,000, and 140,000. The value of wake width at eleven PDR's was obtained for each Reynolds Number. The observations are shown in Fig. 56. These observations provided a bird's-eye view of the entire experiment. It was found that at a Reynolds Number of 80,000, wake width decreased from 2.0 W/DIAM at 77% PDR to a minimum of 1.62 W/DIAM at 22% PDR, representing a reduction of 19%. At a Reynolds Number of 100,000, wake width was reduced from 2.0 W/DIAM at 77% PDR to 1.35 W/DIAM at 15% PDR, representing a decrease of 32%. At a Reynolds Number of 120,000, wake width was reduced from 1.85 W/DIAM at 76% PDR to 1.30 W/DIAM at 14% PDR, for a reduction of 30%. The 140,000 Reynolds Number run showed a reduction from 1.80 W/DIAM at 76% PDR to 1.25 W/DIAM at 10% PDR, representing a reduction of 30%.

These data were somewhat more nebulous in nature than the simple reading of a meter. The results were a function of the observer's ability to determine the initiation of velocity spikes. Thus, no estimate of the error involved is possible.

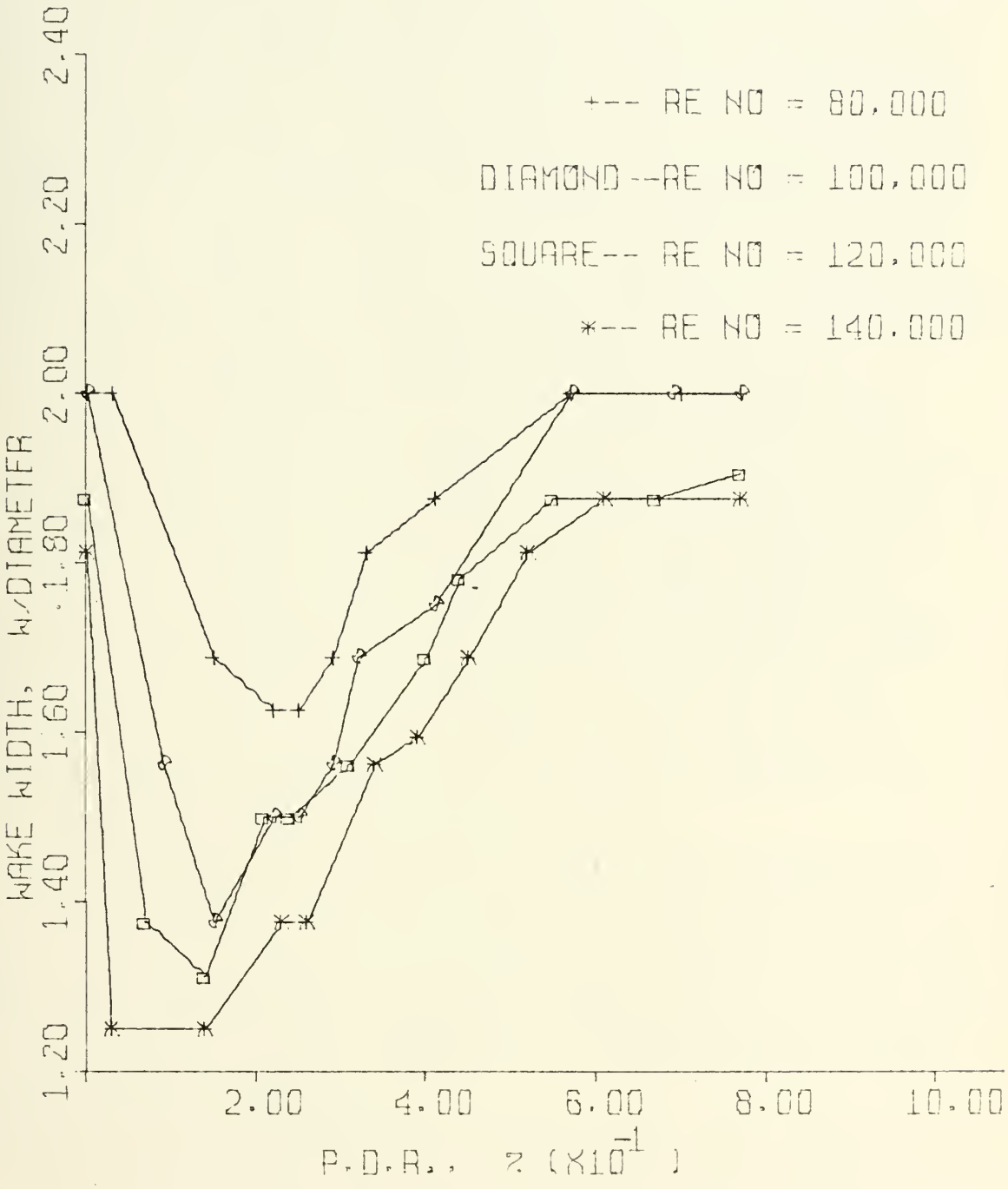

Figure 56: WAKE WIDTH VS. PDR AT X/DIAM = +1.5

E. TURBULENCE INTENSITY VS. REYNOLDS NUMBER

The previously described measurements of turbulence intensity at +1.5 X/DIAM were rearranged to plot turbulence intensity versus Reynolds Number at a given position of the sensor for water flow and a range of PDR's. These plots are presented in Figs. 57 through 62, for Y-coordinate sensor positions of +2.25 Y/DIAM, +2.0 Y/DIAM, +1.75 Y/DIAM, +1.25 Y/DIAM, +0.75 Y/DIAM, and +0.50 Y/DIAM, respectively. Each figure contains plots for water flow and for the four degradation states of 20% PDR, 14% PDR, 6% PDR, and 3% PDR.

Some interesting observations were made. At a given Reynolds Number and sensor position, the turbulence intensity was found to decrease as PDR decreased until a minimum was reached at a certain PDR. The turbulence intensity then increased and attained the value observed in water as PDR decreased to zero. It was further observed that as the Reynolds Number increased, the turbulence intensity at a given point and at a given PDR decreased.

The turbulence intensity at a given point outside the wake could be interpreted as a measure of the influence of wake flow fluctuations at that distance from the wake. Thus, a crude measure of the diffusivity of disturbances in that media could be obtained.

It was observed that as Reynolds Number increased, the diffusion of the signal generated in the wake decreased, for certain conditions of polymer solution flow. At the position +2.25 Y/DIAM, and a Reynolds Number of 80,000, the diffusion

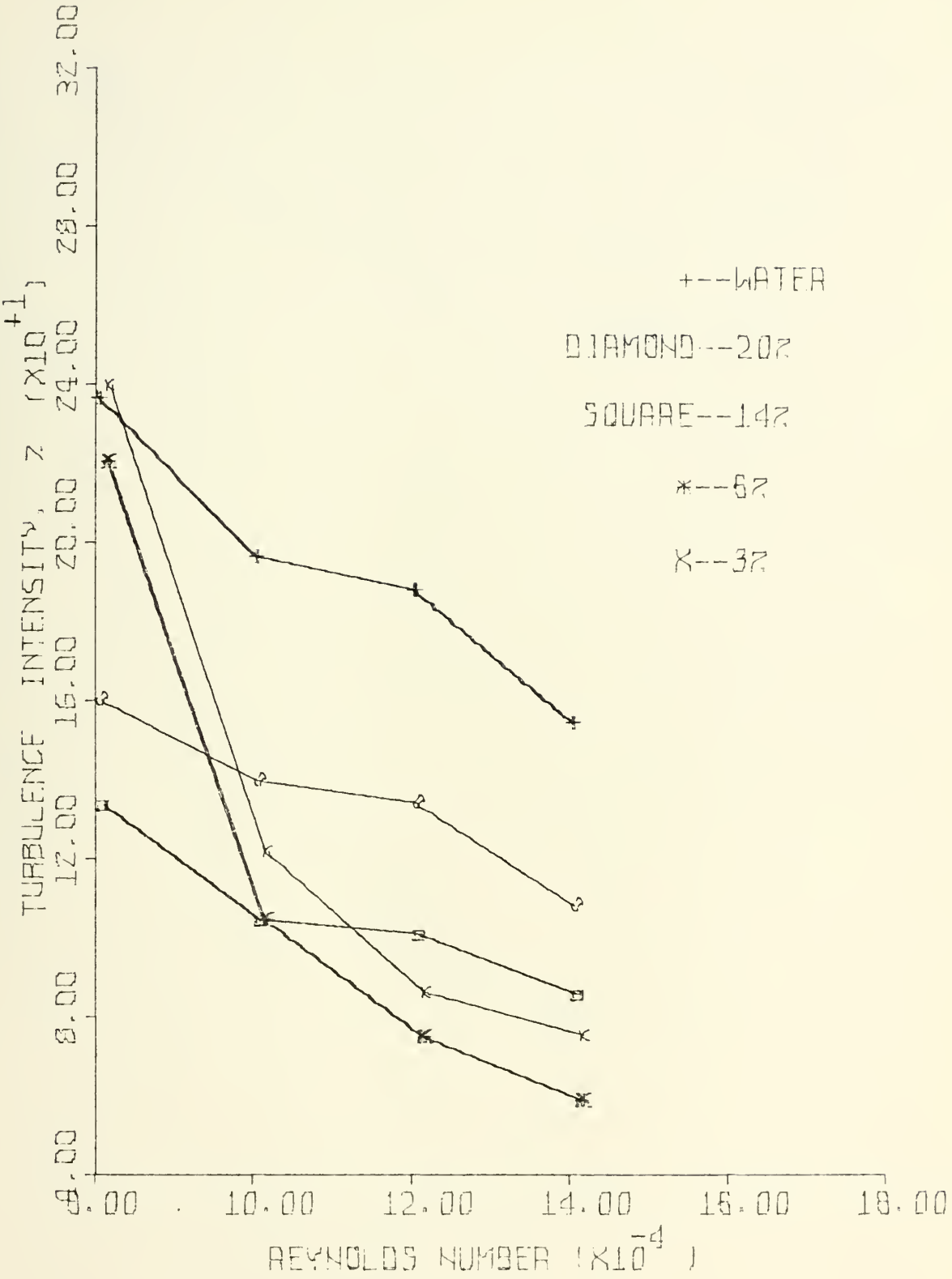

Figure 57: TURBULENCE INTENSITY VS. REYNOLDS NUMBER AT X/DIAM = +1.5, Y/DIAM = +2.25; TAP WATER AND VARIOUS PDR's

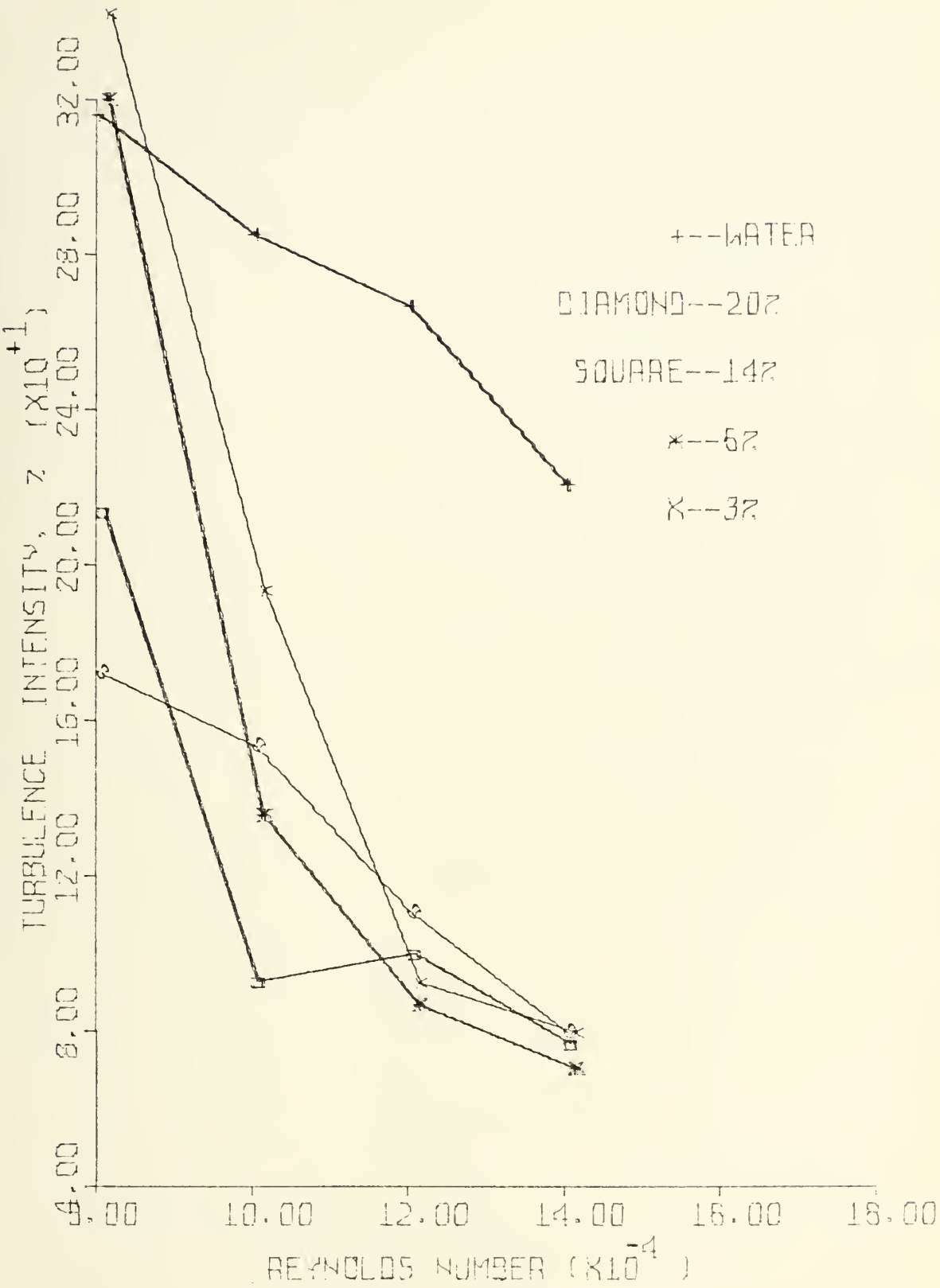

Figure 58: TURBULENCE INTENSITY VS. REYNOLDS NUMBER AT X/DIAM = +1.5, Y/DIAM = +2.0; TAP WATER AND VARIOUS PDR's

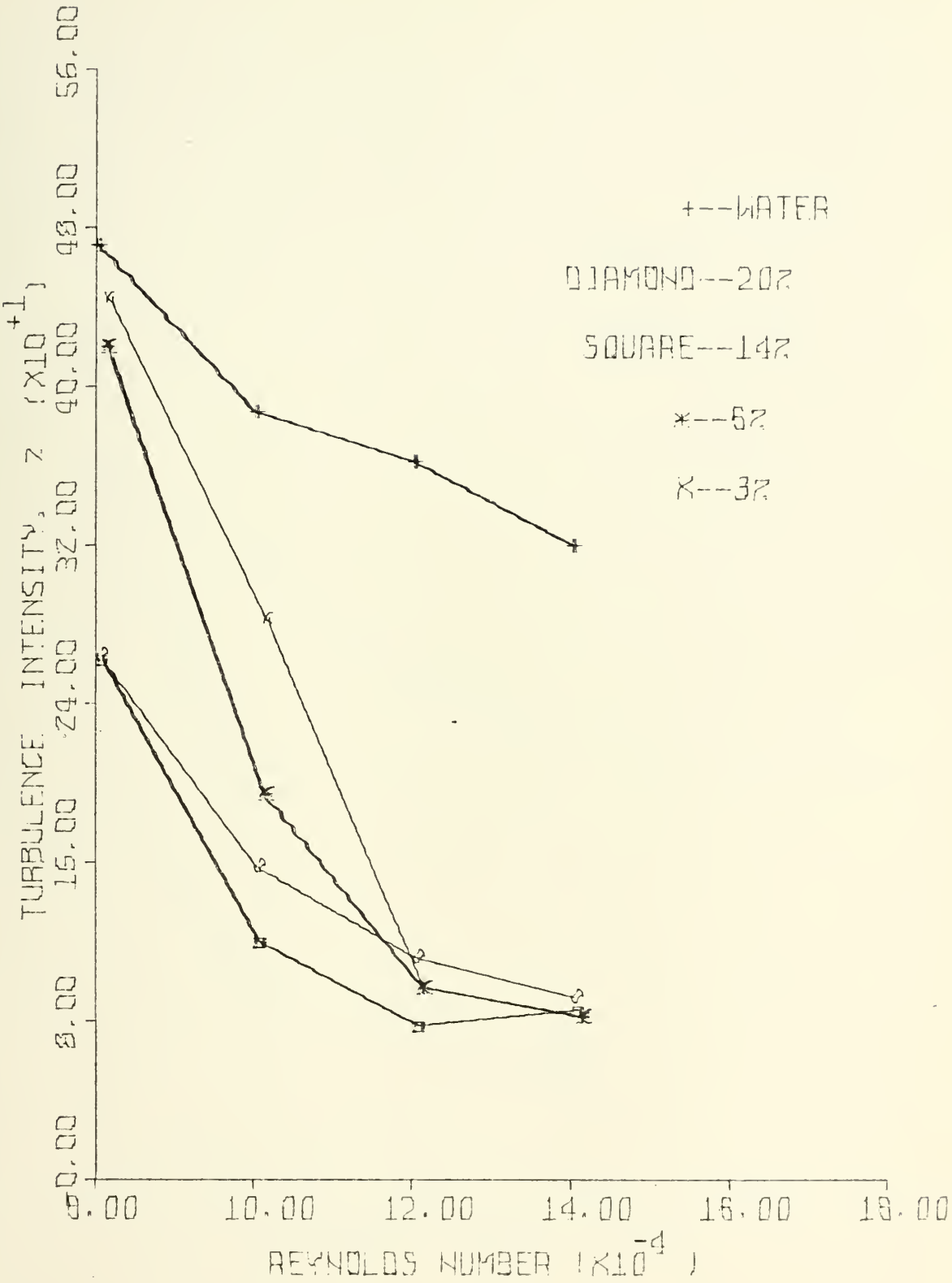

Figure 59: TURBULENCE INTENSITY VS. REYNOLDS NUMBER AT X/DIAM = +1.5, Y/DIAM = +1.75; TAP WATER AND VARIOUS PDR's

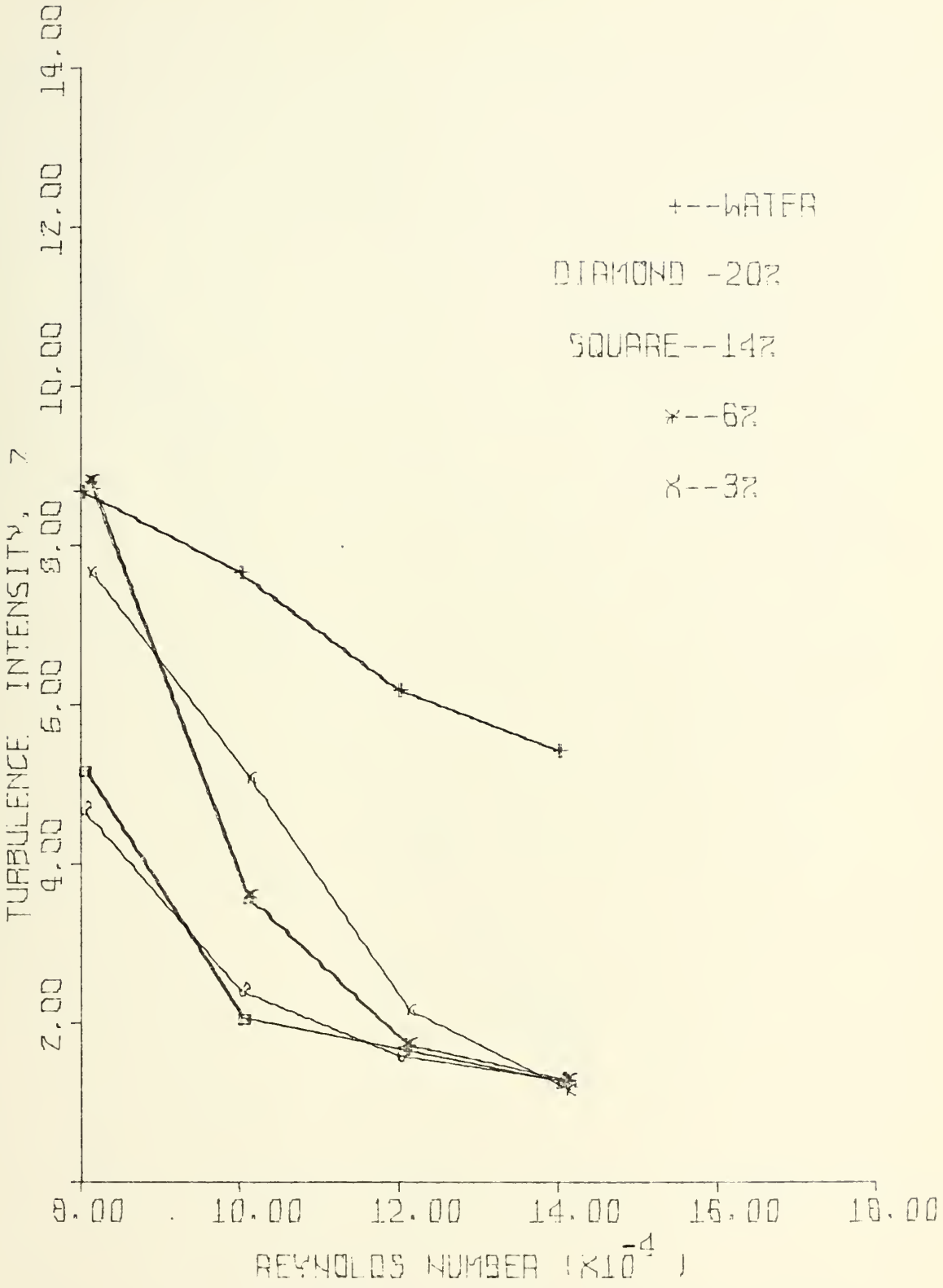

Figure 60: TURBULENCE INTENSITY VS. REYNOLDS NUMBER AT X/DIAM = +1.5, Y/DIAM = +1.25; TAP WATER AND VARIOUS PDR's

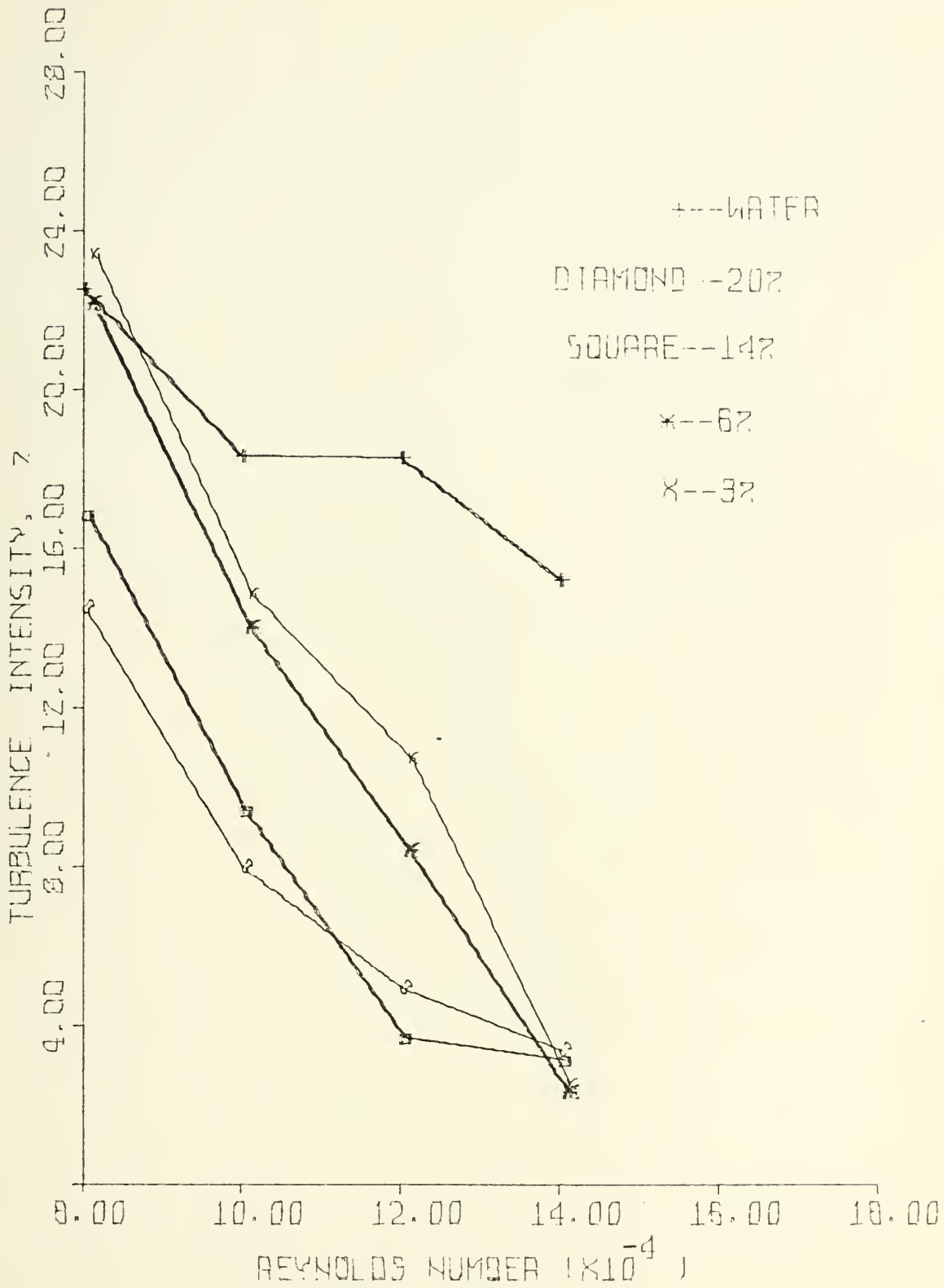

Figure 61: TURBULENCE INTENSITY VS. REYNOLDS NUMBER AT X/DIAM = +1.5, Y/DIAM = +0.75; TAP WATER AND VARIOUS PDR's

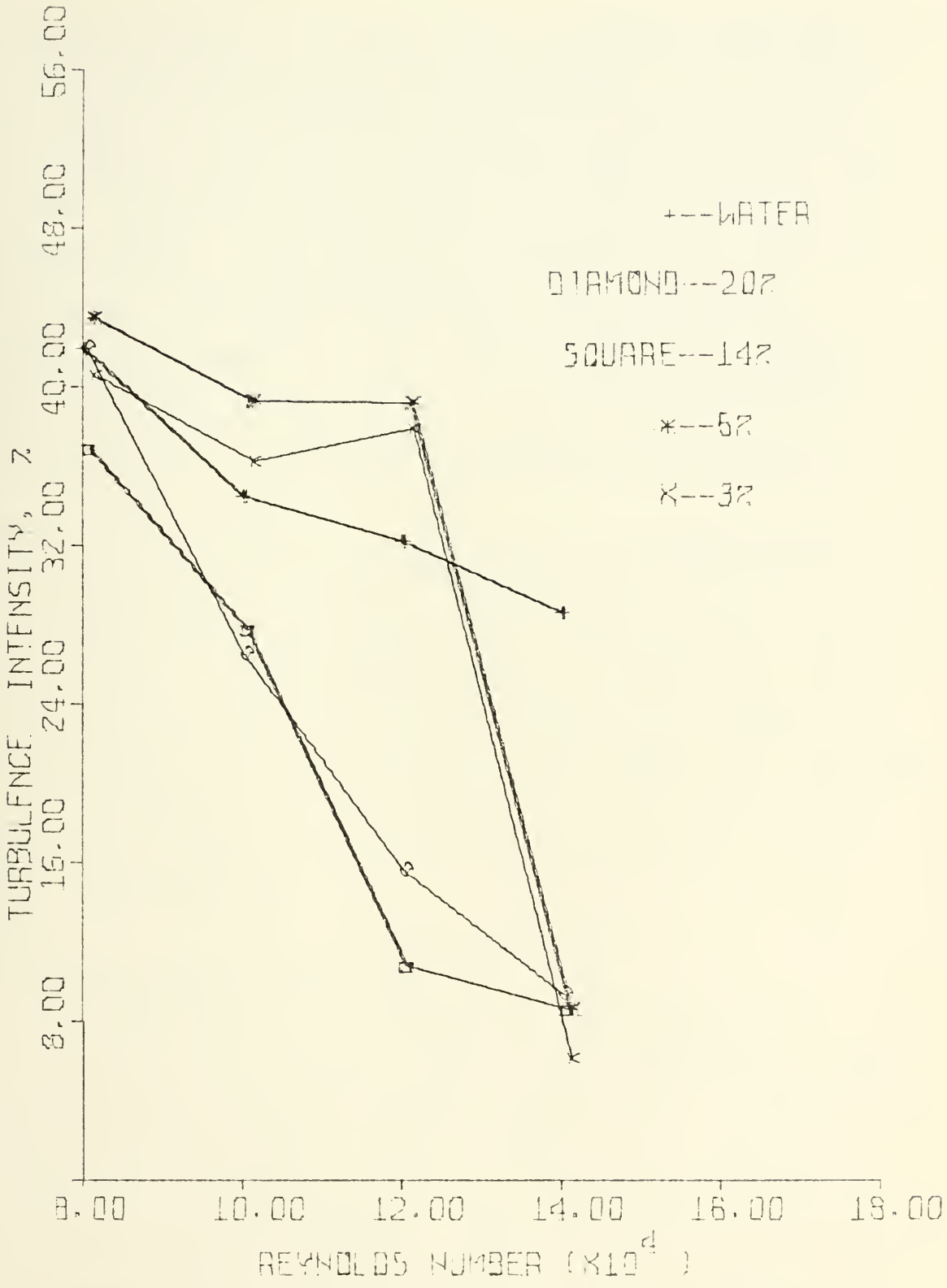

Figure 62: TURBULENCE INTENSITY VS. REYNOLDS NUMBER AT S/DIAM = +1.5, Y/DIAM = +0.50; TAP WATER AND VARIOUS PDR's

in polymer solution of 20% PDR and 14% PDR was suppressed; that is, turbulence intensity had decreased. At 6% and 3% PDR's, however, the turbulence intensity had increased to the level observed in water flow. At a Reynolds Number of 100,000, however, both the 6% PDR and the 3% PDR turbulence intensities were greatly decreased. This indicated a reduction of diffusion to that point in the flow field, due to the increased free stream velocity. Above this Reynolds Number, the diffusion characteristics did not change at this point.

As the points under consideration approached the wake, it was observed that diffusion from the wake to that point increased for a given Reynolds Number of 80,000 and 100,000. At a Reynolds Number of 120,000, an increase in diffusion was first observed at a position +0.75 Y/DIAM. At a Reynolds Number of 140,000, no increase was observed for the PDR's under consideration.

F. MICROSCALE OF TURBULENCE MEASUREMENTS

The microscale of turbulence was measured at an X-coordinate of +1.5 X/DIAM. Results were obtained for the Reynolds Number 80,000, 100,000, 120,000, and 140,000. The results are presented in Figs. 63 through 66, for these respective Reynolds Numbers. Each plot contains the measured microscale profile obtained with water flow, and four profiles for polymer solution flow, with a range of degradation states from 74% PDR to 3% PDR.

In the region above +1.0 Y/DIAM, which was outside the wake, the following observations were made. Microscale of turbulence of the water flow maintained a relatively constant value of 0.07 feet, for all Reynolds Numbers. Polymer solution results were seen to vary with degradation state, but were also constant through the Reynolds Number range under study. It was found that maximum microscale was present at the highest PDR. The microscale progressively decreased with PDR, reached a minimum, and then increased as PDR approached zero. Minimum microscale was observed at a moderately high PDR of 34% to 38% throughout the Reynolds Number range, for the region outside the wake. Generally, the microscale outside the wake of polymer solution flow was reduced to approximately 50% of that obtained with water flow. At high PDR, microscale was found to be 0.045 feet. At moderate PDR, microscale was decreased to the minimum of 0.03 feet. At 14% PDR, microscale had increased to 0.04 feet, and at a minimum PDR of 3%, microscale was found to increase further to approximately 0.045 feet.

Inside the wake region, only a small difference in microscale was observed between polymer solution flow and water flow. The same general trend was preserved, however. Due to the high susceptibility of error in this region, little more can be said.

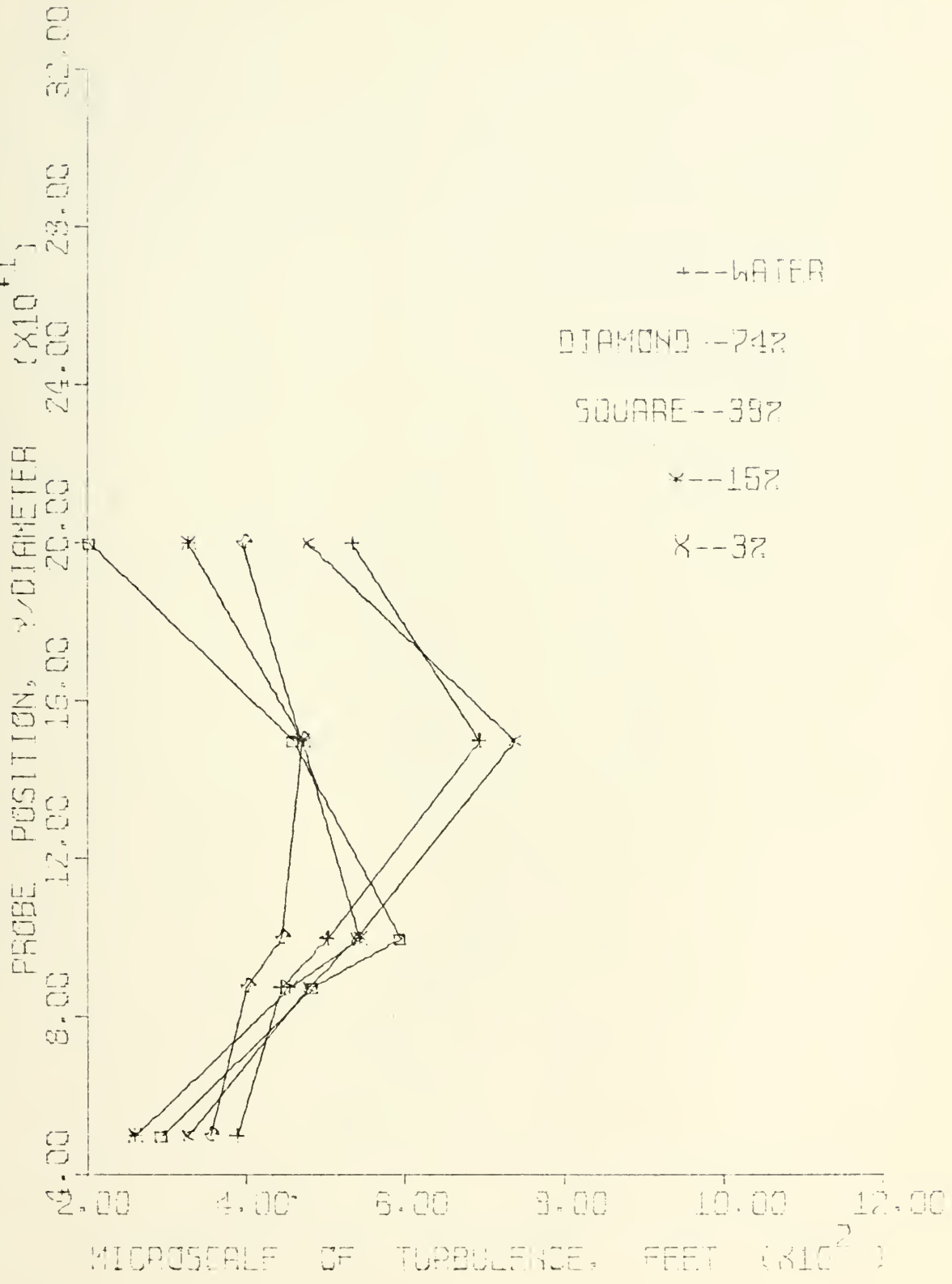

Figure 63: MICROSCALE OF TURBULENCE PROFILES AT X/DIAM = +1.5; RE No = 80,000; TAP WATER AND VARIOUS PDR's

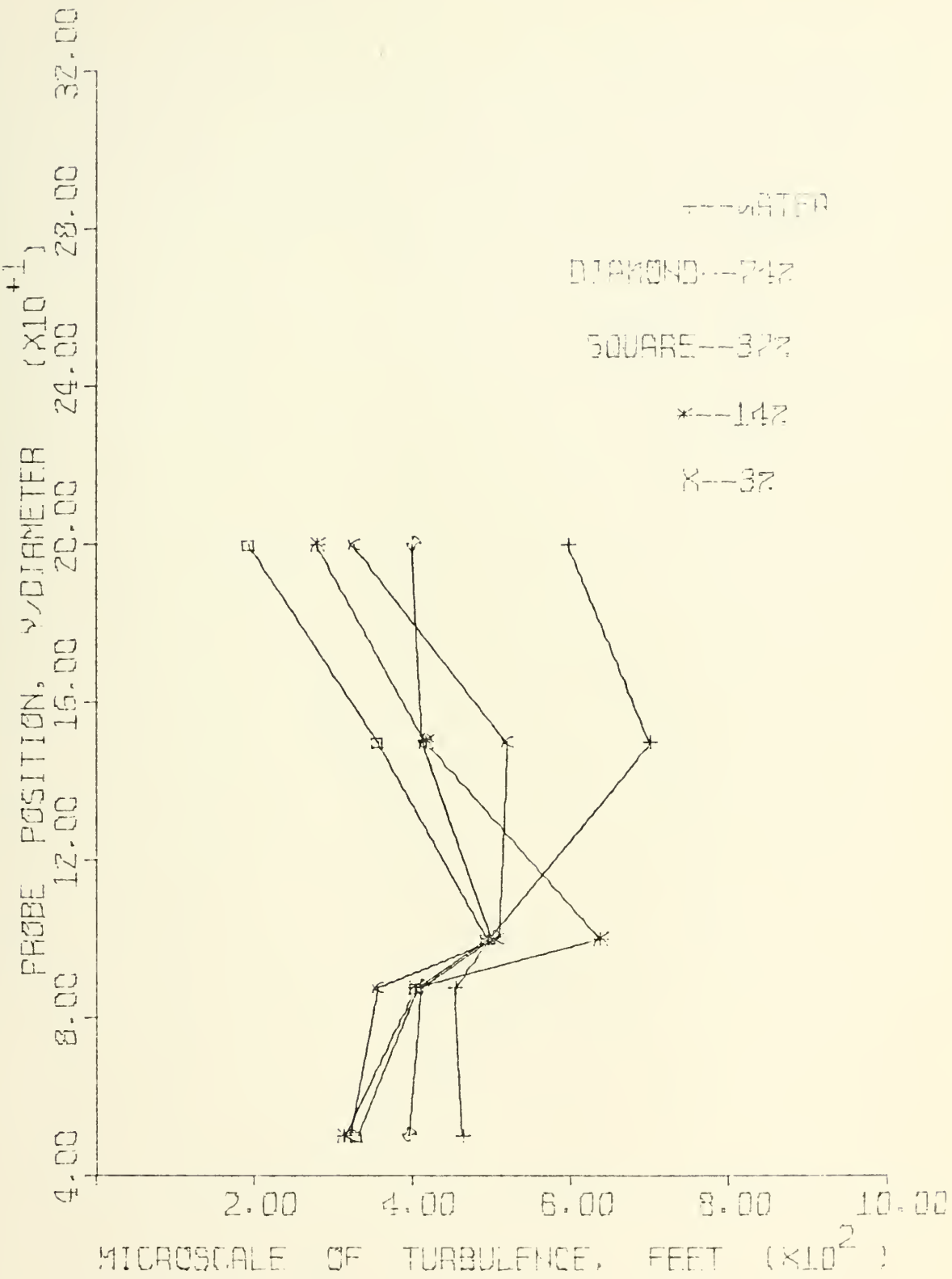

Figure 64: MICROSCALE OF TURBULENCE PROFILES AT X/DIAM = +1.5; RE No = 100,000; TAP WATER AND VARIOUS PDR's

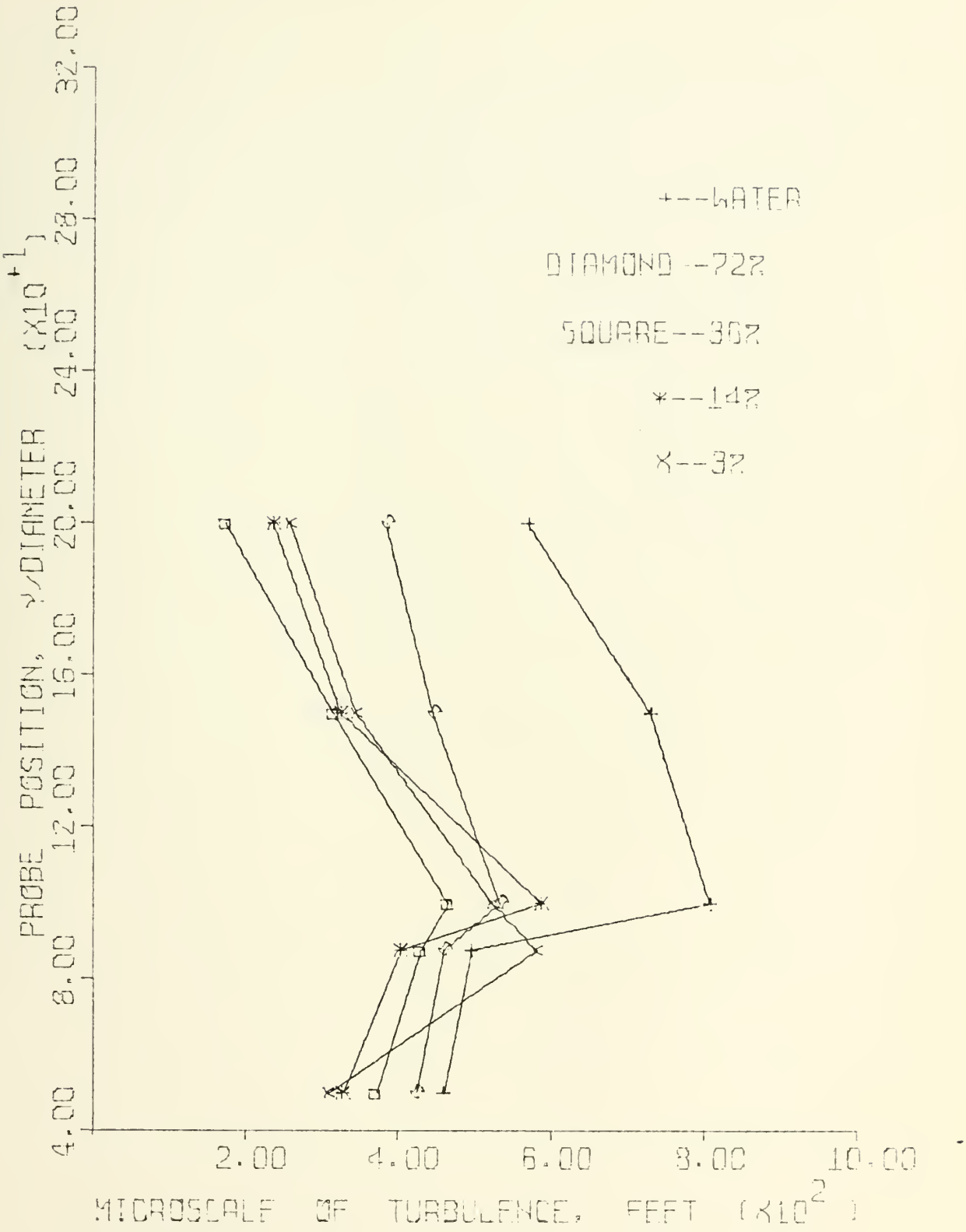

Figure 65: MICROSCALE OF TURBULENCE PROFILES AT X/DIAM = +1.5; RE No = 120,000; TAP WATER AND VARIOUS PDR's

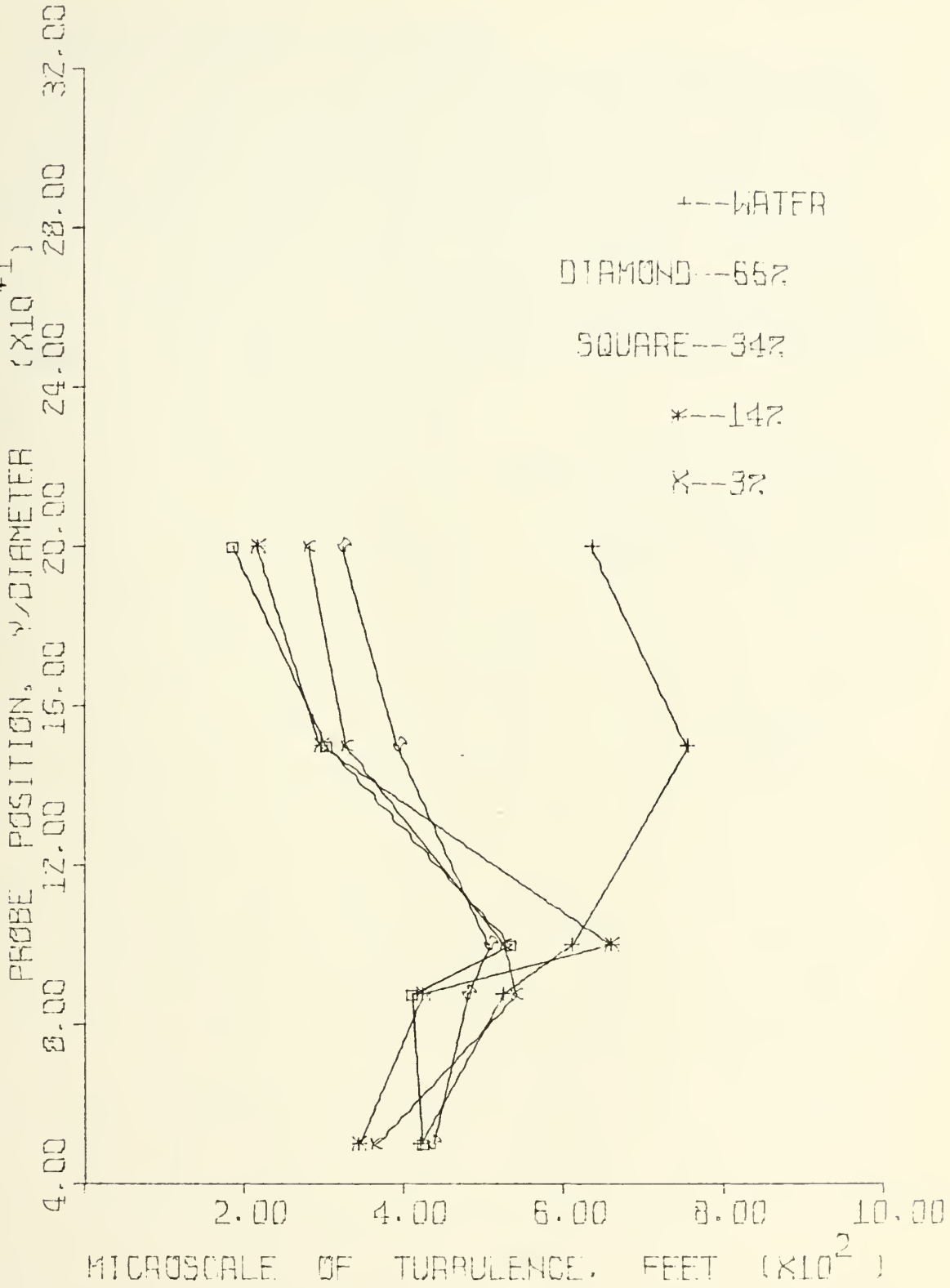

Figure 66: MICROSCALE OF TURBULENCE PROFILES AT X/DIAM = +1.5; RE No = 140,000; TAP WATER AND VARIOUS PDR's

G. FREQUENCY SPECTRUM MEASUREMENTS

Frequency spectra were obtained for five points in the flow field, at an X-coordinate of +1.5 X/DIAM, and the four Reynolds Numbers 80,000, 100,000, 120,000, and 140,000. The data are presented in Figs. 67 through 86. Each plot presents the spectra, at a point in the flow field and for a given Reynolds Number, for water flow and four degradation states of polymer solution flow.

The spectra obtained for the Reynolds Number 80,000 are presented in Figs. 67 through 71. The plots present spectra at Y-coordinates of +2.0 Y/DIAM, +1.5 Y/DIAM, +1.0 Y/DIAM, +0.875 Y/DIAM, and +0.75 Y/DIAM, respectively. At this Reynolds Number, a strong predominant frequency was observed at all points observed for water flow. This predominant frequency was the Strouhal frequency of vortex shedding.

For polymer solution flow, the entire spectra exhibited RMS values much lower than those obtained in water flow. The predominant frequency was also suppressed as the PDR decreased. A maximum suppression was observed at a PDR of 15%, at all five points. The predominant frequency amplitude then increased, and approached the RMS value obtained for water flow. As the points progressed toward the wake, the Strouhal frequency became more predominant, at all degradation states observed, at this Reynolds Number.

The frequency spectra for water flow and polymer solution for a Reynolds Number of 100,000 at the five points under observation are presented in Figs. 72 through 76. The spectra

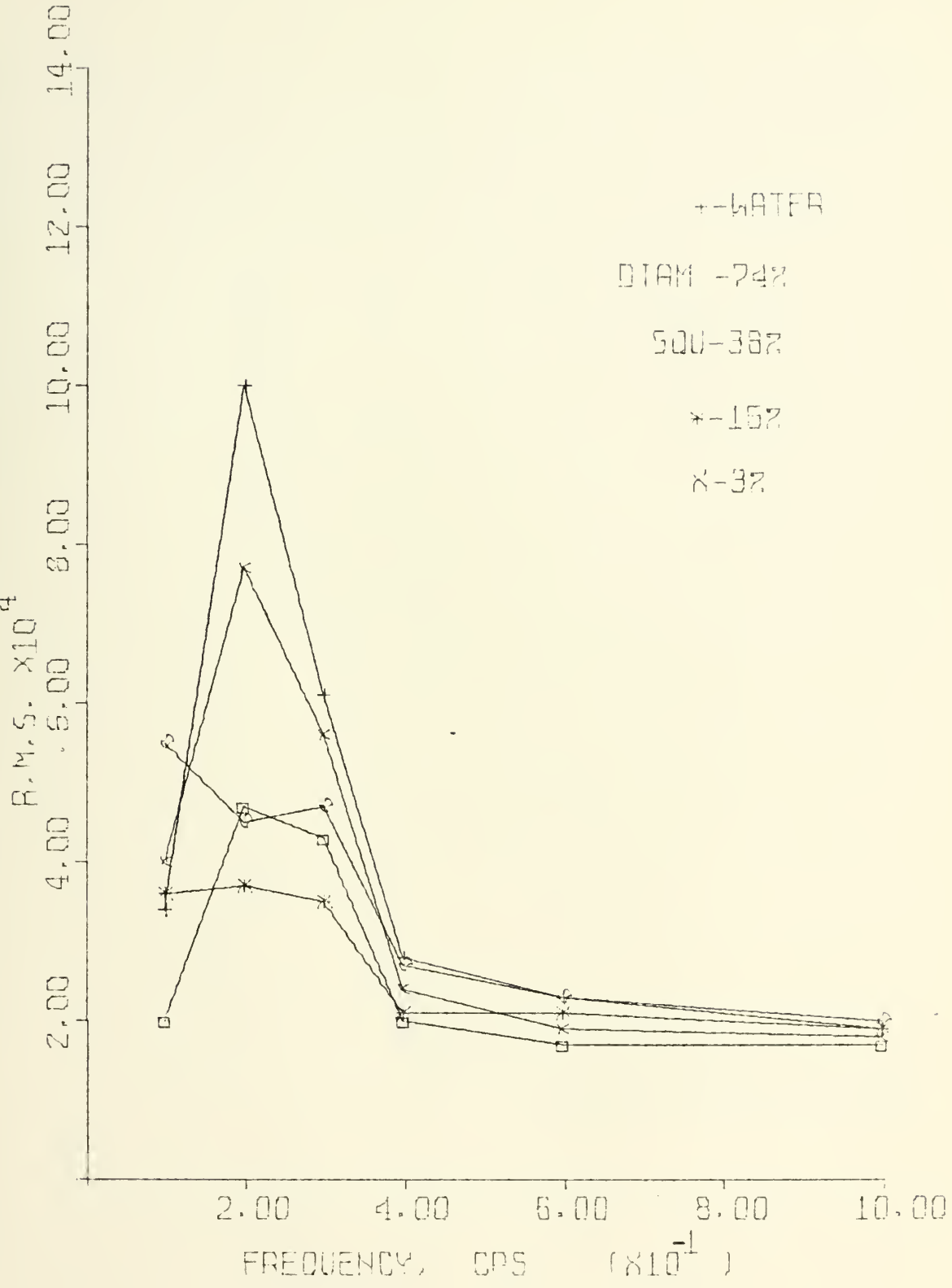

Figure 67: FREQUENCY SPECTRUM FOR TAP WATER AND VARIOUS PDR's AT X/DIAM = +1.5, Y/DIAM = +2.0; RE No = 80,000

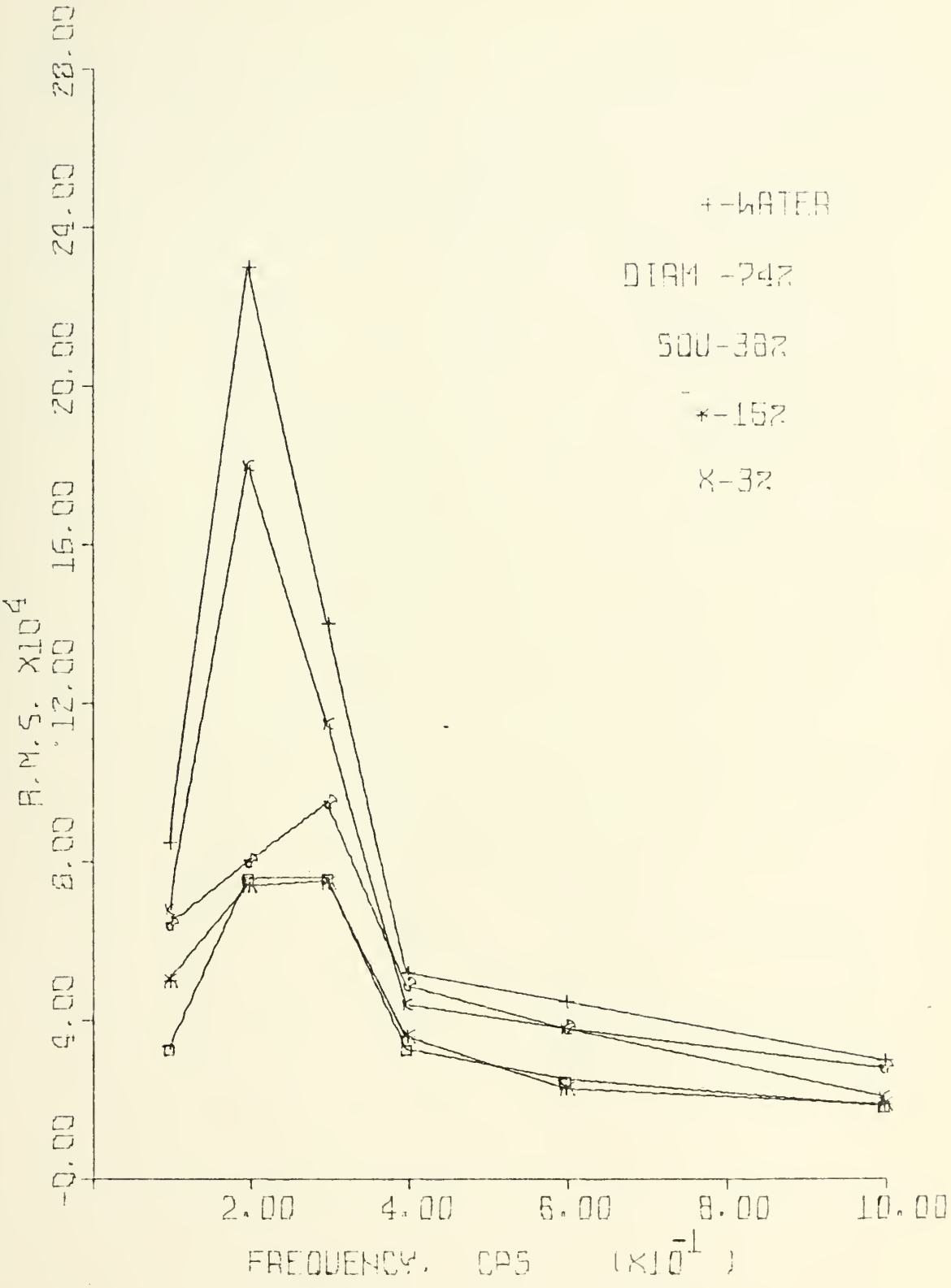

Figure 68: FREQUENCY SPECTRUM FOR TAP WATER AND VARIOUS PDR's AT X/DIAM = +1.5, Y/DIAM = +1.5; RE No = 80,000

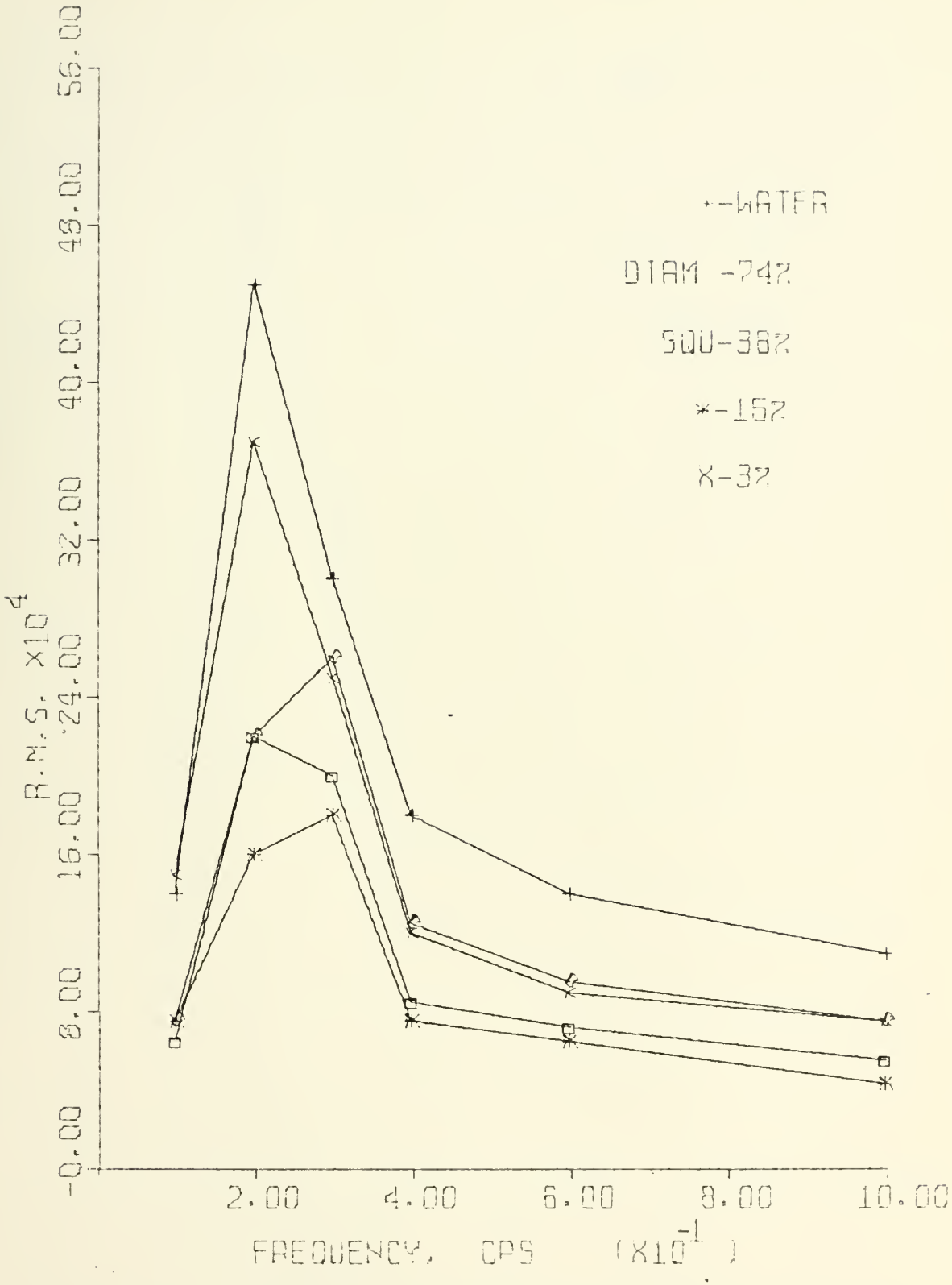

Figure 69: FREQUENCY SPECTRUM FOR TAP WATER AND VARIOUS PDR's AT X/DIAM = +1.5, Y/DIAM = +1.0; RE No = 80,000

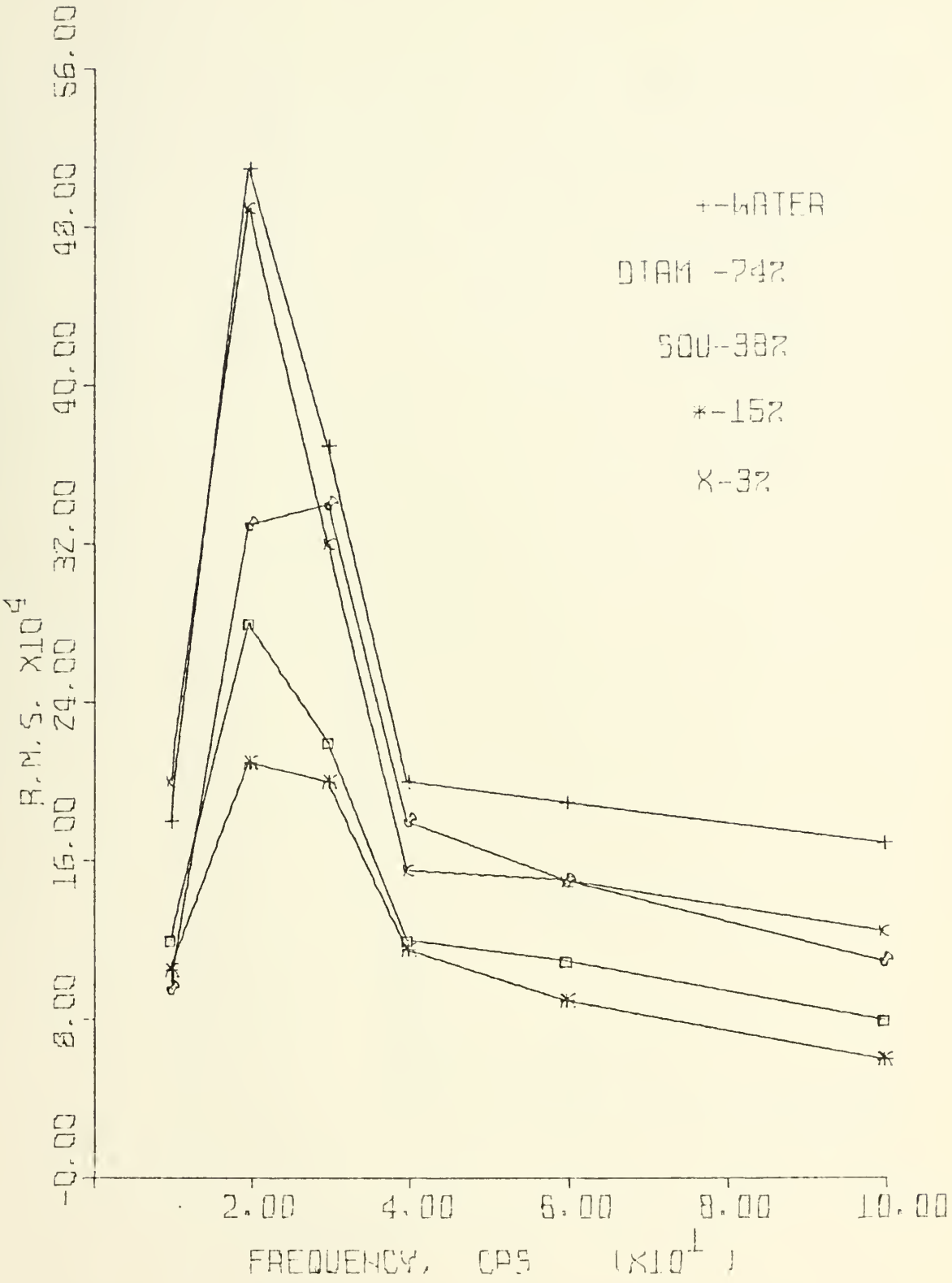

Figure 70: FREQUENCY SPECTRUM FOR TAP WATER AND VARIOUS PDR's AT X/DIAM = +1.5, Y/DIAM = +0.875; RE No = 80,000

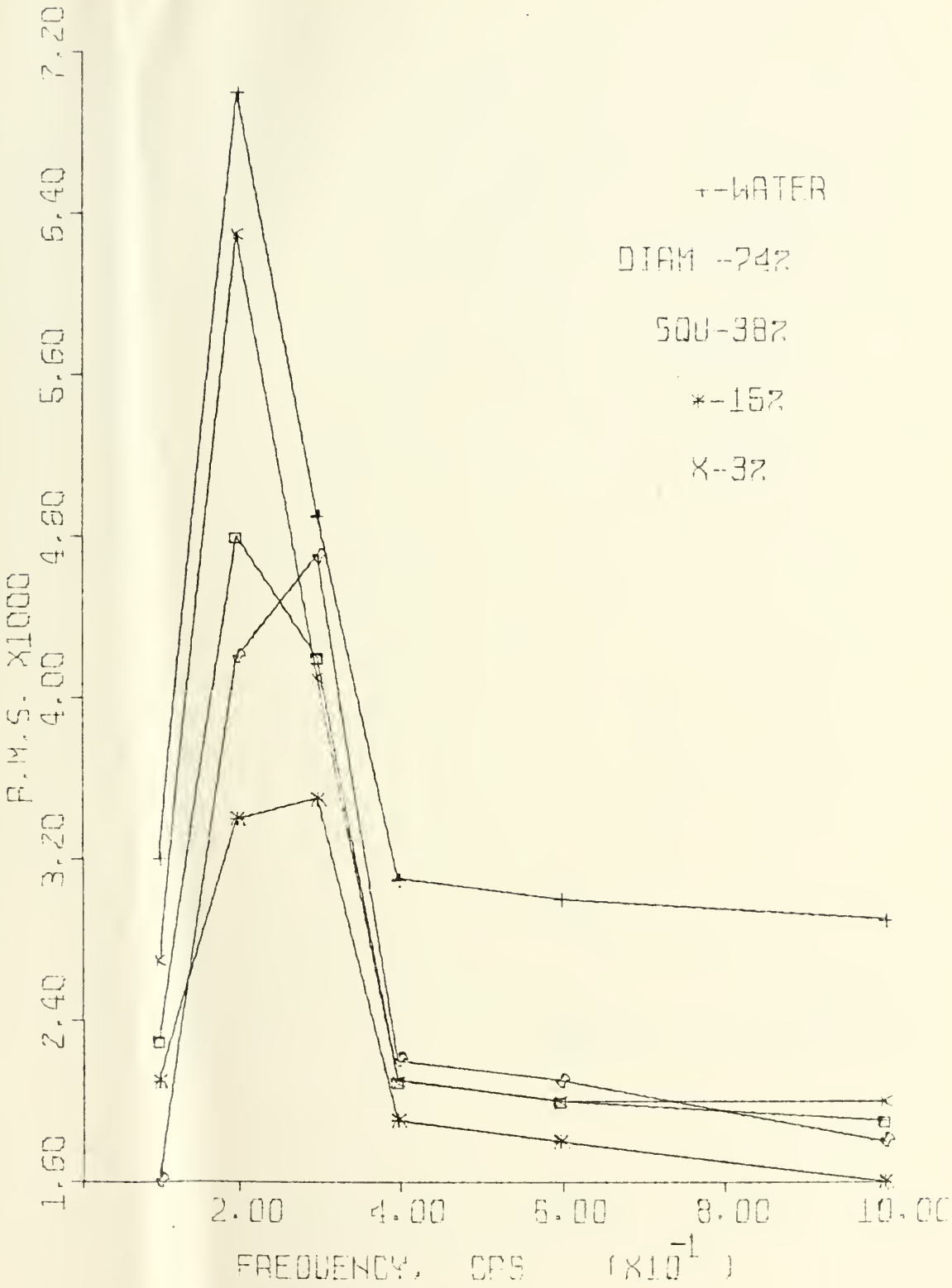

Figure 71: FREQUENCY SPECTRUM FOR TAP WATER AND VARIOUS PDR's AT X/DIAM = +1.5, Y/DIAM = +0.75; RE No = 80,000

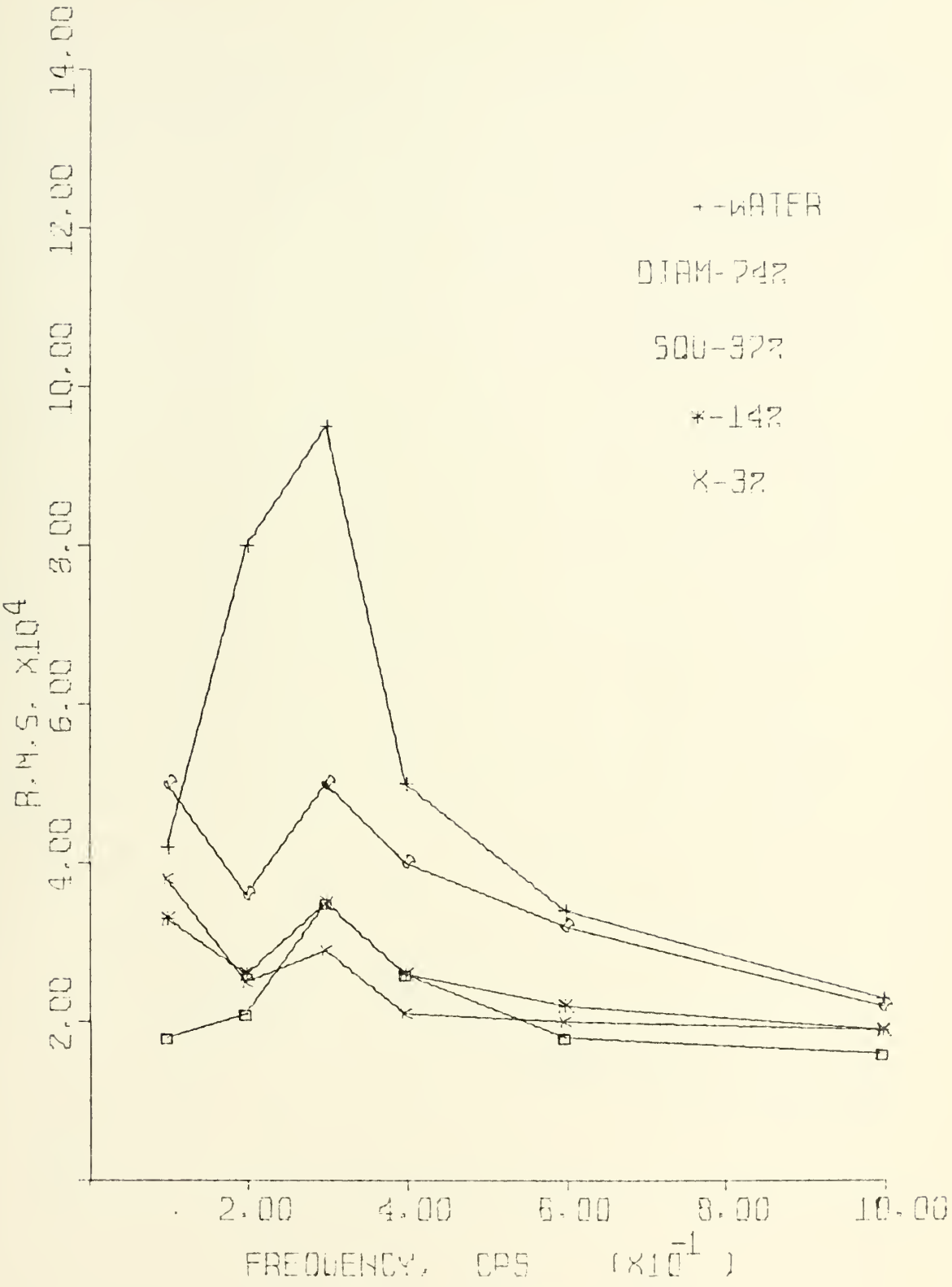

Figure 72: FREQUENCY SPECTRUM FOR TAP WATER AND VARIOUS PDR's AT X/DIAM = +1.5, Y/DIAM = +2.0; RE No = 100,000

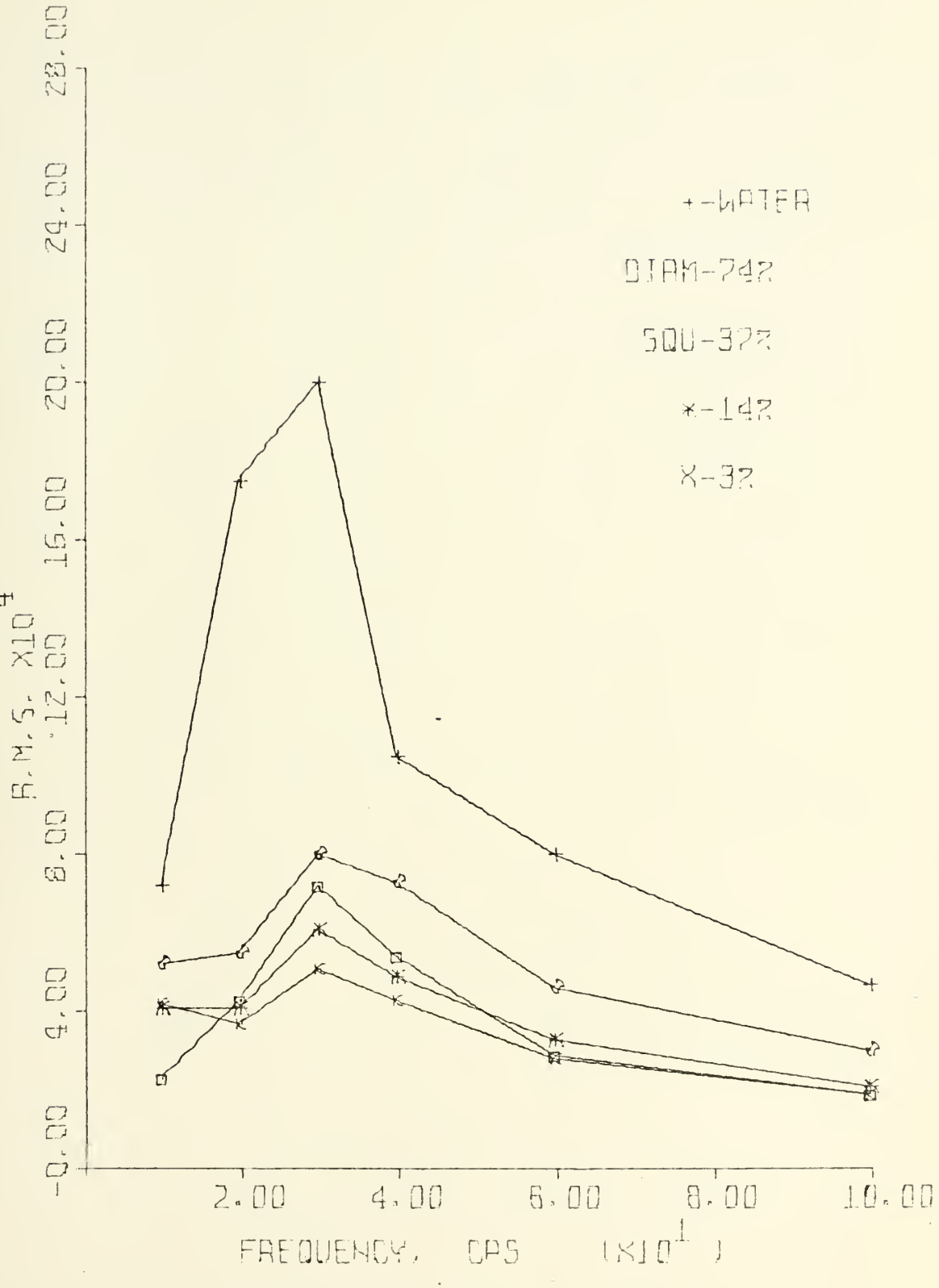

Figure 73: FREQUENCY SPECTRUM FOR TAP WATER AND VARIOUS PDR's AT X/DIAM = +1.5, Y/DIAM = +1.5; RE No = 100,000

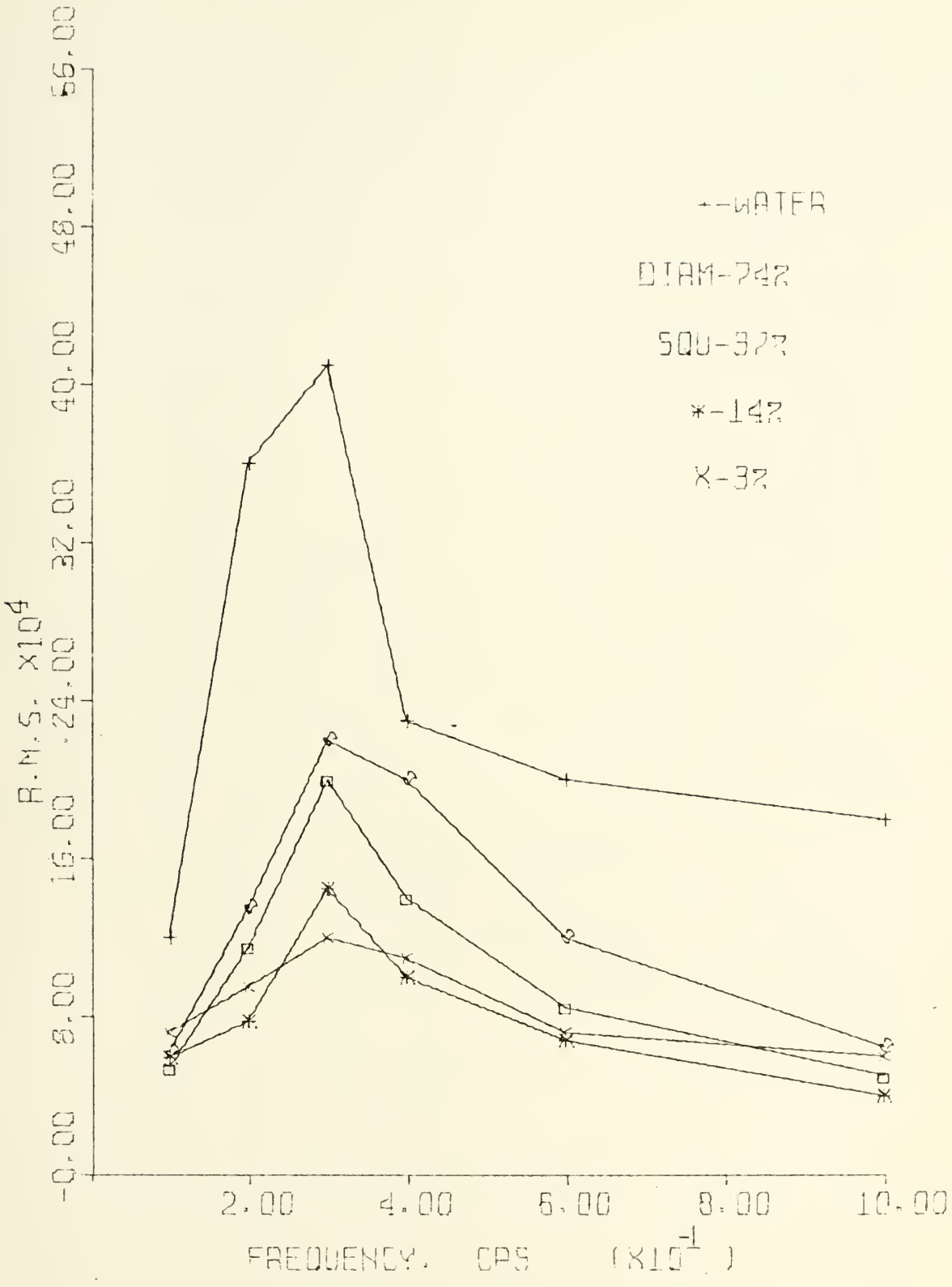

Figure 74: FREQUENCY SPECTRUM FOR TAP WATER AND VARIOUS PDR's AT X/DIAM = +1.5, Y/DIAM = +1.0; RE No = 100,000

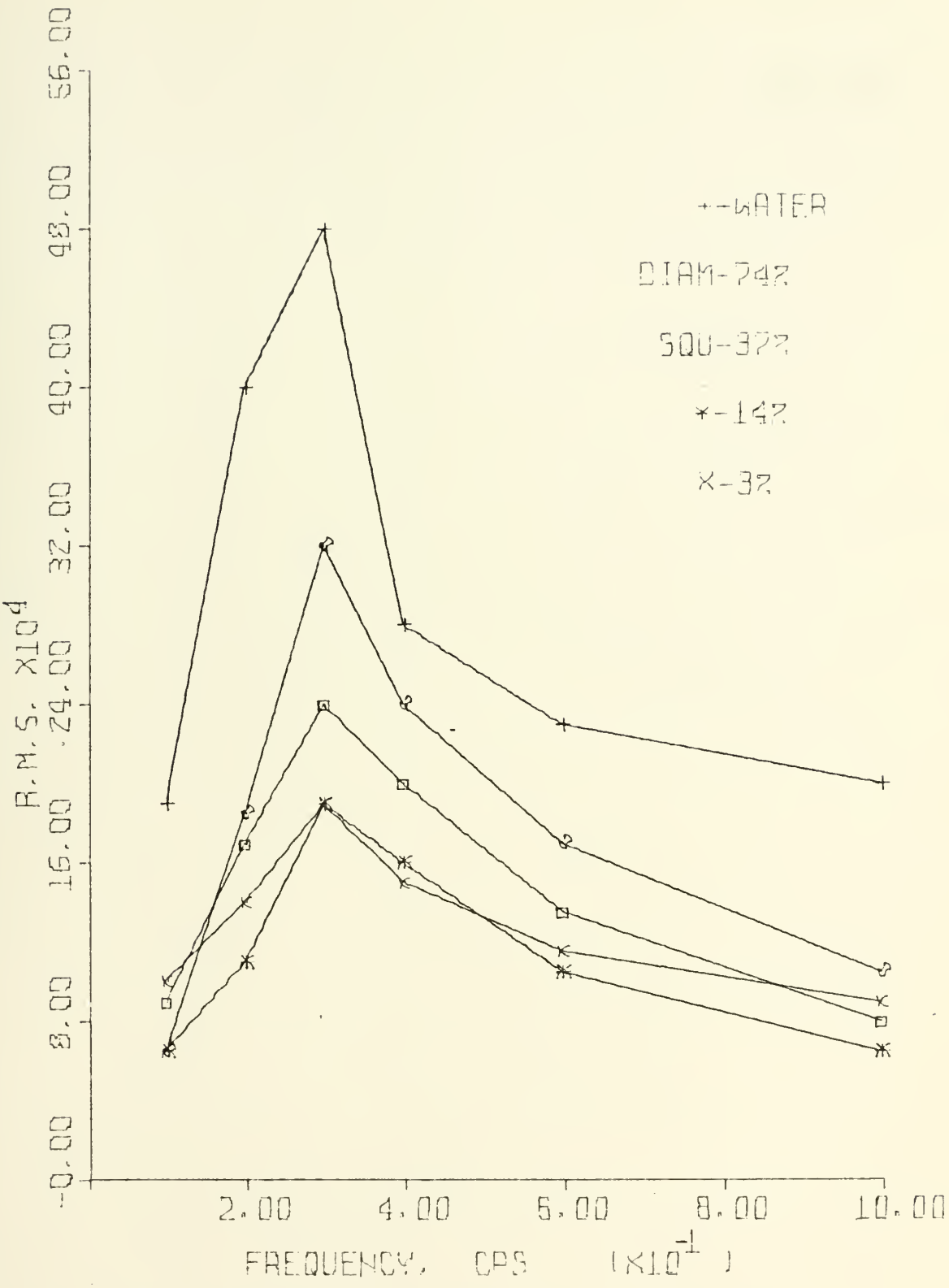

Figure 75: FREQUENCY SPECTRUM FOR TAP WATER AND VARIOUS PDR's AT X/DIAM = +1.5, Y/DIAM = +0.875; RE No = 100,000

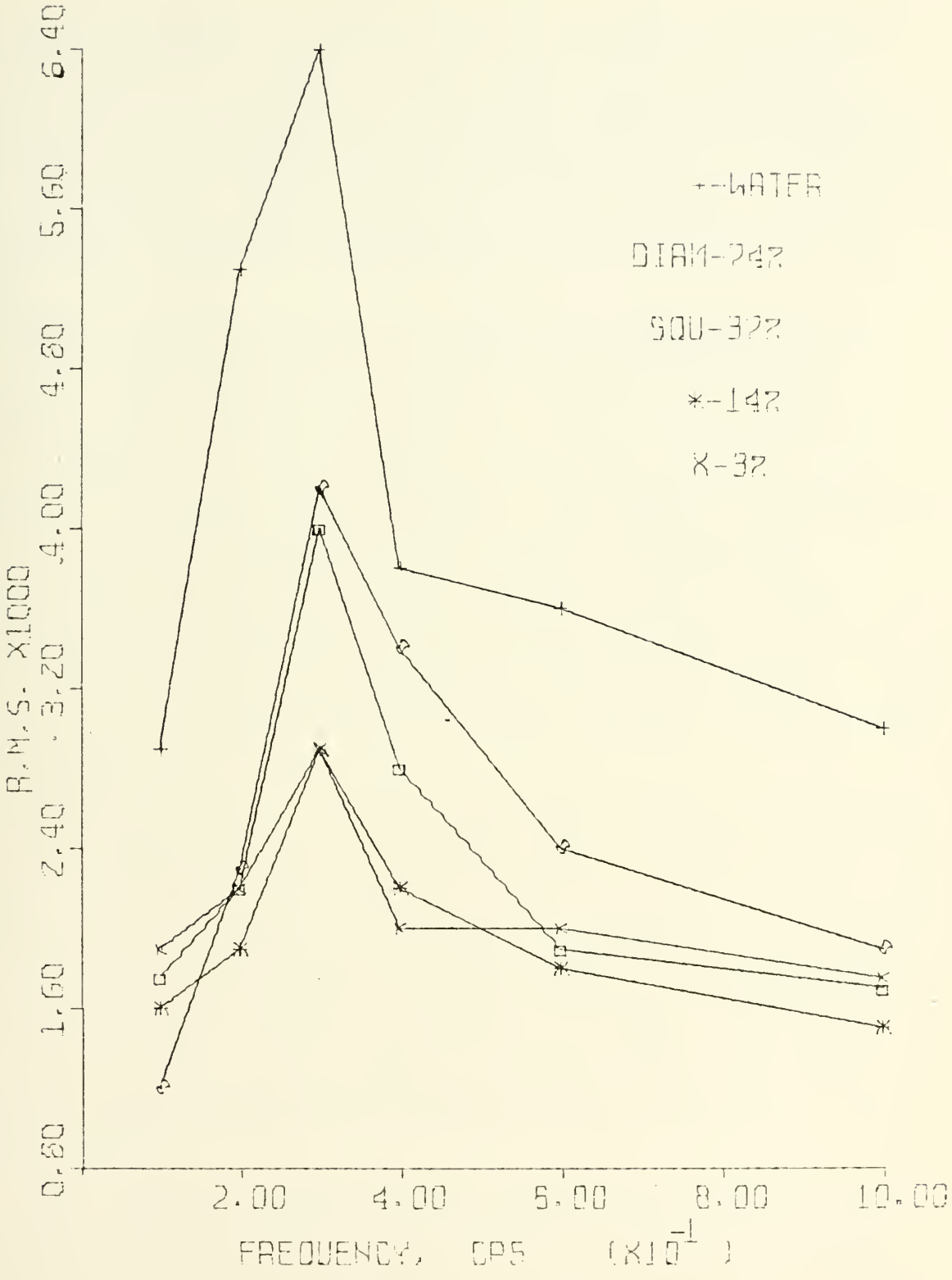

Figure 76: FREQUENCY SPECTRUM FOR TAP WATER AND VARIOUS PDR's AT X/DIAM = +1.5, Y/DIAM = +0.75; RE No = 100,000

obtained for polymer solution flow were for the degradation states 74% PDR, 37% PDR, 14% PDR, and 3% PDR. The water flow spectra exhibited the predominant Strouhal frequency at all five points. The RMS of the Strouhal freuqency increased six-fold as the points progressed toward the center of the wake.

The Strouhal frequency was suppressed considerably in polymer solution flow for all PDR's at +2.0 Y/DIAM and +1.5 Y/DIAM. At +1.0 Y/DIAM, the Strouhal frequency was evident at 37% PDR, but was greatly diminished at 14% and 3% PDR. At +0.875 Y/DIAM and +0.75 Y/DIAM, a suppressed predominant frequency was observed at the same frequency as the water flow. At this Reynolds Number, the entire spectra showed considerable suppression below the RMS values obtained with water flow.

The frequency spectra for water flow and polymer solution flow for a Reynolds Number of 120,000 at the five points under observation are presented in Figs. 77 through 81. The spectra obtained for polymer solution flow were for the degradation states 72% PDR, 36% PDR, 14% PDR, and 3% PDR. The water spectra again exhibited a strong Strouhal frequency at all five points.

The spectra in the polymer solution flow showed several characteristics not previously observed. At the low PDR's, no predominant frequency was distinguishable at +2.0 Y/DIAM, +1.5 Y/DIAM, and +1.0 Y/DIAM. At all five points, the skewness of the spectra curves was shifted to higher frequencies

as the PDR decreased. Maximum suppression was observed at a PDR of 3%.

The frequency spectra for water flow and polymer solution flow for a Reynolds Number of 140,000 at the five points under observation are presented in Figs. 82 through 86. The spectra obtained for polymer solution flow were for degradation states of 66%, 34%, 14%, and 3% PDR's. The water spectra exhibited a Strouhal frequency at all five points. The polymer solution spectra was suppressed with decreasing PDR, at all five points. The spectra also shifted to higher frequencies with decreasing PDR. A maximum suppression was observed at 3% PDR, and maximum shift to higher frequencies was also observed at 3% PDR.

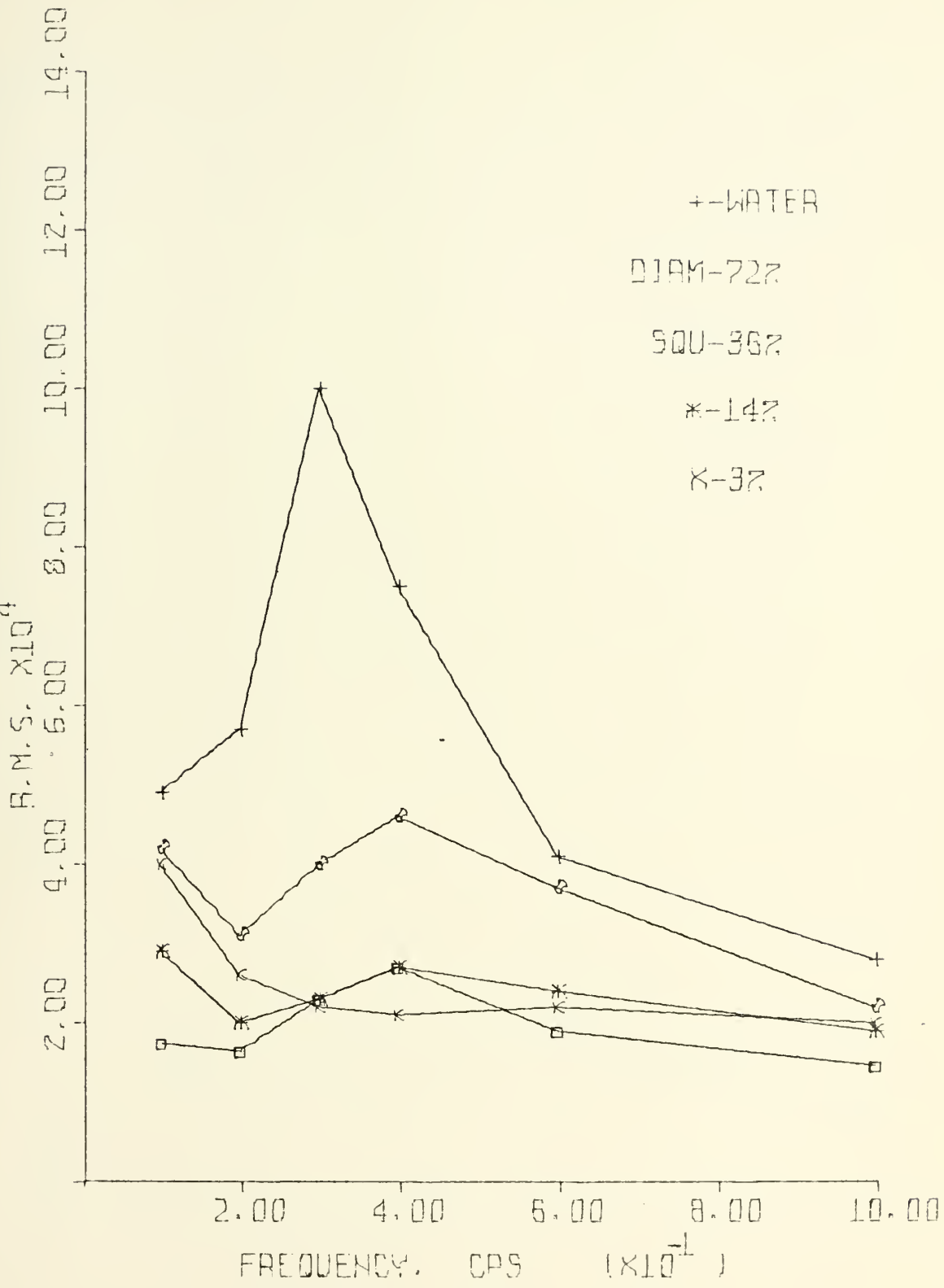

Figure 77: FREQUENCY SPECTRUM FOR TAP WATER AND VARIOUS PDR's AT X/DIAM = +1.5, Y/DIAM = +2.0; RE No = 120,000

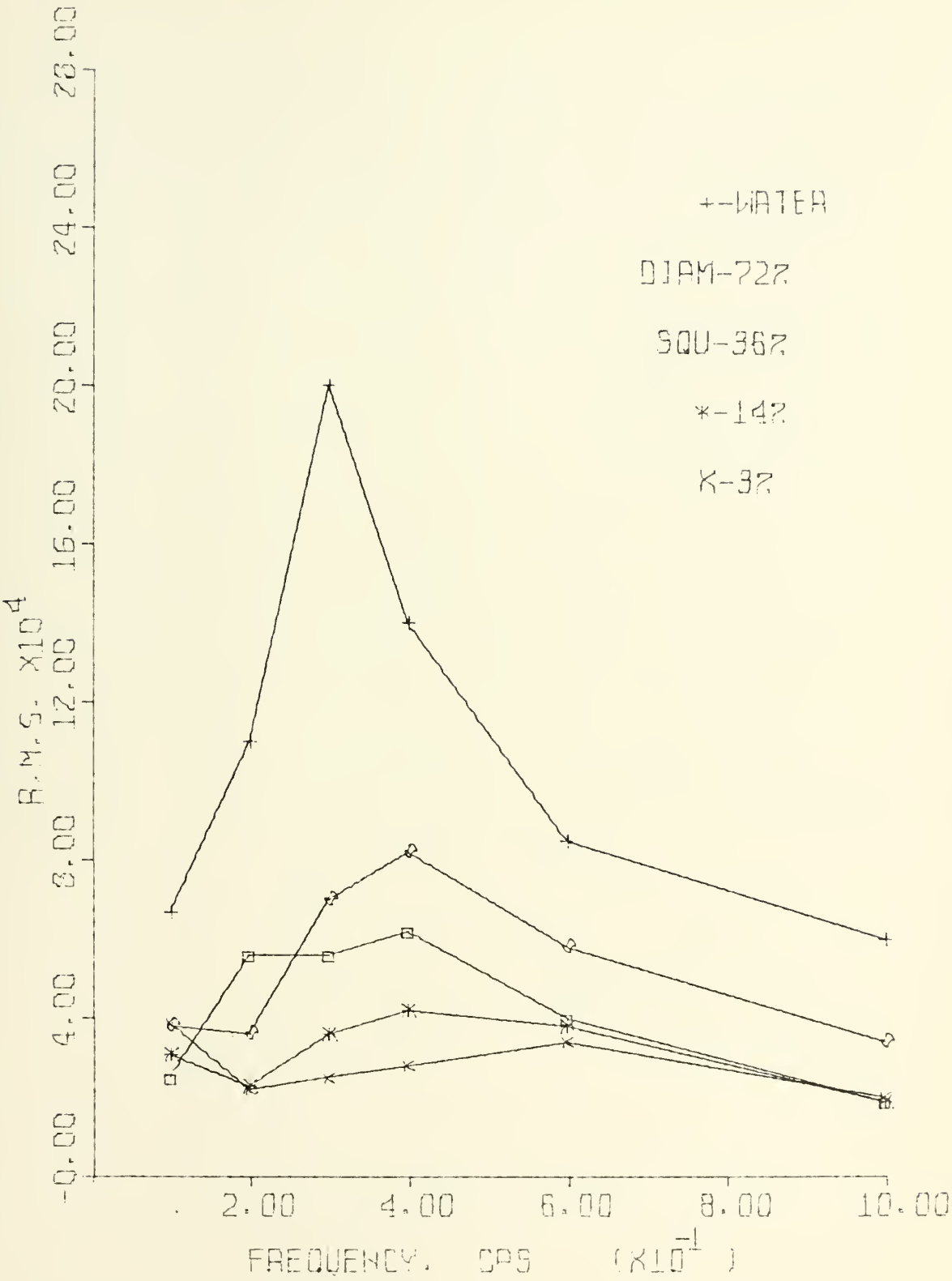

Figure 78: FREQUENCY SPECTRUM FOR TAP WATER AND VARIOUS PDR's AT X/DIAM = +1.5, Y/DIAM = +1.5; RE No = 120,000

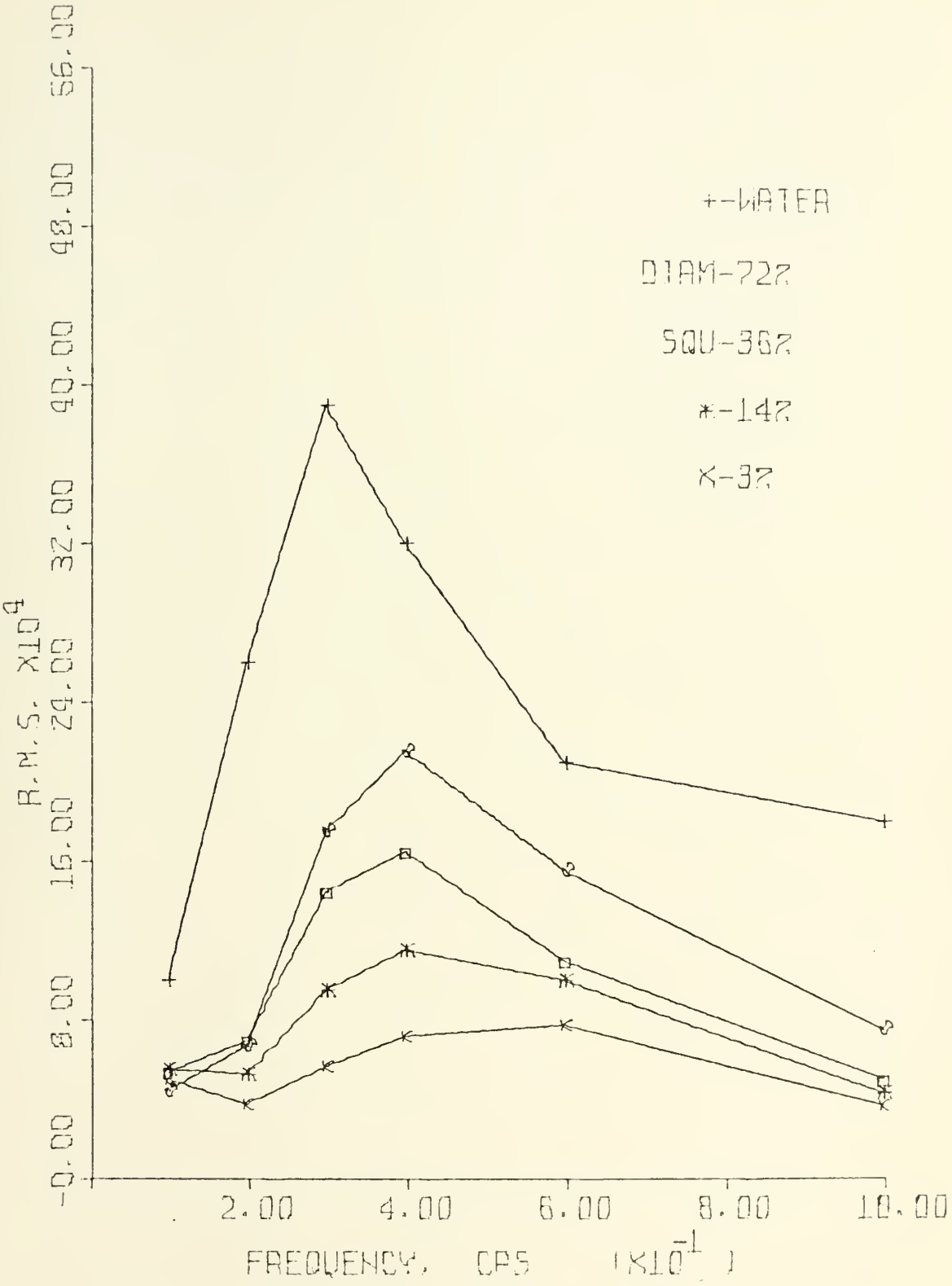

Figure 79: FREQUENCY SPECTRUM FOR TAP WATER AND VARIOUS PDR's AT X/DIAM = +1.5, Y/DIAM = +1.0; RE No = 120,000

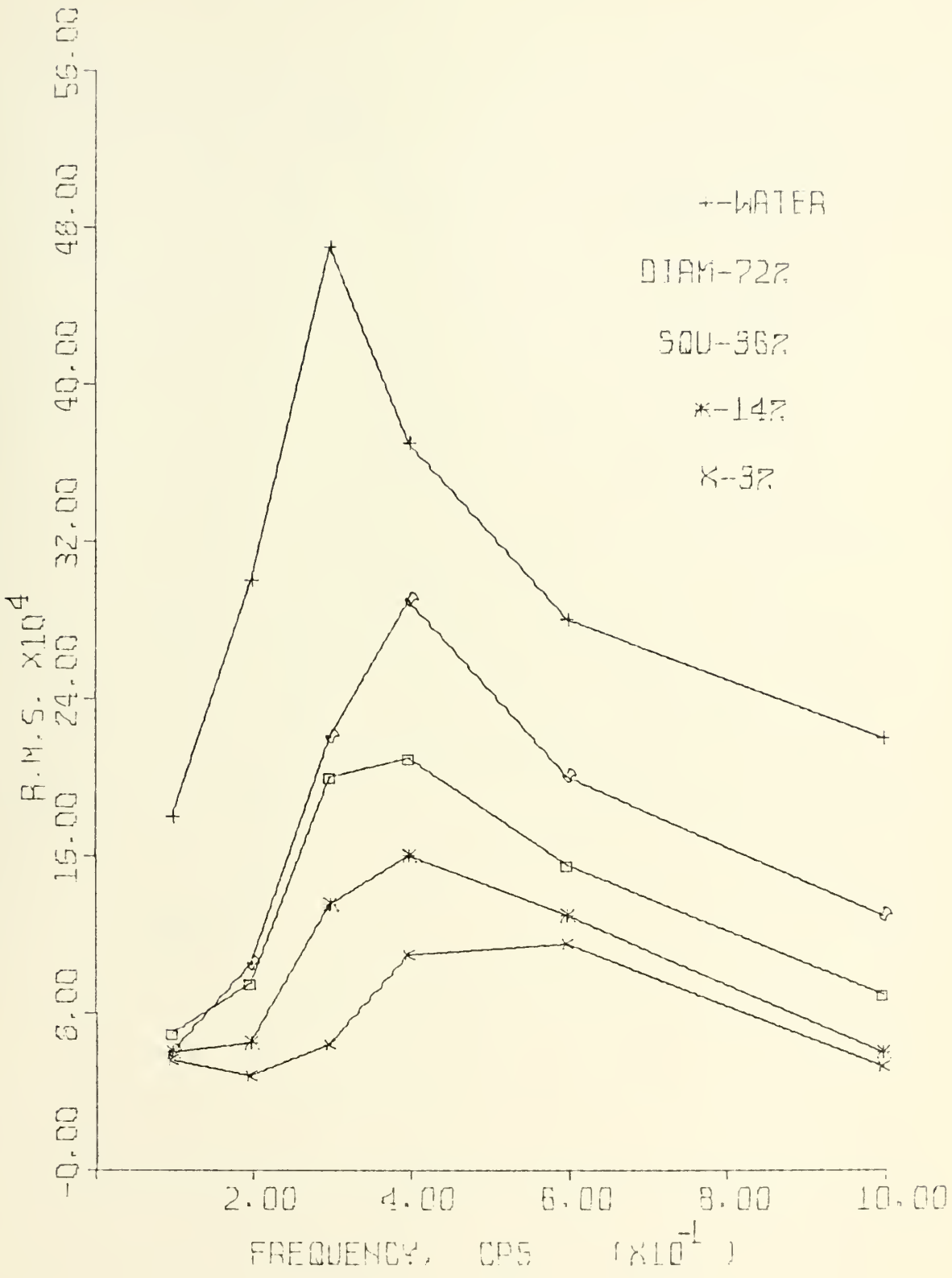

Figure 80: FREQUENCY SPECTRUM FOR TAP WATER AND VARIOUS PDR's AT X/DIAM = +1.5, Y/DIAM = +0.875; RE No = 120,000

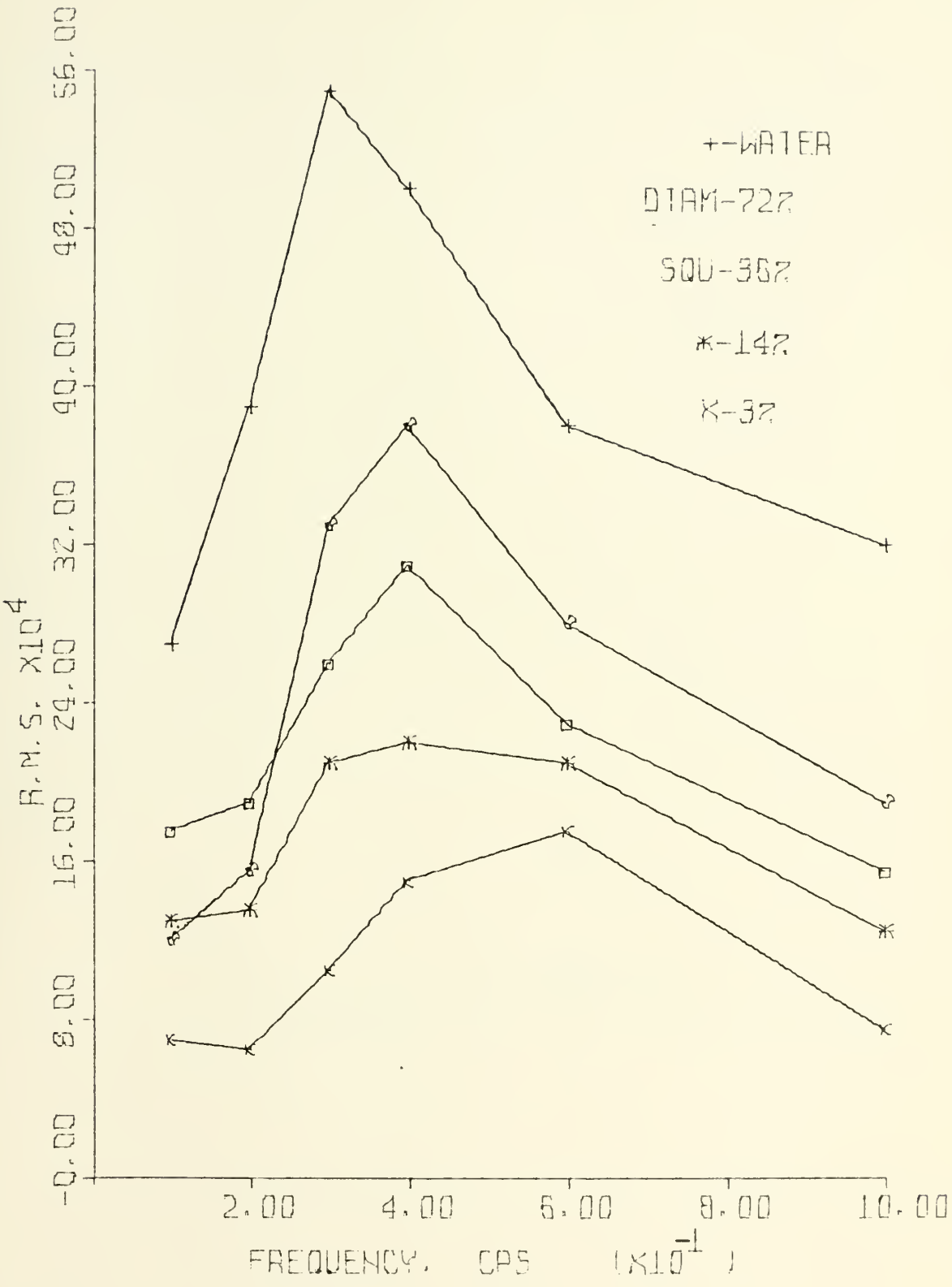

Figure 81: FREQUENCY SPECTRUM FOR TAP WATER AND VARIOUS PDR's AT X/DIAM = +1.5, Y/DIAM = +0.75; RE No = 120,000

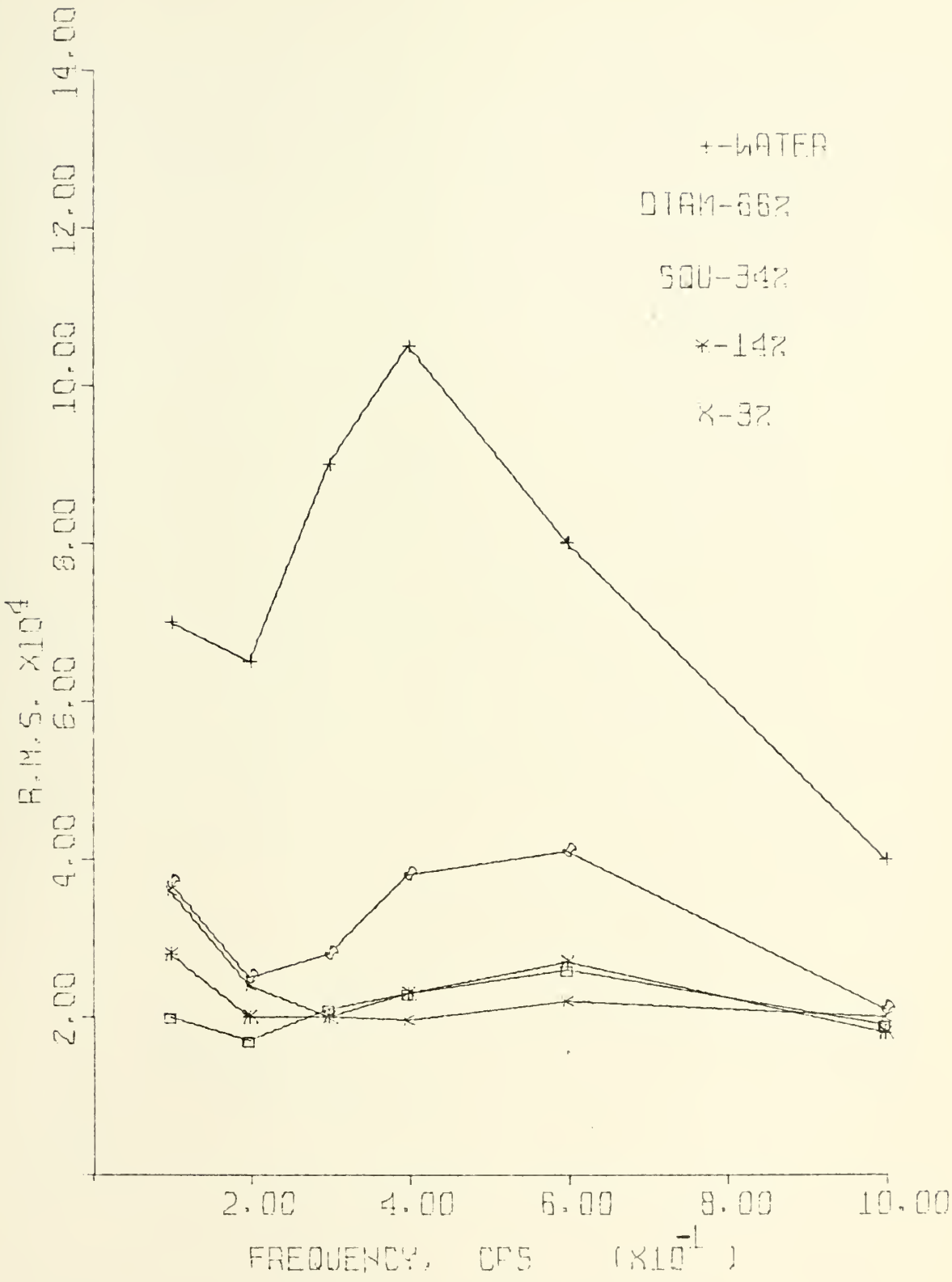

Figure 82: FREQUENCY SPECTRUM FOR TAP WATER AND VARIOUS PDR's AT X/DIAM = +1.5, Y/DIAM = +2.0; RE No = 140,000

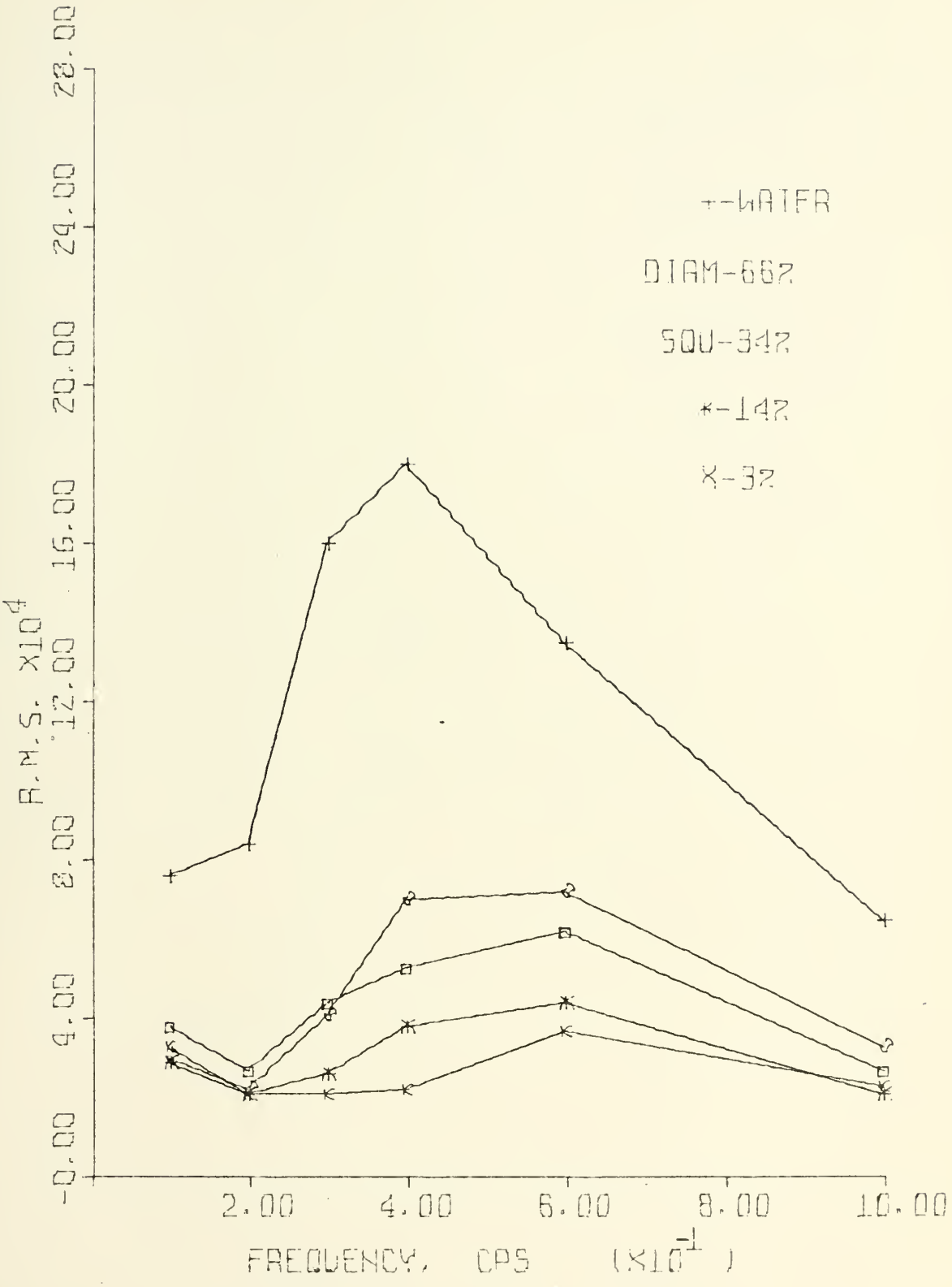

Figure 83: FREQUENCY SPECTRUM FOR TAP WATER AND VARIOUS PDR's AT X/DIAM = +1.5, Y/DIAM = +1.5; RE No = 140,000

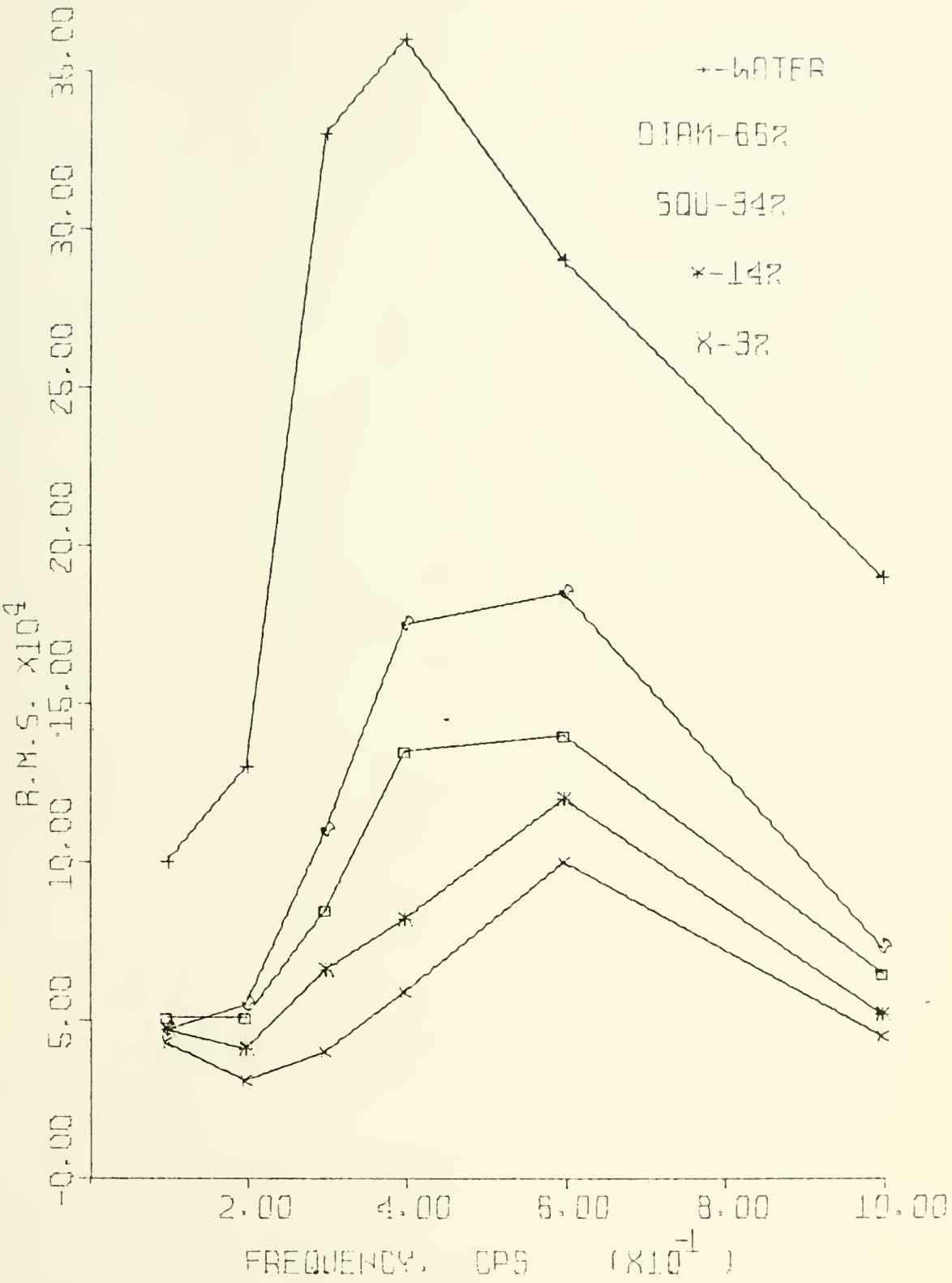

Figure 84: FREQUENCY SPECTRUM FOR TAP WATER AND VARIOUS PDR's AT X/DIAM = +1.5, Y/DIAM = +1.0; RE No = 140,000

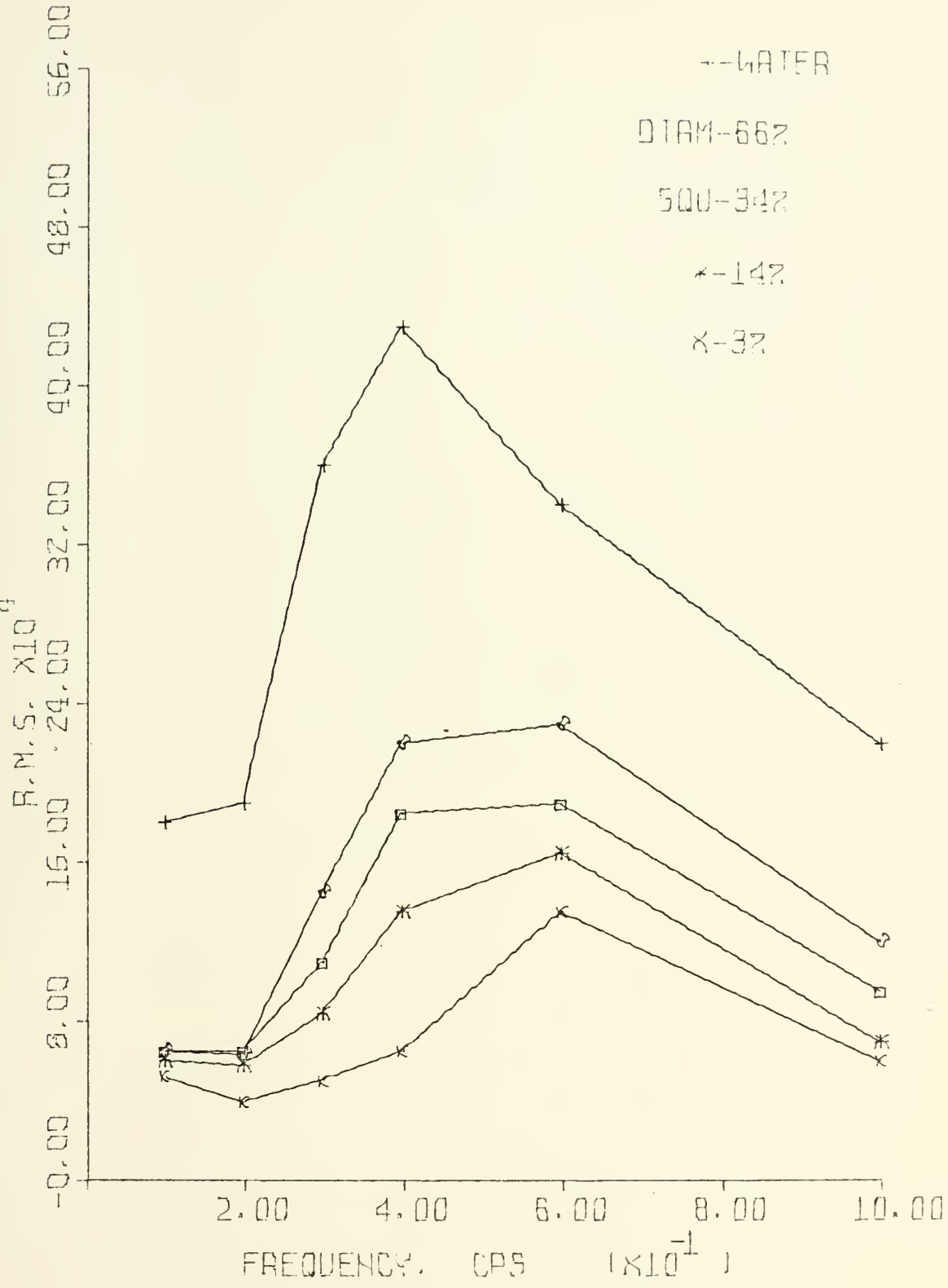

Figure 85: FREQUENCY SPECTRUM FOR TAP WATER AND VARIOUS PDR's AT X/DIAM = +1.5, Y/DIAM = +0.875; RE No = 140,000

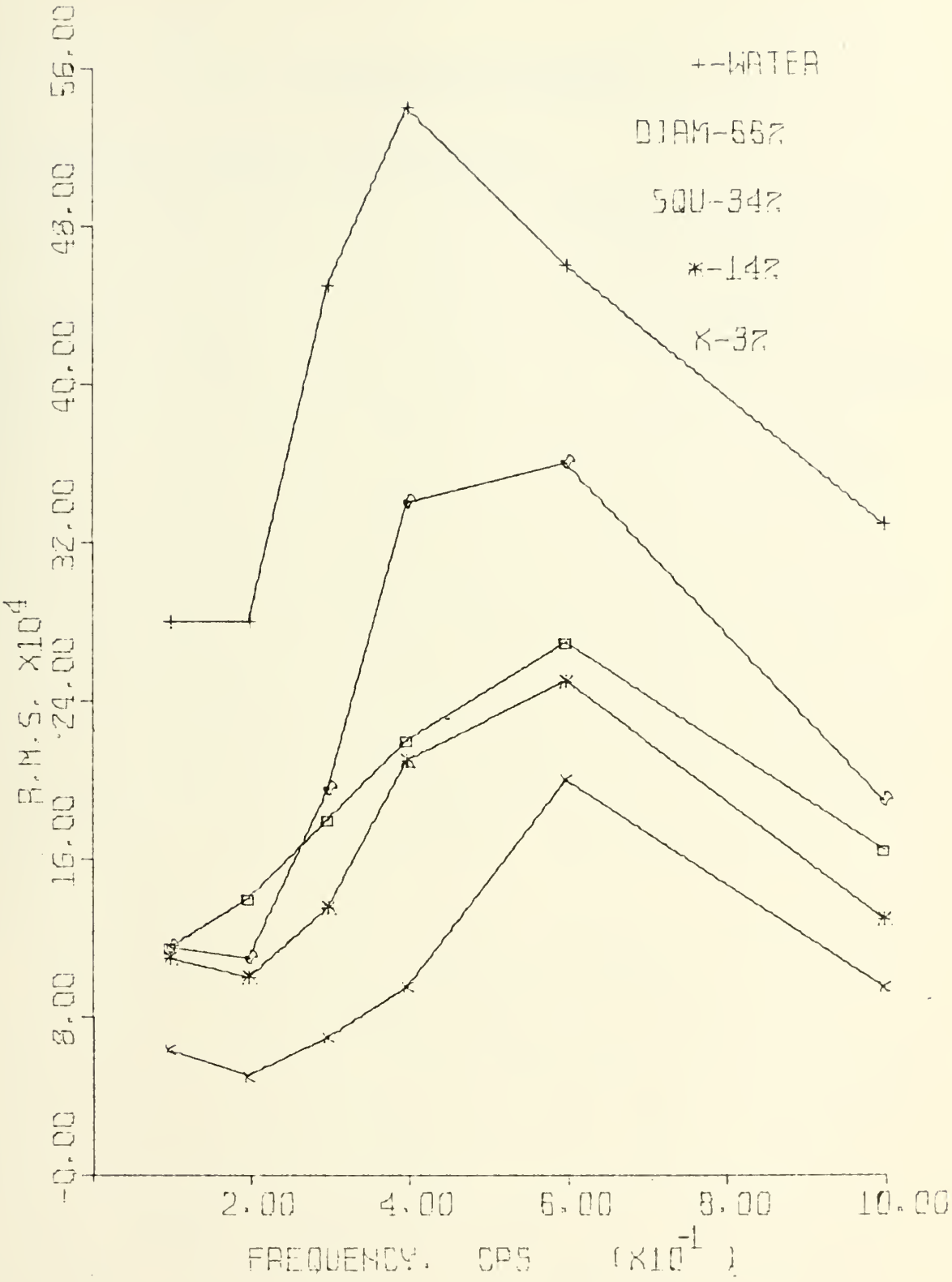

Figure 86: FREQUENCY SPECTRUM FOR TAP WATER AND VARIOUS PDR's AT X/DIAM = +1.5, Y/DIAM = +0.75; RE No = 140,000

IV. DISCUSSION OF RESULTS

A. TURBULENCE INTENSITY MEASUREMENTS

From the data presented in this section, it was observed that the wake width was invariably decreased as the PDR of the polymer solution decreased for all Reynolds Numbers tested. The extent of the reduction was a function of Reynolds Number and PDR. Maximum reduction of wake width occurred at very low PDR's. These observations suggested a decrease in form drag since the area of the low-pressure wake region in contact with the cylinder surface is directly proportional to the form drag. The results agreed favorably with the findings of Sarpkaya and Rainey [Ref. 2] and those of Kell [Ref. 3]. Figure 56, which presented Wake Width versus PDR, was compared with the drag coefficient versus PDR obtained from the work of their experiments. The characteristics were found to be the same.

Measurements suggested a gradual change of wake width at all PDR's, and all Reynolds Numbers. A "drag crisis" region was not observed in this experiment. Since previous experimenters concerned themselves with surface measurements only, and the present investigation was conducted purely off the surface of the test specimen, this difference was reconciled. It was found that the turbulence intensity measurements in the wake were much more violent at the location +1.0 X/DIAM than those obtained at +1.5 X/DIAM. This

observation suggested a rapid decay of turbulent violence as the flow progressed in the longitudinal direction behind the cylinder. Thus, it was reasonable to suspect that the action on the cylinder surface itself was somewhat different also.

The measurements also point to a reduction of disturbance diffusion rate in polymer solution flow. The reduction was found to be dependent upon degradation and Reynolds Number.

B. MICROSCALE MEASUREMENTS

The data presented in this section suggested smaller dissipative eddies in polymer solution flow than in water flow. The size of the dissipative eddies was found to be dependent primarily upon PDR, with fluctuations also present in the transverse direction.

C. FREQUENCY SPECTRUM MEASUREMENTS

The data in this section agreed favorably with the findings of Kell [Ref. 3], who also found a suppression of the entire surface pressure frequency spectra in polymer solution flow. The phenomenon was attributed to an increase of circulation of the vortices. The results of this investigation also suggested an increase in circulation in the wake region due to the large increase in turbulent violence observed there.

The spectrum measurements made outside the wake again pointed to a reduction of the diffusivity of disturbances. This observation was substantiated by the increased suppression

of a distinguishable predominant frequency, as the distance from the center of the wake increased. The trend of the reduction was found to be dependent upon PDR and the transverse distance from the center of the wake. These observations agree with the results of Gadd [Ref. 23] who found that Polyox solution reduced the mixing of dye streaks, as compared to water. His results applied to internal flow, however, and the correlation between internal and external flows of polymer solution has not yet been adequately determined.

D. DISCUSSION OF FLOW MECHANISMS

The data presented in this investigation suggested three phases of solution degradation, the characteristics of which determined the characteristics of the flow field. At high PDR, the polymer solution contained a statistically high percentage of very long, high-molecular weight molecules. Because of the intertwining capabilities at this high PDR, the diffusion of disturbances was not greatly inhibited, since the solution could possibly contain a network of entangled particles, via which diffusion was accomplished. This hypothesis agreed with the "Entanglement Hypothesis" proposed by Kowalski [Ref. 4]. However, as the shearing action of the recirculating pump tore the high-molecular weight molecules apart, the PDR decreased. When the molecules had reached a certain size, entanglement was inhibited. The molecules then uncoiled and aligned themselves in the direction of shear, as the flow progressed about the cylinder.

This hypothesis regarding a preferred molecular orientation was expounded upon by Patterson [Ref. 5]. The molecule in this orientation effectively retarded the diffusion of disturbances toward the outer regions of the flow. The amount of retardation could be characterized by a shear wave speed, as suggested by Sarpkaya and Rainey [Ref. 2]. The data of this experiment suggested that the propagation of disturbances was greatly inhibited at Reynolds Numbers above 100,000. This suggested that the shear wave speed was overpowered by the flow speed, and disturbances were swept downstream before the effect could be observed at a given point. The preferred orientation thus provided an effective barrier to the transfer of momentum normal to the flow direction. The flow field swept past the cylinder at these higher Reynolds Numbers and violently discharged the stored energy of the polymer molecules in the near wake of the flow field. The above hypothesis was justified by the great increase of turbulence intensity measured in the core of the near wake at low PDR's above the Reynolds Number 100,000. This phenomenon caused a reduction in wake width. It was feasible to assume that energy stored by the molecules could also be discharged into the flow as the separation point was reached on the surface of the cylinder since it represents a point of change in the preferred orientation of the molecule. The combined sweeping action of the flow field and the possibility of an interchange of energy as the flow approached the separation point contributed to the reductions observed.

As the polymer solution degraded further, the molecules became less capable of any retarding effect. The characteristics of the flow then approached those observed in water as the PDR approached zero.

The above mechanisms were offered to explain the effects observed.

V. CONCLUSIONS

The results obtained from the phases of this investigation warrant the following conclusions:

1. The turbulence intensity in the wake flow of dilute polymer solution is altered significantly in the transition Reynolds Number range. Turbulence intensity outside the wake progressively decreases, reaches a minimum, and then increases, as the PDR decreases to zero. Concurrently, turbulence intensity in the wake core progressively increases, reaches a maximum, and then decreases with decreasing PDR. The amount of change is dependent upon the degradation state of the solution and upon the Reynolds Number.

2. The width of the near wake is reduced below the value observed for water flow for the Reynolds Numbers tested. The extent of the reduction is dependent upon degradation and Reynolds Number.

3. There is a general suppression of the frequency spectrum observed at points in the wake and outside the wake for polymer solution flows at the X-coordinate +1.5 X/DIAM. The amount of suppression is dependent upon the Reynolds Number, the degradation state, and the distance from the center of the wake.

4. In the wake of polymer solution flow about a circular cylinder, there is a change in frequency distribution above a certain Reynolds Number. The frequency spectra acquire a

skewness toward higher frequencies. This effect is dependent upon Reynolds Number, degradation state, and distance from the center of the wake.

5. The microscale of turbulence in the region outside the wake of polymer solution flow about a circular cylinder is reduced below the value obtained in water flow. The reduction is primarily dependent upon degradation state.

BIBLIOGRAPHY

1. Toms, B. A., "Some Observations on the Flow of Linear Polymers through Straight Tubes at Large Reynolds Numbers," Proc. Int'l. Cong. Rheol. Part II, 1949.

2. Sarpkaya, T. and P. G. Rainey, "Flow of Dilute Polymer Solutions about Circular Cylinders," Report Number: NPS-59SL1021A, Naval Postgraduate School, Monterey, 26 February 1971.

3. Kell, R. E., "The Effect of Dilute Polymer Solution on the Strouhal Frequency of Circular Cylinders," Mechanical Engineer Thesis, Naval Postgraduate School, Monterey, June 1971.

4. Kowalski, T., "The Effect of Dilute Polymer Solutions on the Turbulence Characteristics and the Frictional Drag of External Flows," Doctoral Dissertation, University of Waterloo, March 1969.

5. Patterson, R. W., "Turbulent Flow Drag Reduction and Degradation with Dilute Polymer Solutions, "Div. of Eng. and Applied Physics, Eng. Sci. Lab., Harvard University, 1969.

6. Tulin, M. P., "Turbulence in Weakly Viscoelastic Fluids," Hydronautics Inc., 1965.

7. Goldstein, S., Modern Developments in Fluid Dynamics, Volume II, Oxford, 1938.

8. Rosenhead, L., "Vortex Systems in Wakes," Advances in Applied Mechanics, Vol. III, Cambridge, 1953.

9. Humphreys, J. S., "On a Circular Cylinder in a Steady Wind and Transition Reynolds Numbers," J. Fluid Mechanics, v. 9, pt. 4, pp. 603-612, 1960.

10. Schmidt, L. V., "Measurements of Fluctuating Air Loads on a Circular Cylinders," J. Aircraft, Vol. 2, No. 1, pp. 49-55, January 1965.

11. Keefe, R. T., "An Investigation of the Fluctuating Forces acting on a Stationary Circular Cylinder in a Subsonic Flow Stream and of the Associated Sound Field," Institute of Aerophysics, UTIA Report No. 76, September 1971.

12. Prendergast, V., "Measurement of Two-Point Correlations of the Surface Pressure on a Circular Cylinder," UTIA T. N. No. 23, July 1958.

13. el Baroudi, M. Y., "Measurement of Two-Point Correlations of Velocity near a Circular Cylinder Shedding a Karman Vortex Street," UTIA T. N. No. 31, January 1960.

14. Kovasznay, L. S. G., "Hot-Wire Investigation of the Wake behind Cylinders at Low Reynolds Numbers," Proc. Roy. Soc., A, 198, 174, 1949.

15. Bloor, M. S., "The Transition to Turbulence in the Wake of a Circular Cylinder," J. Fluid Mechanics, Vol. 19, p. 290, 1965.

16. Gerrard, J. H., "A Disturbance-Sensitive Reynolds Number Range of the Flow past a Circular Cylinder," J. Fluid Mechanics, Vol. 22, pp. 187-196, 1965.

17. Gerrard, J. H., "The Mechanics of the Formation Region of Vortices behind Bluff Bodies," J. Fluid Mechanics, Vol. 25, Part 2, pp. 401-13, 1966.

18. Roshko, A., "Experiments on the Flow past a Circular Cylinder at Very High Reynolds Number," J. Fluid Mechanics, 1960.

19. Hinze, J. O., Turbulence, McGraw-Hill, 1959.

20. Metzner, A. B. and G. Astarita, "External Flows of Viscoelastic Materials: Fluid Property Restrictions on the Use of Velocity-Sensitive Probes," AIChE Journal, May 1967.

21. Smith, K. A., E. W. Merrill, H. S. Mickley, and P. S. Virk, "Anomalous Pitot Tube and Hot-Film Measurements in Dilute Polymer Solutions," Chemical Engineering Science, Vol. 22, pp. 619-626, 1967.

22. "Polyox Water Soluble Resins," Union-Carbide Corporation, 1960.

23. Gadd, G. E., "Effects of Drag-Reducing Additives on Vortex Stretching," Nature, Vol. 217, March 16, 1968.

INITIAL DISTRIBUTION LIST

		No. Copies
1.	Defense Documentation Center Cameron Station Alexandria, Virginia 22314	2
2.	Library, Code 0212 Naval Postgraduate School Monterey, California 93940	2
3.	Asst Professor T. M. Houlihan, Code 59 Hm Department of Mechanical Engineering Naval Postgraduate School Monterey, California 93940	1
4.	ENS. John N. Schimmels, USN 1947 N. 37th Street Milwaukee, Wisconsin 53208	1
5.	Department of Mechanical Engineering, Code 59 Naval Postgraduate School Monterey, California 93940	1

UNCLASSIFIED

Security Classification

DOCUMENT CONTROL DATA - R & D

(Security classification of title, body of abstract and indexing annotation must be entered when the overall report is classified)

1 ORIGINATING ACTIVITY (Corporate author)

Naval Postgraduate School
Monterey, California 93940

2a. REPORT SECURITY CLASSIFICATION

UNCLASSIFIED

2b. GROUP

3 REPORT TITLE

A Study of the Wake Region of the Flow of Dilute Polymer Solution about Circular Cylinders

4 DESCRIPTIVE NOTES (Type of report and inclusive dates)

Master's Thesis; December 1971

5. AUTHOR(S) (First name, middle initial, last name)

John Norman Schimmels

6. REPORT DATE	7a. TOTAL NO. OF PAGES	7b. NO. OF REFS
December 1971	152	23

8a. CONTRACT OR GRANT NO.	9a. ORIGINATOR'S REPORT NUMBER(S)
b. PROJECT NO.	
c.	9b. OTHER REPORT NO(S) (Any other numbers that may be assigned this report)
d.	

10. DISTRIBUTION STATEMENT

Approved for public release; distribution unlimited

11. SUPPLEMENTARY NOTES	12. SPONSORING MILITARY ACTIVITY
	Naval Postgraduate School Monterey, California 93940

13. ABSTRACT

The wake region of the flow of dilute polymer solution about a circular cylinder was studied. Polyox WSR-301 at a concentration of 25 WPPM was dissolved in tap water. The investigation was performed in the drag transition flow regime. Turbulence intensity, wake width, microscale of turbulence and frequency spectra were measured at various points in the wake region of water flow and polymer solution flow.

The polymer additive suppressed turbulence intensity outside the wake and caused a corresponding increase in the wake core. The effect was dependent upon degradation and Reynolds Number. Frequency spectra were also suppressed. The amount of suppression was dependent upon degradation, Reynolds Number and distance from the wake center. Microscale was reduced outside the wake, as a function of degradation only. Wake width was reduced, dependent upon degradation and Reynolds Number. Results indicated a premature transition which was dependent upon the above factors.

DD FORM 1 NOV 65 1473 (PAGE 1)

S/N 0101-807-6811

UNCLASSIFIED

Security Classification

A-31408

KEY WORDS	LINK A		LINK B		LINK C	
	ROLE	WT	ROLE	WT	ROLE	WT
Polymer Flow						
Circular Cylinders						
Bluff Body						
Turbulence Intensity						
Wake						
Microscale of Turbulence						
Frequency Spectrum						

Thesis
S33675 Schimmels
c.1
133156
A study of the wake region of the flow of dilute polymer solution about circular cylinders.